Snow avalanches in central Svalbard: A field study of meteorological and topographical triggering factors and geomorphological significance

MARKUS ECKERSTORFER

Ph.D. Thesis
Longyearbyen 2012

Arctic Geology Department, The University Centre in Svalbard, Norway

Department of Geosciences, Faculty of Mathematics and Natural Sciences, University of Oslo, Norway

Series of dissertations submitted to the
Faculty of Mathematics and Natural Sciences, University of Oslo
No. 1283

ISSN 1501-7710

Cover: Inger Sandved Anfinsen.
Printed in Norway: AIT Oslo AS.

Produced in co-operation with Akademika publishing.
The thesis is produced by Akademika publishing merely in connection with the thesis defence. Kindly direct all inquiries regarding the thesis to the copyright holder or the unit which grants the doctorate.

Abstract

Snow avalanches are a natural phenomenon occurring in snow covered alpine areas all over the world. A complex process combining gravity, topographical conditions, physical and mechanical properties of snow and meteorological conditions control avalanche release. Due to this process complexity, avalanche research has a remarkable interdisciplinary nature, from physical geography, to geomorphology, meteorology, geophysics, engineering and natural hazards. Hazard related avalanche research is of most importance, as an improved process understanding of how, when and where avalanches release is crucial for avalanche warning and forecasting. Besides this natural hazard focus, avalanches are also studied to improve the understanding of their geomorphological role. Their importance as rock sediment erosion, transport and depositional agents in high relief terrain is of main interest.

Surveying the scientific literature indicates that until 2009 no basic avalanche research has been published in Svalbard. This is somewhat surprising, as the alpine Svalbard landscape with its snow cover, existing for a maximum of 10 months per year, is prone to avalanching. In addition, with the permanent settlement Longyearbyen, where the University Centre in Svalbard is located, infrastructure certainly exists to conduct year-round slope process studies, with very easy field access to avalanche terrain. Moreover there is an increasing population that is living and working in an active landscape, visited also by an increasing number of tourists.

Therefore my PhD thesis is a field based and interdisciplinary study of the meteorological and topographical triggering factors and the geomorphological significance of avalanches in central Svalbard. All data was obtained by direct observations, data recording by instruments and by direct measurements in the field between 2003 – 2012; with my own data gathering beginning in 2008, but primarily during my 4 year PhD study from 2009 to 2012. Thus, it should be kept in mind, that results and conclusions are based on a short but unique dataset.

The main characteristic of the snow climate in central Svalbard is a thin, discontinuous snowpack that is highly stratified with several ice layers and meltform layers overlying a persistent depth hoar base. Depth hoar and secondly facets are the most prominent weak layers in the snowpack.

The main characteristic of the avalanche regime in central Svalbard is the dominance of cornice fall avalanches, due to the sedimentary plateau mountain topography, the

lack of high vegetation and a prevailing winter wind direction. The timing of cornice fall avalanche releases is identified to be within 3-5 weeks after cornices start deforming rapidly enough that tension cracks open between the cornice and the snow of the plateau. Slab avalanches are the second most observed avalanche type. For the release of natural dry slab avalanches the best meteorological predictor variable are sums of precipitation and snowdrift in periods of 24, 48 and 72 hours before an avalanche day. This is in agreement with previous studies from other areas. Wet slab and slush avalanches had the longest runout distances observed. Such were studied during two mid-winter wet avalanche extreme events in January 2010 and March 2011. Both these extreme cycles resulted from slowly passing low-pressure systems, with air temperatures several degrees above freezing, and 100-year record monthly rainfalls. Analyzing the occurrence of such extreme meteorological conditions for the last 100 years, no correlation between a warming climate and wet avalanche cycle frequency was found. In conclusion, low-pressure frequency and magnitude largely determine avalanche activity at present in Svalbard. As the low-pressure frequency is modeled to decline in the North Atlantic in a warming climate, avalanche activity will be reduced. However, cornice fall avalanches are mainly controlled by the topography and the prevailing winter wind direction, and will therefore increase in dominance.

The geomorphological role of avalanches as sediment transport agents is significant, primarily due to rock erosion, transportation and deposition by the cornices and cornice fall avalanches. Cornices can increase rock weathering and thus erosion by keeping the ground thermal regime underneath them ideal for ice segregation. The weathered rock debris is then eroded from the backwall by plucking as the cornice detaches from the plateau. Cornice fall avalanches, consequently can transport rock debris downslope throughout winter and spring. Therefore, high rockwall retreat rates with associated large avalanche sedimentation on the avalanche fans below have been quantified for leeward facing slopes in Longyeardalen. This identified cornice fall avalanches as the most efficient geomorphological slope process at present and during the Holocene.

The conducted research focusing on the natural hazard perspective and on the geomorphological effects of avalanches represents the first basic research on the natural phenomenon snow avalanche in central Svalbard. Hopefully my study will trigger more research on avalanches in Svalbard, but also be a useful basis for a future avalanche forecasting service in Svalbard.

Acknowledgements

My greatest thanks go to my supervisor Hanne H. Christiansen and my friend Ulli Neumann. Hanne offered me to join the Cryoslope project for two months in spring 2008 without knowing me. She then paid my rent for the rest of 2008 and fought for the PhD position I could apply for. It was a pleasure working with you for the last 5 years Hanne, and I am looking forward to our future collaborations. I was given a great degree of freedom in my work and could pick the directions I wanted to go to.

Everything I know about living and working in the High Arctic I know from Ulli. You have quite a different and refreshing angle towards life and many of your talents I would like to call my own. I always tried to mimic your relaxed attitude and I hope I managed some time. I really miss spending time with you on skis and snowmobiles, in front of released avalanches and on top of weather stations.

I would like to thank Ole Humlum and Lena Rubensdotter for being my scientific mentors. You are both incredible scientists. Much of the work I have done in my PhD goes back to your initial ideas Ole. Lena, you are crazy and you know it.

I also want to thank "my" MSc students and buddies Stephan Thomas Vogel and Wesley Pickle Farnsworth. It was a pleasure to hang with you guys in snow pits, on and underneath cornices, under bars, on rocky and sandy beaches, in Russian swamps and on North American golf courses. Besides all that fun, we cranked out some good science, and yea, I ski so much better than both of you.

I owe gratitude to Jordy Hendrikx and Karl Birkeland from Montana State University for hosting me in spring 2012. Jørgen Haagensli for his enthusiasm about my work and for borrowing me equipment. Mike Retelle for proofreading my thesis. Some of the good folks at UNIS and Svalbard like Jordan, Sara, Pål, Espen, Rasmus and Kim, only to name a few.

Last but not least, I want to thank my family, especially my parents for understanding that I chose to move 3000 km north.

I feel lucky that I could live in Svalbard, experience its fascinating nature and try to reveal some of its secrets. I also found Juni there and I am thankful for the great life we share.

Hell yea what a ride, I would do it again in a heartbeat!

Max,
Salema, Algarve, Portugal
July 2012

List of papers

Paper 1:
Eckerstorfer, M., Christiansen, H.H. 2011. The "High Arctic maritime snow climate" in Central Svalbard. *Arctic, Antarctic and Alpine Research.* 41/1. 11-21. doi: 10.1657/1938-4246-43.1.11

Paper 2:
Eckerstorfer, M., Christiansen, H.H. 2011. Topographical and meteorological control on snow avalanching in the Longyearbyen area, central Svalbard 2006-2009. *Geomorphology.* 134. 186-196. doi:10.1016/j.geomorph.2011.07.001

Paper 3:
Eckerstorfer, M., Christiansen, H.H. 2011. Relating meteorological variables to the natural slab avalanche regime in High Arctic Svalbard. *Cold Regions Science and Technology.* 69. 184-193. doi:10.1016/j.coldregions.2011.08.008

Paper 4:
Eckerstorfer, M., Christiansen, H.H. 2012. Meteorology, topography and snowpack conditions causing two extreme mid-winter slush and wet slab avalanche periods in High Arctic maritime Svalbard. *Permafrost and Periglacial Processes.* 23. 15-25. doi:10.1002/ppp.734

Paper 5:
Vogel, S., **Eckerstorfer, M.,** Christiansen, H.H. 2012. Cornice dynamics and meteorological control at Gruvefjellet, Central Svalbard. *The Cryosphere.* 6. 157-171. doi:10.5194/tc-6-157-2012

Paper 6:
Eckerstorfer, M., Christiansen, H.H., Vogel, S., Rubensdotter, L. 2012. Snow cornice dynamics as a control on plateau edge erosion in central Svalbard. *Earth Surface Processes and Landforms.* doi: 10.1002/esp.3292

Paper 7:
Eckerstorfer, M., Christiansen, H.H., Rubensdotter, L., Vogel, S., Siewert, M. submitted. The role of cornice fall avalanche sedimentation (in the valley Longyeardalen, central Svalbard). *Journal of Geophysical Research – Earth Surface.* 20 p.

Table of contents

1. Introduction

The interdisciplinary nature of snow avalanche science and its relevance

Figure 1: Three cornice fall avalanches that released on 14 May 2012. The two large cornice fall avalanches additionally triggered slab avalanches and run over the road between Longyearbyen and a part of town called Nybyen.

Snow avalanches (hereafter also called avalanches) are rapid mass movements occurring in snow covered mountain areas all over the world (McClung and Schaerer, 2006) (Figure 1). Since avalanches are rare events, their study is as exciting as it is challenging. Due to their complexity, avalanche research has a remarkable interdisciplinary nature, crossing several boundaries within the field of physical geography, including natural hazards, meteorology, geomorphology and hydrology, as well as in the fields of geophysics and engineering.

Avalanches have been studied by physical geographers since the late 19th century (Cornell, 1873). In these early days of avalanche science, snow was regarded as sediment that accumulates in layers, and the geology and geomorphology of snow was of special interest (Paulcke and Welzenbach, 1928; Seligman, 1936; Welzenbach, 1930). But these Geographers from the Alps also noted the hazardous nature of avalanches (Figure 2). As the number of avalanche fatalities lies nowadays at around 250 persons per year worldwide (Schweizer, 2008), the study of their release mechanisms and dynamics are crucial for a better understanding of the processes involved. This research should lead to an improved predictability of release location and timing (Schweizer,

2008). The prediction of current and future snow instability in space and time, relative to a given trigger level is crucial in decreasing avalanche fatalities (McClung and Schaerer, 2006).

Figure 2: Engraving by D. Herrliberger after D. Duerringer, Topographie der Eidgenossenschaft, 1754. The artwork shows one of the first known graphical representations of an avalanche, threatening a mountain village in the Alps.

Some research has its focus on avalanches as a type of mass movement on hill slopes (Selby, 1993). Avalanches are widely regarded as sediment erosion, transportation and deposition agents, thus being of geomorphological significance. Especially in favourable climatic and lithological settings, avalanches are an efficient sediment transport mode from high to low relief (Caine, 1976; Decaulne and Saemundsson, 2006; Heckmann et al., 2005; Luckman, 1977; Luckman, 1978a; Luckman, 1978b). Avalanches also contribute to the mass balance of glaciers (Barsch and Jakob, 1998; Bell et al., 1990; Scherler et al., 2011) and provide rock sediment and snow to rock glaciers (Humlum et al., 2007). However, the importance of avalanches as geomorphological agents in the alpine cascade is often underrated (Sass et al., 2010). Avalanches are considered as subsidiary sediment transport agents, rather than the dominant one. There are a number of studies quantifying the geomorphological work of avalanches from the Canadian Rocky Mountains (Luckman, 1988), or northern Swe-

den (Rapp, 1960a; Rapp, 1960b). These studies reported significant geomorphological work of avalanches, quantified by direct measurements (Luckman, 1978b), however, ranked it second after rockfall as the dominant debris transport agent. Studies, solely dealing with avalanche sedimentation are sparse and originate from the observation of single events for example in New Zealand (Ackroyd, 1987) and the Himalayas (Bell et al., 1990).

Therefore, geomorphological field studies, such as this PhD study, are of great importance for an enhanced understanding of the geomorphological impact of avalanches and their significance in rock debris erosion, transportation and deposition.

2. Scope of thesis and research questions

A survey of the literature indicates that until 2009 no basic avalanche research had been conducted at the regional scale in central Svalbard. My PhD study takes advantage of a number of critical factors that combine to provide an ideal field site for a geographical analysis of avalanches. The unique location of the University Centre in Svalbard (UNIS) provides year-round, easy field access to nearby avalanche prone terrain. In central Svalbard, the long-lasting mountain snow cover, alpine terrain, and the lack of any high vegetation, are conditions that favour avalanche activity. Lastly, the Longyearbyen community is highly active in recreation, including snowmobile travel, skiing and hiking making avalanche studies highly relevant. Taking advantage of this world-class field laboratory on periglacial slope processes and its controls has been the main focus of this PhD study.

Therefore this study addresses some classic questions in physical geography:

- How do physical features such as meteorological and snowpack conditions vary through time (through a snow season from September or October to June) and space (in the high relief landscape of central Svalbard), as controls for present-day avalanche activity? Furthermore, what is the geomorphological significance of these avalanches in terms of sediment erosion, transportation and deposition?

Basic, field-based research was carried out on meteorological and topographical factors determining the spatial and temporal dynamics of the snow cover and its consequent control on avalanche release.
A simple question on avalanche formation is:

- Where and when does what kind of avalanche occur and additionally how and why? (Schweizer et al., 2003).

Furthermore basic, field-based research was carried out on the erosional effect of avalanches and their role as sediment transport agents.
A simple question on the geomorphological significance is:

- How much rock debris is eroded and transported downslope by avalanches and what are the controlling processes. Furthermore, what does that mean for the periglacial landscape evolution?

The first part of this PhD study on avalanche formation is of interest for future avalanche scientists working in Svalbard, as well as a future establishment of an avalanche warning and forecasting service. The second part of this study on the geomorphological significance of avalanches is of interest for physical geographers working on periglacial slope processes, sediment budgets, erosion and weathering. Furthermore, this study provides the first basic results on snow dynamics in High Arctic Svalbard, useful for snow science, snow hydrology, climatology and meteorology.

3. Snow avalanche theory: Types of snow avalanches and their trigger mechanisms

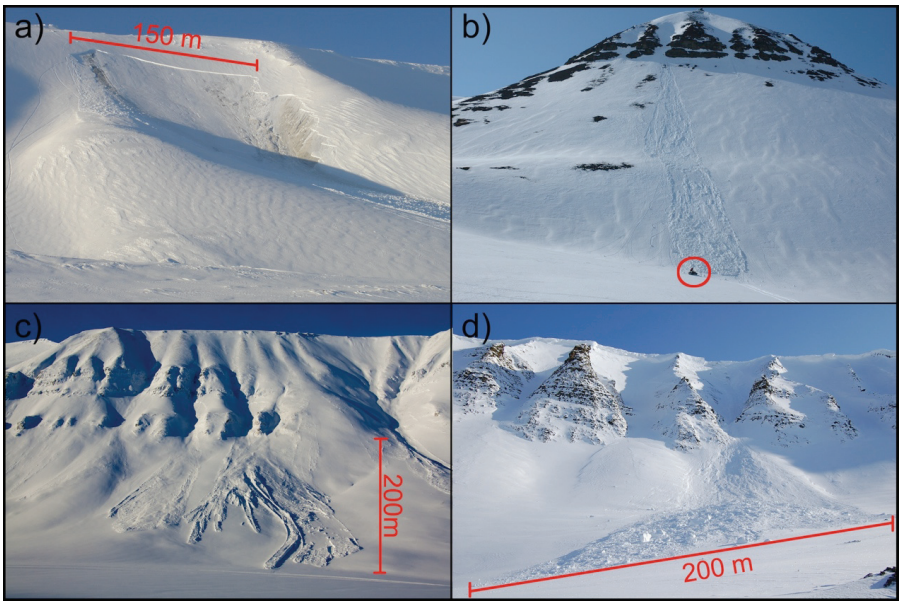

Figure 3: Types of avalanches. a) Slab avalanche on Nordenskiöldtoppen, artificially triggered by a snowmobile on 15 March 2009. b) Loose snow avalanche on Karl Bay Fjellet in Todalen, naturally released on 26 April 2008. Snowmobile in red circle for scale. c) Slush avalanche on Karl Bay Fjellet in Todalen, naturally released on 18 March 2011. d) Cornice fall avalanche on Gruvefjellet at Larsbreen, naturally released on 2 April 2010. Place names are given in Figure 4 and Figure 5.

A complex process combining gravity, topographical and meteorological conditions, and mechanical properties of snow must take place for an avalanche to release (McClung and Schaerer, 2006; Schweizer et al., 2003). Two general avalanche types are distinguished, loose and slab avalanches, occurring both in dry and wet snow (McClung and Schaerer, 2006). Dry slab avalanches release starts with a failure in a thin weak layer, or at an interface, underlying a cohesive slab layer. Slab avalanches are distinguishable by characteristic crowns, from where the avalanche bulk detaches (Figure 3a). Slab avalanches cause most human fatalities (McClung and Schaerer, 2006). In over 90 % of all avalanche accidents, the victims trigger the avalanche themselves (McCammon and Haegeli, 2006). Therefore slab avalanche mechanics are of special interest in hazard related avalanche science. For a dry slab avalanche to release, a weak layer must fail in compression and shear. The potential energy gained through this weak layer collapse then drives the development of a fracture, communi-

cated by the overlying slab (Gauthier and Jamieson, 2010; Heierli et al., 2008). Loose snow avalanches start at a point with a cohesion-less layer and entrain snow in a spreading triangular pattern (Figure 3b).

Topography largely controls where avalanches start and how far they run. The most important factor is slope inclination and the majority of slab avalanches releases between 35-45 ° (McClung and Schaerer, 2006). Meteorological factors, favourable for slab avalanche release are wind velocity and direction, precipitation and air temperature, as well as direct solar radiation over various time scales, all dynamically interacting with the terrain (McClung and Schaerer, 2006).

Avalanches are also distinguished by their triggering mode, classified into natural and artificial releases. Natural avalanches are of special interest for avalanche forecasting, as natural causes such as a certain amount of precipitation or wind loading lead to overcoming the strength of a weak layer, which eventually fractures and induces a slab avalanche. Cornice fall avalanches are regarded as natural releases, triggered by a collapsing cornice (Figure 3d) (Greene et al., 2004). Cornices are wedge-like snowdrifts that form on lee sides of ridges and slope inflections (Latham and Montagne, 1970; Montagne et al., 1968). Fundamental work on cornices was carried out in the European Alps, due to their particular shape and their ability to trigger avalanches when collapsing (Paulcke and Welzenbach, 1928; Seligman, 1936; Welzenbach, 1930). John Montagne, working in the Bridger Range, Montana, did extensive cornice studies, focusing on deformation processes inside the cornice mass, and attributed snow creep and glide to the opening of tension fractures between the cornice mass and the ridgeline, which seemed to be a requirement for entire cornice collapses (Montagne et al., 1968).

Avalanches are also classified into dry and wet avalanches. One type of wet snow avalanche is a slush avalanche (Figure 3c). Slush avalanches were first observed in the Arctic, as water-saturated snow flowing along stream channels due to intense spring thawing (Washburn and Goldthwait, 1958). Slush avalanches release due to a hydraulic gradient developing from an increasingly inclined meltwater table within the snowpack, so that friction at a bed surface can be overcome (McClung and Schaerer, 2006; Scherer et al., 1998). This happens due to either intensive spring melting of snow or rain on snow events (Hestnes, 1998).

4. Study area and sites

Figure 4: Nordenskiöld Land in central Spitsbergen, Svalbard's main island (see inlet map). The red square indicates the study area around Svalbard's main settlement Longyearbyen (Figure 5). The key sites, Nybyen, Larsbreen, and Gangskaret are indicated with red dots.

Studies were performed around Longyearbyen, the main settlement in Svalbard. Longyearbyen is located at 78° 13'N, 15° 47'E in the centre of Svalbard's main island Spitsbergen on the eastside of Isfjorden, a large fjord stretching from the west coast inland (Figure 4). The study area is about 17 km^2 large (Figure 4, red square), and studies were focused along the 70 km long snowmobile route referred to as the "Little Round" around Longyearbyen (Figure 5, grey line). This study area was chosen for the Cryoslope Svalbard Research project (2006-2009) with the aim of monitoring periglacial slope processes, their effect on traffic and infrastructure in the Longyearbyen area and their response to a future changing climate (Eckerstorfer et al., 2008). Two sites in the valley Longyeardalen, the Nybyen and Larsbreen slope systems (Figure 4, Figure 5), were used for an integral study of cornice fall avalanches, their meteorological control and geomorphological significance. The mountain pass Gangskaret, at the junction of Todalen, Gangdalen and Bødalen (Figure 4, Figure 5) was used for comprehensive snowpack studies.

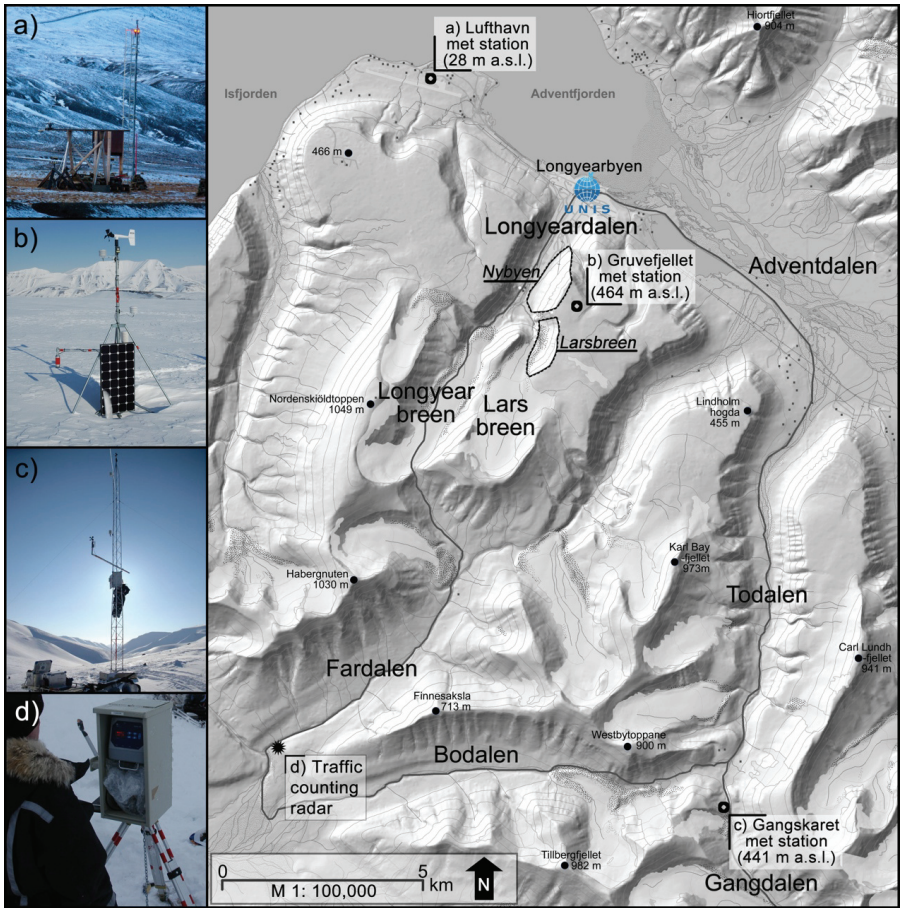

Figure 5: Topographic map of Longyearbyen and the snowmobile route "Little Round (grey line). a) Lufthavn meteorological station. b) Gruvefjellet meteorological station. c) Gangskaret meteorological station during maintenance. d) Traffic counting radar, deployed in the valley Fardalen between 11 March and 14 May 2009. e) Both key study sites, the Nybyen and Larsbreen slope systems are indicated.

4.1 Geology and geomorphology

The landscape around Longyearbyen lies in the Central Tertiary Basin, consisting of horizontal-lying, sedimentary bedrock of Early Permian to Eocene age (Major et al., 2001). This geological setting determines the extensive plateau mountain topography (Figure 4, Figure 6), rising to an average elevation of 450 – 550 m a.s.l. The highest peaks in the area display a rather alpine topography, reaching as high as 1000 m a.s.l. (Figure 5). Longyearbyen is located in the valley Longyeardalen, a typical, glacio-fluvially eroded U-shaped valley, deglaciated around 10,000 BP (Svendsen and Mangerud, 1997). The mountain slopes consist mainly of coarse weathered talus or

more fine-grained weathered material (Sørbel et al., 2001), shaped by a combination of gravitational processes mainly avalanches, rockfalls and debris flows (Larsson, 1982). Additionally smaller V-shaped gullies or ravines cut into the plateau edges, formed between protruding bedrock noses that are more resistant to erosion and weathering. The ravines are in many places funnel-shaped, with one or more contributing couloir that extends upwards to the plateau edge. Beneath the ravines, the slope system largely consists of talus deposits, mainly avalanche fans, reworked by debris flows. The mountains and lowlands are underlain by continuous permafrost (Christiansen et al., 2010), with a thickness range from less than 100 m near the coasts to more than 500 m in the highlands (Humlum et al., 2003). The permafrost at Svalbard is very variable in temperatures, depending mainly on ground material properties and snow cover. Ground temperatures in Adventdalen at 15 m depth vary from -3.2 °C at the solifluction sheet in Endalen, to -5.3 °C at the mountain plateau of Gruvefjellet (Christiansen et al., 2010) (Figure 5). The periglacial landscape makes up 40 % of Svalbard's landmass, even more so in the Longyearbyen area, where glaciation is less extensive.

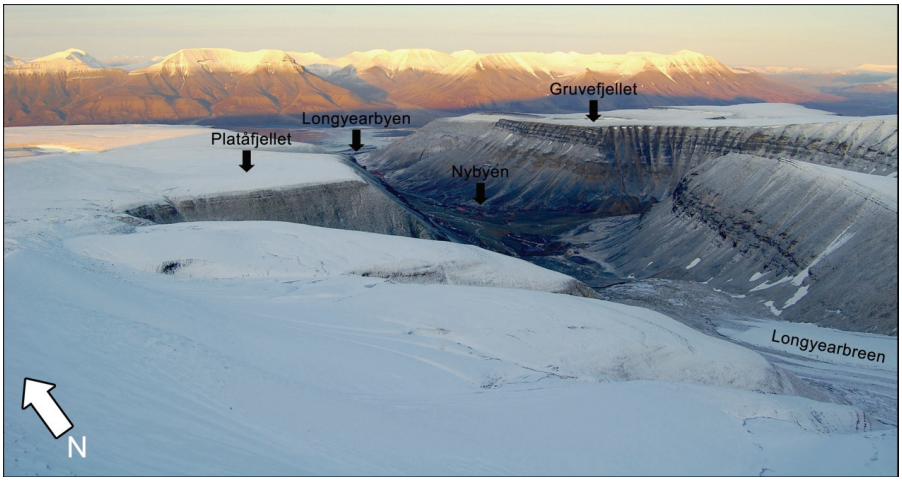

Figure 6: View from the mountain Nordenskiöldtoppen towards NNE down into the valley Longyeardalen. The infrastructure of Longyearbyen is visible at the mouth of the valley next to the waters of Adventfjorden. The characteristic plateau mountain topography is visible on both sides of Longyeardalen, with Platåfjellet to the left and Gruvefjellet to the right.

4.2 Climate and meteorology

Weather in the Arctic is characterized by an alternating pattern of high and low-pressure systems (Schaerer, 1986; Serreze and Barrett, 2008). This pattern is relatively weak in summer and stronger in winter, reflected by seasonal and daily air temperature fluctuations in Longyearbyen (Figure 7). The synoptic air flows over the Svalbard area are determined by the general low-pressure area near Iceland, and relatively high-pressures over Greenland (Hanssen-Bauer et al., 1990). During the winter season, meridional moisture transport along the North Atlantic cyclone track brings warm air temperatures and precipitation to Svalbard (Dickson et al., 2000). From the north, cold anticyclonic air masses change with these moist cyclonic air masses resulting in large air temperature variations during the winter (Figure 7).

Svalbard is located near the confluence of ocean currents and air masses of different thermal character (Humlum et al., 2007). The extent of large scale phenomena such as the Siberian High, an intense, cold anticyclone, influence especially winter air temperature conditions (Humlum et al., 2003). When the Siberian High extends to the west, covering parts of Europe, airflow over the Nordic Sea is strong and southerly, causing advection of warm air to the Svalbard region. Conversely, when cold polar air masses extend over Svalbard, a strong westerly airflow blows over northern Europe, creating heavy precipitation (Humlum et al., 2003). The climate sensibility is also enhanced by rapid variations in the sea ice extent that is coupled with both atmospheric and oceanic circulations (Humlum, 2002).

Thus, the area around the Svalbard archipelago is recognized as one of the most climatically sensitive in the world (Rogers et al., 2005). This climatic sensitivity was recognized early by Ahlmann (1953) and later by Rogers et al. (2005), and also mentioned in the third IPCC report (Houghton et al., 2001). The linear air temperature trend 1912-2010 from Svalbard airport is 0.23°C per decade (Humlum et al., 2011). This air temperature record is a homogenized composite record, established from different stations around Isfjorden. In Figure 7 the distinct 1920 warming period between 1917 – 1922 can be seen, which changed the mean annual air temperature (MAAT) at sea level from -12.2°C to -4.9°C. Following this air temperature rise, the Svalbard airport record is characterized by a warm period lasting to around 1955, a relatively cold period lasting to about 1990, and a renewed warming lasting until present (Figure 7). This late warming trend parallels observations from other places in the Arctic.

During the last two decades, the MAAT in the Svalbard region has increased by 1.0 – 1.2°C per decade, with an intensified winter warming of 2-3°C per decade (Førland et al., 2011). Førland et al. (2011) used downscaled global climate models forced with observed greenhouse gas emissions, and predict (point prediction) a warming for the Svalbard Longyearbyen – Airport area from 1961-90 to 2071-2100 equaling 0.6°C per decade for annual air temperatures and 0.9°C per decade for the winter season. Humlum et al. (2011) on the other hand modeled future air temperature development based on Fourier and wavelet analysis and suggest that the observed late 20th century warming is not likely to continue, but rather to be followed by variable, lower air temperatures for at least the next 20 – 25 years.

The MAAT in 2011 at sea level in Longyearbyen was -3.4°C; the 1912-2010 average is -6°C (Figure 7). The warmest years on record were 2006 with -1.7°C and 2007 with -2.5°C (Figure 7). The warmest winter season was in 2005 – 2006 with an average air temperature of -4.7°C, in 2008-2009 it was -6.5°C (Figure 7). Annual precipitation at sea level in Longyearbyen was 199 mm water equivalent (w.e.) in 2011, the average for the almost 100 year long record is 196 mm w.e (Figure 7). Data from surrounding meteorological stations (Met.no, 2012), however, suggest a significant vertical precipitation gradient, of 15-20 % per 100 m in coastal regions, and somewhat smaller (5-10 %) in the central part of Spitsbergen (Humlum, 2002). There is also a problem with precipitation measurements, since most precipitation gauges are raised above ground and thus influenced by the constant wind action, underestimating the amounts of precipitation. Humlum (2002) therefore used a 100 % upward correction for modeling the late 20th century precipitation in central Svalbard.

Wind is constantly blowing, with average annual wind speeds of around 5 m/s in 2011 (Met.no, 2012). Due to its constancy and strength and the lack of any high vegetation, winds significantly redistribute snow in the landscape. Some parts are completely blown free of snow for most of the winter while in lee sides, snow accumulates up to several meters thick. The prevailing winter wind direction over central Svalbard is from the SE (Met.no, 2012), local wind directions may vary due to topographical channeling effects (Christiansen et al., in press).

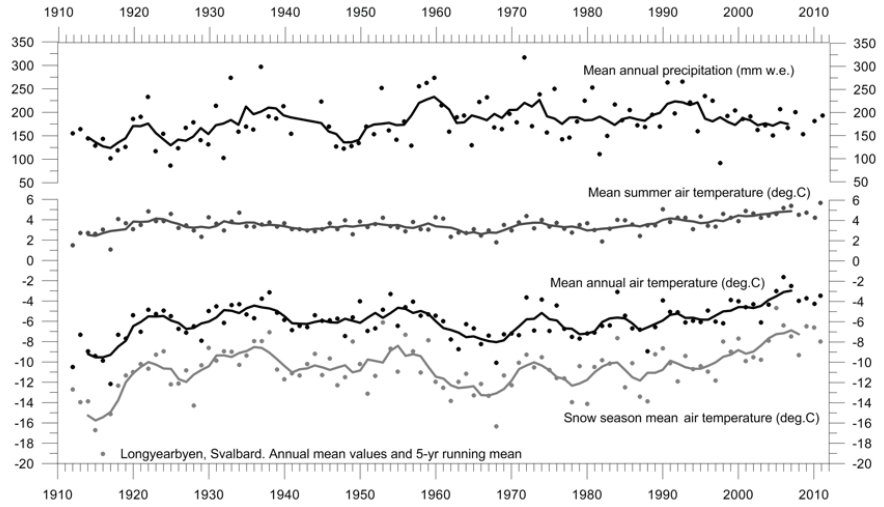

Figure 7: Mean annual precipitation and air temperature at Longyearbyen, Svalbard from 1912 - 2011, showing annual observations (points) and running 5 year average (solid lines). Snow season is October - May, summer is June - September. Data from Norwegian Meteorological Institute (Met.no, 2012).

5. Snow avalanche accidents and protection measures in Svalbard

The Svalbard archipelago consists of a high relief, mountain landscape (Figure 8). The main island's name "Spitsbergen" means "pointy mountains" in a wider sense, given by the first explorers who sailed Spitsbergen's west coast in the 16th century, astonished by the rugged, alpine topography (Arlov, 1996). Naturally, avalanches occur in Svalbard's mountainous landscape, which is snow covered permanently inland and at higher grounds, for at least 8-10 months of the year (Figure 1).

Figure 8: The west coast of Svalbard's main island Spitsbergen, seen from the airplane. The particular location is the strand flat of Kapp Linné, transitioning into the mountain Griegsaksla. Such mountains along the coast were sighted by the first explorers, thus leading to the islands current name.

Alfred Jahn described (1976) the disastrous slush flow avalanche that occurred in June 1953 and destroyed the hospital of Longyearbyen, killing 2 people, injuring another 12. The hospital was located at the mouth of Vannledningsdalen (Figure 9). The wife of the Governor of Spitsbergen, L. Balstad (Balstad, 1956) reported this event. Vannledningsdalen was at this time a deep gully (depth up to 30 m), low inclined (10-15°), starting from a large, flat cirque as the snow catchment area, surrounded by steep slopes. L. Balstad reported: *"In the uppermost part of the couloirs which forms the Vannledningsdalen valley, close to the mountain top, melting snow masses were gliding down the slope towards the valley. The speed of the avalanche was growing; nearly 100 m further down, it struck against heaps of hard, old snow and pushed them forward ahead together with ice and stones."* An ice dam was blocking the gully and

a surplus of melt water had therefore accumulated in the cirque above. A sudden release of that ice dam resulted in a violent down flow, with the water carrying away the snow and ice in the gully as well as large masses of rock debris. Afterwards, protective ridges along the river Vannledningselven, as well as two about 70 m long snow fences were constructed, to protect the infrastructure below the valley (Figure 9). In addition, the slush avalanche risk is reduced nowadays by excavating a channel in Vannledningsdalen each spring. Shortly before the onset of snowmelt, a caterpillar drives up and down the valley, excavating a deep channel to ensure good drainage of water from the critical upper valley section. Since this procedure was initiated, no slush avalanche has occurred during spring melting. Only in 1989, when the caterpillar operation was cancelled due to worry for increasing costs, a slush avalanche released (Humlum et al., 2010). On 20 January 2012 a mid winter slush avalanche, however, released in Vannledningsdalen, destroying a pedestrian bridge (Figure 9b, c).

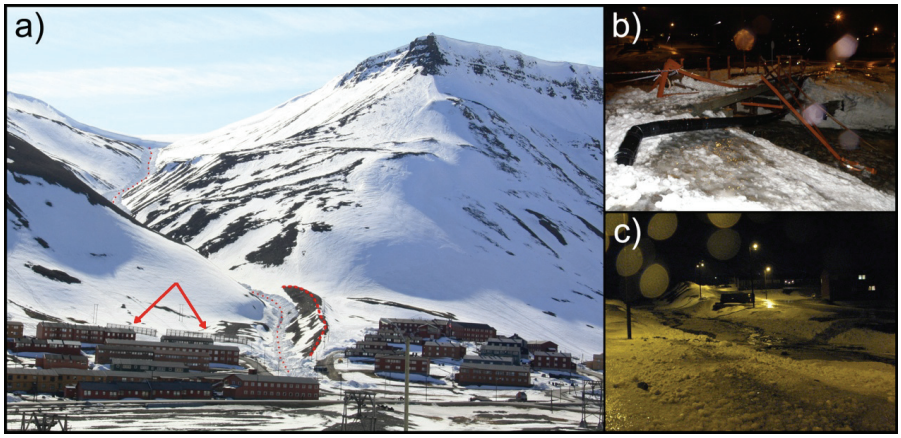

Figure 9: Vannledningsdalen, April 2010. a) Avalanche protective measures (avalanche fence and an artificial ridge, indicated by the red arrows and the dashed red line respectively) have been constructed at the mouth of the valley. The excavated channel, carried out by a bulldozer can be seen (red dotted line), as well as the flat snow accumulation area at the head of the valley. The slush avalanche from 1953 destroyed buildings on the orographic left side of the valley, now protected by the dam. b) and c) A slush avalanche, releasing on 20 January 2012, destroyed a pedestrian bridge at the mouth of Vannledningsdalen.

On 11 June 1992 Sysselmannen was called to a slush avalanche accident in Lifdefjorden, in northwestern Spitsbergen (Sysselmannen, 1992). One person was missing in the avalanche and the other 10 persons of his party had already given up the search.

In 1996, Store Norske Spitsbergen Kulkompani, the local mining company, and Svalbard Sammfunnsdrift A/S, contracted the NGI (Norwegian Geotechnical Institute) to

carry out an avalanche hazard evaluation for two particular areas in Longyearbyen. One area was Haugen, the part of Longyearbyen situated underneath the valley Vannledningsdalen (see 1953 slush avalanche disaster), (Hestnes, 1996b) and the other was an area close to the church, where a new kindergarten was planned (Hestnes, 1996a). For both locations, Hestnes calculated a likelihood for a disastrous avalanche of 1/1000 per year and concluded that a fair chance of a debris flow or slush avalanche event is given. Hestnes furthermore suggested not building the kindergarten in Haugen as well as the establishment of an avalanche forecasting service.

Erik Hestnes from NGI carried out the first monitoring of avalanches in the Longyearbyen area in the winters 1996, 1998 and 1999. Again, the Longyearbyen community was the contractor for this report about snowpack characteristics, avalanches and their runout distances (Hestnes, 1999). Hestnes and his college Bakkehøi spent three days in 1996 and one day in 1999 in the field, observing a total of 76 avalanches. They calculated an average runout inclination for all avalanches of 25.5° with most avalanches releasing in the aspect sector SSE-S (Hestnes, 1999). In their five excavated snow profiles they found a highly stratified snowpack with a hard middle part consisting of facets or meltforms, several ice layers inside and wind slabs on top.

In 2001 an avalanche killed two persons. Two young snowmobile drivers triggered a slab avalanche on the mountain Håbergnuten in the valley Fardalen, south of Longyearbyen (Figure 5). NGI reported that the accident happened after a snowstorm, with winds from SW. It took the rescue teams 17 hours to locate the first victim after spending much time searching for the artificially released avalanche, since many natural avalanches released on that particular day. After another two hours, the second victim was found with the help of a ground penetration radar (GPR), the methodology is presented in Instanes et al. (2004). The weak layer that fractured in the accident was depth hoar (Lied and Bakkehøi, 2001).

A slab avalanche took the lives of two snowmobilers again in March 2004 in Malardalen, NE of Longyearbyen. The victims were found after 20 hours of search at 3 m depth (NGI, 2010).

On 15 March 2009 a snowmobile driver drove up the 40 - 44° steep south facing slope of Hiorthfjellet (Figure 5). On his second loop he triggered a slab on depth hoar as the weak layer, tried to outrun it and fell off the snowmobile (Figure 10a). A second slab buried him under 3 m of snow and he died in the hospital later that day. On the

same day, another snowmobile driver triggered a slab avalanche on the mountain Nordenskiöldtoppen (Figure 5), but could outrun the avalanche.

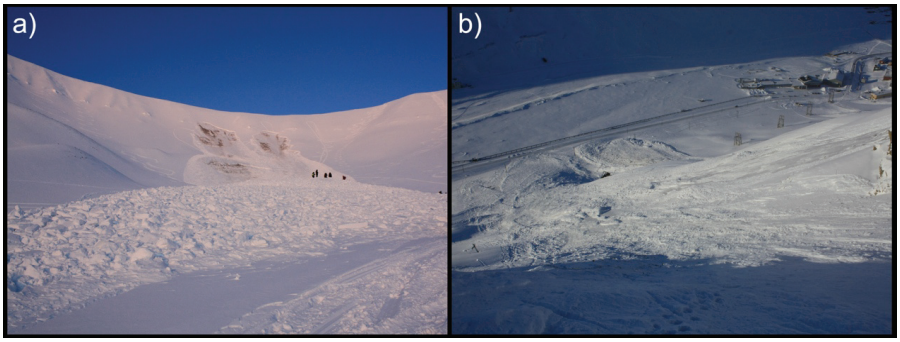

Figure 10: a) Snowmobile triggered slab avalanches on the mountain Hiorthfjellet, opposite of Longyearbyen, 15 March 2009. The snowmobile driver triggered the left slab; the second slab on the right buried the driver, where people are gathered in the middle of the picture. b) Natural (right) and artificial (left) triggered cornice fall avalanches on 29 March 2009.

End of March 2009 a falling cornice from the mountain Gruvefjellet collapsed and triggered a slab avalanche that destroyed historical mining infrastructure (Figure 10b). As a protection measure, the local government tried to control the remaining cornice with explosives. During installing of the explosive charges the cornice remains collapsed and triggered another slab avalanche on the slope beneath (Figure 10b). Both slabs ran over the street between Longyearbyen centre and Nybyen on the southern end of the valley, and a student had a narrow escape.

The cornice situation in Nybyen, where over 100 students and tourists live every spring caught also the attention of Erik Hestnes from NGI (Hestnes, 2000). Hestnes noted that several avalanches had reached the buildings in the past, and NGI raised the concern of this actual avalanche hazard. But explosives were not recommended since the artificial avalanches are consequently larger than natural once. NGI moreover suggested snow fences on the edge of the plateau might reduce the size of the cornices. These constructions should have been 100 m long, 4.5 m high and be located 80 m from the rim (Hestnes, 2000). Such snow fences were never constructed; instead, several snow piles were pushed together to protect the infrastructure in Nybyen in spring 2008, after we raised concerns that falling cornices could release large slab avalanches.

At present Longyearbyen is home to over 2000 people and annually, up to 85,000 tourists stay overnight, and around 39,000 people land by boat for some hours (Sentralbyrå, 2011). Thus, people living and visiting Svalbard, following their daily life and recreational as well as touristic activities, expose themselves to avalanche hazard during the winter and spring months. Snowmobiles are the main mean of transport in winter and in 2008, 2627 snowmobiles were registered (Sentralbyrå, 2011). Snowmobiles are used for recreational trips and commuting by the community and for excursions by tourists. In spring 2009, between 11 March and 14 May, we placed a traffic counting radar in the valley Fardalen, south of Longyearbyen (Eckerstorfer et al., 2009) (Figure 5d). Inhabitants and tourist groups frequently use this valley as a transit route to the Russian mining settlement Barentsburg. In this two months period, 7311 snowmobiles passed the radar, 51 % came from Longyearbyen, suggesting that most traffic was on a daily base. 123 avalanches (61 % of the total amount observed in winter 2008/2009) released along the snowmobile track "Little Round" in the period when the traffic counting radar was operating. From these 123 avalanches, 29 % released along the snowmobile track that is used, coming and going to Longyearbyen, when passing the radar. Thus most traffic during winter and spring took place in the most active avalanche period.

In the period 2000 – 2009, five people died in avalanches in Svalbard and many others had narrow escapes. Recently, on 20 January 2012, a slush avalanche released in the valley Vannledningsdalen and destroyed a pedestrian bridge in Longyearbyen (Figure 9b, d); another slush avalanche crossed the main road to the airport. On 14 May 2012 three cornice fall avalanche released on the mountain Gruvefjellet, two of them buried the road between Longyearbyen and Nybyen 20 m wide and 1 m high (Figure 1, Figure 5). However, to date, there is no avalanche warning system established in the Longyearbyen area, but increasing numbers of fatalities and infrastructure loss, along with increasing numbers of inhabitants and tourists demand basic avalanche research as a basis for future forecasting.

6. Snow avalanche research history in Svalbard

Historically, the interest in avalanches in Arctic regions was more a geomorphological one. Avalanches were studied amongst other periglacial slope processes of apparently more scientific interest like debris flows, rock falls and solifluction (French, 2007). Therefore, there are a number of studies on the geomorphological impact of avalanches in Svalbard.

Jonas Åkerman carried out a periglacial slope process monitoring in Kapp Linné, on the western tip of Isfjorden (Figure 4). In his paper on talus morphology and processes, Åkerman (1984) noted avalanche sedimentation as a result of sediment-rich avalanches, with the highest frequency at a late phase of the snow melt period. This was also found by Marie-Françoise André, a French geomorphologist, who described in greater detail the geomorphologic work of spring avalanches (André, 1990). However, she found no convincing evidence of the significance of avalanches as sediment transport agents, as annual avalanches only slightly reshaped talus slopes, yet major episodic slush avalanches did create substantial boulder tongues (André, 1990). André (1996) also put this conclusion forward in a paper on the geological control of slope processes in northwest Spitsbergen. Still, from these episodic slush avalanche events, André found geomorphologic evidence and came up with a recurrence interval of 80-500 years for major events (André, 1995).

Slush avalanches were of great interest for researchers between the 1970s and 1990s. Two papers by German geomorphologists, that carried out a Svalbard expedition in 1972, focused on extensive debris flow and slush avalanche activity in Longyeardalen after heavy precipitation (Thiedig and Kresling, 1973; Thiedig and Lehmann, 1973). Thiedig and Lehmann (1973) concluded that during snowmelt or heavy precipitation and the continuous permafrost preventing rain or meltwater from draining into the ground, favourable conditions for slush avalanche release were met. Slush avalanches were also mentioned by Jahn (1976), a polish geographer, who described them as a type of mass movement that are a distinct geomorphologic factor of Arctic slopes. The author defined slush avalanches as a flowage of water-saturated snow along stream courses during the spring snow melt. Because of the transport of soil debris and rock by slush avalanches, characteristic talus fans deposit (Jahn, 1976). In the mid 1980's, the Swedish geomorphologist Anders Rapp published a paper on extreme rainfall and rapid snowmelt causing mass movements in central Svalbard (Rapp,

1985). He mentioned that slush avalanches are relatively frequently repeated with return periods between several years and some decades, and are restricted to fixed tracks. Slush avalanches were later also mentioned in a publication by Scherer et al. (1998), who observed them during a German Expedition in northern Svalbard. They were particularly interested in the meteorological and snowpack conditions prior to the slush avalanches, and concluded that the crucial elements for a release due to snowmelt are the timing of energy input and meltwater flow through the snowpack (Scherer et al., 1998). Slush avalanches were also very briefly mentioned by Winther et al. (2003) in their review of snow research in Svalbard. The authors state that most research on snow has been performed in the late 20th century on snow distribution, snowmelt, snowpack characteristics and remote sensing of snow rather than avalanches (Winther et al., 2003).

Snow distribution became of interest for one researcher from the University Centre in Svalbard (UNIS). Christian Jaedicke conducted research in his PhD thesis (Jaedicke, 2001) and in several publications on drifting snow and snow accumulation in complex Arctic terrain. He investigated the snow drift losses from valleys to the open sea and found these to be of minor influence for the valleys water balance (Jaedicke, 2002). Jaedicke's snow drift model supported the idea that most glaciers in central Svalbard gain their mass as a result of their leeward aspects (Jaedicke, 2001) (Figure 4).

Another specific type of avalanche, the cornice fall avalanche, was first mentioned by Humlum et al. (2007), when they introduced avalanche-derived rock glaciers. This particular rock glacier type forms by the supply of rock debris and snow from avalanches, that are released by collapsing cornices.

It took almost 50 years, from the first mentioning of an avalanche in Svalbard by Mrs. Balstad (Balstad, 1956) until Erik Hestnes, snow and avalanche researcher from the NGI proposed that Longyearbyen be developed into a expanding centre of Arctic education and tourism and several geohazards interfere with the infrastructure (Hestnes, 2000). He also highlighted, that skiing and snowmobiling might be hazardous in certain periods. As principal problems, Hestnes for example identified drifting snow to have negative consequences for visibility, determining snow accumulation around infrastructure as well as the increase in avalanche danger (Hestnes, 2000). Hestnes furthermore concluded, that to prevent accidents, evacuation and relocation of people, closing of roads, skiing areas and snowmobile routes should be done by qualified personnel, able to evaluate the hazard.

In 2003, Jonas Ellehauge, a Danish MSc. student at the University Centre in Svalbard studied the influence of meteorological and topographic conditions on avalanches in the Longyearbyen area (Ellehauge, 2003). Ellehauge was the first to establish a winter and spring avalanche-monitoring program, where all observations were stored in a database. This was the start of the Cryoslope project 2006-2009, and the initiation of my PhD work.

7. Methodology

This PhD study is built entirely on field based methods. The periglacial slope and snow process monitoring included direct field observations as well as running and maintenance of field instruments. During the four years of the PhD project (2009-2012) including 2008, when I worked as a field assistant for the Cryoslope Svalbard research project, I spent a total of 159 days in the field (Figure 11). According to UNIS field safety regulations, a field party always contained two persons. In the following the different methods I used are explained in more detail.

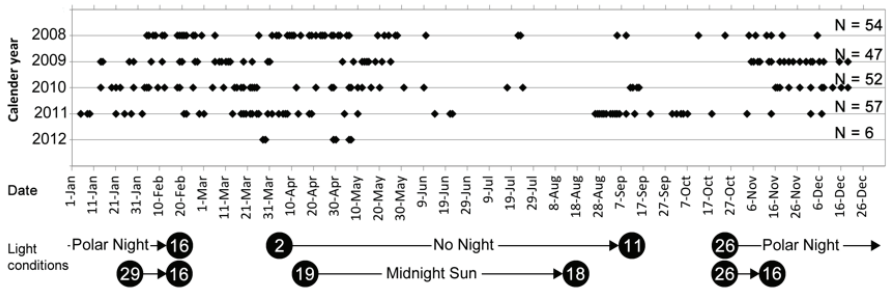

Figure 11: Timing of the fieldwork that this thesis is based on during 5 calendar years from 2008 to 2012. In spring 2012 (January – April) I did an exchange visit to Montana State University. Fieldwork was also carried out during the rest of 2012, but data is not included in this thesis.

7.1 Manual field snow avalanche monitoring

Avalanche activity was monitored from the snow season 2006/2007 to 2009/2010 along the snowmobile route "Little Round", as well as on the glacier Larsbreen, situated in the valley Longyeardalen (Figure 5). Some additional observations were carried out in the snow seasons 2010/2011 and 2011/2012, with a large focus on the Nybyen and Larsbreen slope systems (Figure 12). Photographs and GPS positions (avalanche snow-debris front) were collected for every single avalanche and the date and time of the event as well as the observation were noted. The avalanche type, trigger mechanism and their spatial extent, including release point elevation, slide distance, vertical fall height, debris width, length and area were determined and put into the Cryoslope Svalbard database. Additionally, slope aspect, curvature and angle were noted at the avalanche release site. Now, 824 avalanches are in the Cryoslope Svalbard database, with the last entry made on 1 June 2010. All avalanche observations were carried out

according to the observation guidelines by the American Avalanche Association (Greene et al., 2004). For more detailed studies on the topographic parameters of avalanches, the field estimations were revised by drawing the outlines of the avalanches in ArcGIS.

7.2 Manual field snow cover monitoring

Manual field snow cover monitoring was carried out from the snow season 2008/2009 to 2010/2011 along the snowmobile route "Little Round", most extensively at Gangskaret, as well as on the glacier Larsbreen, situated in the valley Longyeardalen (Figure 5). At each snow pit location, full profiles and stability tests were carried out. A full snow profile included excavating a pit down to the ground surface, investigating temperatures and layering. Snow temperatures were measured every 10 cm and at standard height of 1.5 m above snow surface. Single snow layers were identified and their characteristics, including crystal form and size, hand hardness and water content, noted. Special emphasis was given to notable weak layers in the snowpack, with large, poorly bounded snow crystals. In these pits, stability tests, to identify weak layers and their fracture propensities, were carried out. I used both the Compression Test (CT) (Jamieson, 1999) and Extended Column Test (ECT) (Simenhois and Birkeland, 2009) to evaluate the snowpack stability. In performing these tests, a snow column was cut out from all sides and increasing loading steps by hitting on top of the column were applied. If a fracture in a weak layer occurred, the loading step was noted, together with the shear quality of the fracture. The ECT test in addition provided information on the fracture propagation potential of a weak layer, needed for a slab avalanche to release. At various sites, wooden stakes, with miniature temperature loggers (iButtons (Lewkowicz, 2008)) were installed at 10 cm spacing from the ground surface upwards, to measure the thermal properties of snow and its interaction with the ground and atmosphere temperatures over an entire snow season (Figure 12g). These snow stakes were also used to calculate the local snow depth at any time through the snow season. iButtons were also installed on the Gruvefjellet plateau edge, on one vertical boom and two horizontal booms of a temperature logging construction (TLC), to monitor the seasonal cornice dynamics in great detail (Figure 12g). All snowpit observations were done according to the observation guidelines by the American Avalanche Association (Greene et al., 2004).

7.3 Automatic time-lapse photography and shock logger monitoring

Automatic time-lapse cameras from the company Harbotronics, equipped with a intervalometer (DigiSnap), an internal battery pack and a solar charger were installed at several locations along the "Little Round" snowmobile track (Figure 12a, b, c, d). Typical photo intervals ranged between 1 and 6 photos per day. These cameras provided useful information on snow cover duration and depth (Christiansen, 2001), quantifiable in combination with the iButton snow stakes. At the two slope systems, Larsbreen and Nybyen, the time-lapse cameras provided accurately the release timing of cornice fall avalanches (Figure 12a, c, d).

High sensitivity miniature shock loggers (TGP-0605) from the company TinyTag, recording any acceleration in the range from 0 to 5g, perpendicular to the surface of the box were installed at the Nybyen and Larsbreen slope systems (Figure 12e). The shock loggers were screwed directly onto large boulders in a vertical transect on an avalanche fan at Larsbreen, and a horizontal transect, spanning over five avalanche fans, at Nybyen. With the addition of the time-lapse photography, very accurate cornice fall avalanche timing could be determined.

7.4 Manual snow avalanche sedimentation quantification

Avalanche sedimentation was quantified by the use of permanently deployed sediment traps (16 m^2 plastic sheets) (Figure 12f) or the use of 4-8 m^2 large snow inventories on melting avalanche deposits at the Nybyen and Larsbreen slope systems (Figure 5i, h) (Luckman, 1978b). All rock sediment within the traps or snow inventories were collected and weighed. The snow inventories had to be carried out on melting avalanche snow deposits, freshly exposing the transported sediment. A clear avalanche-snow boundary with the underlying previous years sedimentation was needed to correctly quantify the winter's avalanche sedimentation. This work was thus mainly done between mid June to late July at both Nybyen and Larsbreen, when snow melting had progressed significantly. The permanent sediment traps were emptied in September, when all the avalanche debris had melted out at Larsbreen. Avalanche sedimentation was quantified at Nybyen and Larsbreen for up to eight years, with my contribution

between 2008 and 2012. Both locations belong to the highly instrumented and monitored sites, including frequent field monitoring, automatic time-lapse photography and shock logger monitoring (Figure 12).

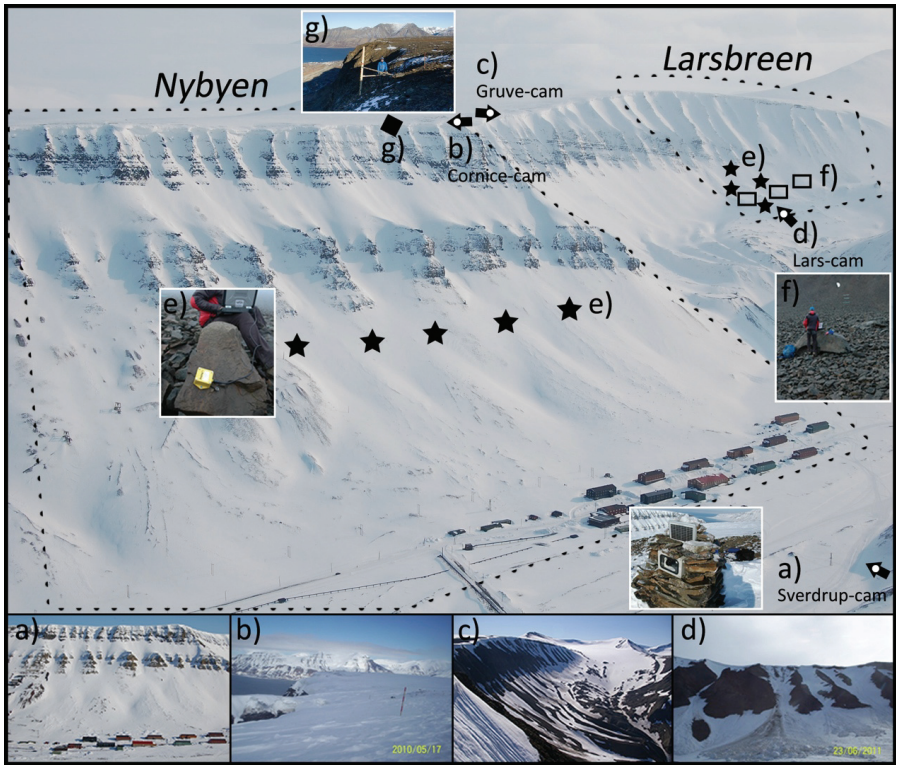

Figure 12: Photo of the key study sites Nybyen and Larsbreen. a) Example photo from the automatic time-lapse cameras a) Sverdrup-cam, b) Cornice-cam, c) Gruve-cam, d) Lars-cam. e) Miniature shock loggers, screwed onto rocks on a horizontal (Nybyen) and vertical (Larsbreen) transect. f) Permanently deployed, 16 m^2 large sediment traps. g) Temperature recording construction (TRC) with miniature temperature loggers (iButton) placed with 10 cm spacing on a horizontal and two vertical booms.

7.5 Cornice dynamics monitoring

Cornice dynamics monitoring was carried out on the Gruvefjellet plateau edge above the Nybyen slope system. Former Cryoslope Svalbard MSc.-student Stephan Vogel helped to establish this site. The automatic time-lapse camera setup includes one camera taking pictures from the opposite valley side towards the plateau edge (Sverdrup-cam) and the slope beneath, while the other camera is placed on the plateau edge, perpendicular to it (Cornice-cam) (Figure 12a, b). Snow stakes in front of the Cornice-cam

helped to quantify the size and extent of the cornice throughout the snow season. To get more high-resolution data, I installed snow stakes with iButtons on the plateau edge (TRC, Figure 12g), to monitor cornice accretion and melt dynamics. Additionally, temperatures at the ground surface for studying the cornices' role in frost weathering and sediment plucking, as well as its internal temperature gradients, responsible for deformation in the form of tension cracking and downslope creep, were installed.

7.6 Meteorological data

Three meteorological stations were used in my PhD project. The official meteorological station of Longyearbyen is located at the airport, on a raised marine beach, 28 m a.s.l. around 200 m from the fjord (Figure 5a). It records hourly, standard meteorological data, freely available through the e-climate service of the Norwegian Meteorological Institute (met.no).

The Gruvefjellet meteorological station is owned by UNIS established in the central part of the Gruvefjellet plateau mountain at 464 m a.s.l. in August 2001 (Figure 5b). Due to its location, the station records the regional airflow with only minor topographical disturbance, recording hourly, standard meteorological data, as well as permafrost data to a depth of 5 m (since 2008). The station is online on the UNIS webpage, where also historical data can be downloaded.

The Gangskaret meteorological station was established on a mountain pass at 441 m a.s.l. in February 2008 by the Cryoslope Svalbard project (Figure 5c). Due to its inland location, the instruments record a higher degree of continentality than the other two stations with lower average air temperatures and higher maximum precipitation rates. This station records hourly, standard meteorological data at standard height as well as at 10 m above ground.

8. Results

In the following, short summaries of the papers included in this PhD thesis are given.

8.1 Eckerstorfer, M., Christiansen, H.H. 2011. AARE.

The "High Arctic maritime snow climate" in Central Svalbard. Arctic, Antarctic and Alpine Research. 41/1. 11-21. doi: 10.1657/1938-4246-43.1.11.

Worldwide, three main snow climate types are established; maritime, continental and transitional (McClung and Schaerer, 2006). This classification is mainly based on characteristics of the snowpack like snow depth, layering, and most common snow crystal forms and weak layers, influenced by the dominant meteorological patterns in a mountain area. In central Svalbard, no such snow climate classification exists, but avalanche forecasting is based on weather observations and the investigation of structural weaknesses in the snowpack. Knowing the type of snow climate thus provides important knowledge about the avalanche regime.

During the course of two snow seasons, 2007/2008 – 2008/2009 we dug 109 snow pits in different valleys, aspects and altitudes along the "Little Round' snowmobile track (Figure 5). Meteorological and avalanche observations were also collected in both snow seasons.

Our results show that due to the very slow onset of the snow cover in autumn, large temperature gradients within the snowpack favour rapid constructive metamorphism, resulting in the growth of depth hoar. Depth hoar comprised 15 % of the entire snowpack in both observation seasons. Due to the large, cup-shaped snow crystals rather poor ability to bond, depth hoar is regarded as a weak layer that is very persistent in time. In both snow seasons, depth hoar was the most observed weak layer in the snowpack, thus also the lower third of the snowpack was regarded as the weakest. The second most observed weak layer was comprised of faceted crystals, forming above ice layers, dominantly found in the middle third of the snowpack.

The continuous permafrost in the study area influences mainly the bottom snowpack temperature, by keeping it cool. Due to large air temperature fluctuations in winter and a steady cold ground, large temperature gradients are created in the upper and middle parts of the snowpack, enabling the growth of weak, faceted snow layers.

In conclusion, the snowpack in central Svalbard is generally cold, thin and spatially highly variable in depth. The snowpack has a weak base consisting of depth hoar, overlain by wind slabs and ice layers. The ice layers are due to the significant maritime influence, which makes Longyearbyen the warmest place in the High Arctic. We therefore propose in this paper an additional snow climate called the "High Arctic Maritime Snow Climate". Although it has some continental characteristics, the maritime influence is most dominant.

8.2 Eckerstorfer, M., Christiansen, H.H. 2011. Geomorphology.

Topographical and meteorological control on snow avalanching in the Longyearbyen area, central Svalbard 2006-2009. Geomorphology. 134. 186-196. doi:10.1016/j.geomorph.2011.07.001.

Avalanche activity and its characteristics largely depend on the meteorology and topography of an area. The ability to understand and predict seasonal avalanche activity patterns, dominant types and meteorological triggers are key factors necessary for developing avalanche forecasting and assessing future avalanche activity.

In this study, we used data from the Cryoslope Svalbard research project database and analyzed the three snow seasons 2006/2007 – 2008/2009. In this study, we characterize the avalanche regime in Svalbard for the first time.

Out of 824 avalanches in the database, a total of 423 avalanches were analyzed, being larger than 100 m^3 in their debris extent. Our results show that the most dominant avalanche type are cornice fall avalanches, with 45.2 % of the total. This is due to the dominant plateau mountain topography and a prevailing winter wind direction from SE, forming cornices on the NW-facing, leeward plateau ridges. These cornices eventually fail, triggering cornice fall avalanches on the slope beneath. There is a clear seasonal pattern in avalanche activity due to their dominance and delayed release timing, towards May / June. Only minor activity takes place in autumn and early winter when only small snow amounts are accumulated. The majority of releases are from April onwards, when maximum amounts of snow exist in the landscape. During cold, stable high-pressure periods, lasting up to 4 weeks, avalanche activity is slowed down to an absolute minimum. Maximum avalanche activity was observed during and shortly after snowstorms, induced by passing low-pressure systems. In the three years observation period, we counted 19 major avalanche cycles, in which 80 % of all observed avalanches released.

As the cornice fall avalanches are largely topographically controlled, we expect only a minor shift in the future avalanche type distribution in a future changing climate. Due to a projected decline in low-pressure systems generated in the North Atlantic in a warming climate (Zahn and von Storch, 2010), these storm-induced avalanches will decrease. Thus cornice fall avalanches will become a more pronounced natural hazard for Longyearbyen.

8.3 Eckerstorfer, M., Christiansen, H.H. 2011.CRST.

Relating meteorological variables to the natural slab avalanche regime in High Arctic Svalbard. Cold Regions Science and Technology. 69. 184-193. doi:10.1016/j.coldregions.2011.08.008.

Natural dry slab avalanche releases are of special interest from a geohazards point of view. This type of avalanche releases without artificial stress increase on a weak layer buried in the snowpack. Rather a stress increase due to a natural loading process during new precipitation, wind loading or air temperature fluctuations is responsible for their release.

We therefore studied the four major meteorological variables air temperature, wind speed, precipitation and snowdrift for 0, 24, 48 and 72 hours prior to an avalanche and a non-avalanche day.

The avalanche dataset used for this study came from the Cryoslope Svalbard Research project database, including 156 natural dry slab avalanches that released on 20 avalanche days from 2007 to 2010. We used a Wilcoxon rank sum test and linear regressions to determine the meteorological variables that could best predict an avalanche day.

Minimum, maximum and average wind speeds were significantly higher on avalanche days than on non-avalanche days, therefore being good discriminators of avalanche and non-avalanche days. The best possible meteorological predictor variables were though sums of precipitation and snowdrift, 24, 48 and 72 h before an avalanche day. While precipitation was measured directly, snowdrift is a product of sum of hourly precipitation and average wind speed to the fourth power. The results are logic for the high arctic barren landscape, were natural dry slab avalanche activity is highly controlled by wind activity. Still, the avalanches released equally in all slope aspects, since their release is also largely controlled by the internal structure of the snow pack (e.g. occurrence of a weak layer).

8.4 Eckerstorfer, M., Christiansen, H.H. 2012. PPP.

Meteorology, topography and snowpack conditions causing two extreme mid-winter slush and wet slab avalanche periods in High Arctic maritime Svalbard. Permafrost and Periglacial Processes. 23. 15-25. doi:10.1002/ppp.734.

Slush avalanches are a type of wet avalanche, frequently releasing due to intense spring melting in the Arctic. In this paper, we report on two extreme mid-winter slush avalanche and wet slab avalanche periods due to rain on snow events (Figure 3c). Both extreme cycles resulted from slow passing low-pressure systems, with air temperatures several degrees above freezing and 100-year record monthly rainfall.

The slush and wet slab avalanches released due to a decrease in snowpack strength induced by water from rain percolating through the snowpack and being blocked by an existing ice layer. This ice layer then got further lubricated until a loss of friction caused the releases.

Prior to both extreme events, end of January 2010 and mid March 2011 favourable snowpack conditions existed for wet snow avalanche releases. A coarse-grained snowpack allowed rapid water infiltration and a for water impermeable ice layer, acted as the sliding plain. With the absence of such ice layers, percolating water would have been blocked by the frozen ground, still the avalanches could have entrained some sediment.

In both cycles, the wet snow avalanches started very likely as wet slab avalanches. Some wet slab avalanches released into narrow river gorges thus blocking the gorge exits, so the water level in the snowpack could rise sufficiently to consequently release a slush avalanche. These slush avalanches were confined solely to these river-cut gorges with a lower starting zone inclination then the wet slab avalanches, and with deposits consisting of flow lobes and levees. During both extreme cycles, the wet snow avalanches were extreme in their sizes and runout distances. Wet snow avalanches crossed the snowmobile track at several locations along the Little Round, burying it, in places, up to several meters deep.

To assess the possibility of future wet snow avalanche activity in a warming climate we studied the almost 100-year-old meteorological record existing from the Longyearbyen airport meteorological station. We identified four potential wet snow avalanche cycles with meteorological conditions, being maximum amount of precipitation and maximum air temperature continuously over at least 24 hours similar to the actual observed ones. These four potential cycles cluster in the mid to early 1990s. A

correlation between mean winter temperatures and potential wet snow avalanche cycles was, however, not found. Moreover, the frequency and duration of low-pressure systems are the dominating controls.

8.5 Vogel, S., Eckerstorfer, M., Christiansen, H.H. 2012. TC.

Cornice dynamics and meteorological control at Gruvefjellet, Central Svalbard. The Cryosphere. 6. 157-171. doi:10.5194/tc-6-157-2012.

This paper is the result of Stephan Vogel's MSc.-thesis at the University Centre in Svalbard and the University of Oslo. I took part in designing the project, co-supervised Stephan and helped him with fieldwork. I contributed to the data analysis, construction of figures and writing of the manuscript.

Cornice fall avalanches had been identified as the dominant type in central Svalbard, endangering infrastructure and travelling in and around Longyearbyen (Paper 4). We therefore chose to monitor the seasonal snow dynamics and their meteorological control of a cornice on the plateau edge of Gruvefjellet, right above Nybyen during the period 2008-2010 (Figure 12). The aim was to get more insight into the dynamical response of cornices and their collapse to meteorological influence.

The monitoring setup included two automatic time-lapse cameras in combination with snow stakes, manual crack width measurements and frequent field visits to the plateau. Our results show that the cornice accreted when wind speeds averaged 12 m/s, blowing towards the plateau edge. Scouring took place when winds blew against the cornice exceeding maximum speeds of over 30 m/s.

Several cornice tension cracks between the snowpack on the plateau and the cornice mass were observed, leading to a complete detachment of the cornice. These tension cracks then linearly opened with a rate roughly between 0.5 and 1 cm per day, simply due to snow creep. Four observed tension cracks resulted in full cornice collapses, after two to five weeks when the crack was first observed. Due to their overhanging mass, these cornices got pulled down by gravity and failed, releasing cornice fall avalanches. A total of 180 cornice fall avalanches was observed, their size was largely determined by the size of the cornices that collapsed. The amount of snow on the slope did not play a role in the actual cornice fall avalanche size. No significant distinction in meteorological conditions between avalanche and non-avalanche days could be made; this relationship still remains elusive. However, the majority of cornice fall avalanches released in the period May-July at the very end of the snow season.

8.6 Eckerstorfer, M., Christiansen, H.H., Vogel, S., Rubensdotter, L. 2012. ESPL.

Snow cornice dynamics as a control on plateau edge erosion in central Svalbard. Earth Surface Processes and Landforms.

The cornices on the leeward plateau edge of Gruvefjellet are annual cornices. During field visits in several summers we had noted that the rock sediment on the plateau edge was freshly weathered, and unlike the rocks of the blockfield on the plateau, free of lichens. We moreover observed rock debris incorporated into cornices, visible in open tension cracks during winter fieldwork. These observations lead to the study on the erosional significance of cornices. Moreover, the dynamics causing tension fractures between the plateau snowpack and cornice had not yet been studied in great detail. Therefore we instrumented the plateau edge with a profile of ground surface temperature loggers and a miniature temperature logger stake (Figure 12g), to be buried by the cornice for snow temperature observation. Together with an automatic time-lapse camera (Figure 12b), we could thus monitor the seasonal cornice dynamics and its control on backwall weathering and erosion in great detail.

Our results show, that a vertically fully accreted cornice was in place after the first snowstorm, and it reached its horizontal maximum extent in April. Tension cracks opened due to differential creeping rates between accretion layers, resulting in high shear stresses between the plateau snowpack and the cornice. Once these tension cracks opened further, we could observe rock sediment incorporated into the cornice mass. This rocky sediment was released on the slope below either when the cornice collapsed or melted. We found that, due to autumn rain and spring cornice-melt, water is supplied to the loosened rocks on the plateau edge. When the cornice is in place for eight months, the backwall ground surface underneath the thickest part of the cornice remains in the frost-cracking window, efficiently enabling frost cracking by ice segregation. This weathered sediment is incorporated in the cornice during its onset and plucked out, once a tension crack opens and the cornice deforms downslope. Therefore, the cornices favour conditions for frost weathering and actively erode the plateau edge and transport the weathered sediment downslope. The weathered sediment also falls down after the cornice melts away in late spring. A highly actively weathered plateau edge becomes visible in summer, unlike places without seasonal cornices.

8.7 Eckerstorfer, M., Christiansen, H.H., Rubensdotter, L., Vogel, S., Siewert, M. subm. JGR-ES.

The role of cornice fall avalanche sedimentation (in the valley Longyeardalen, central Svalbard). Journal of Geophysical Research – Earth Surface.

The quantification of the geomorphological work of rapid slope processes is of importance when studying the alpine sediment cascade and the overall landscape evolution in alpine areas. The role of snow avalanches as sediment erosion, transportation and accumulation agents is often underrated, and ranked behind rock fall and debris flows in their significance. As a result of avalanche sedimentation, quantifiable through the calculation of avalanche sedimentation rates (kg/yr or mm/yr) and rockwall retreat rates (mm/yr), avalanche fans form.

In the present past, a number of studies suggested that avalanche sedimentation by cornice fall avalanches on the NW facing slopes of the valley Longyeardalen is of high significance. Humlum et al. (2007) reported from a cornice fall derived rock glacier, having its root at the foot of the Larsbreen slope system. Siewert et al. (2012) calculated Holocene rockwall retreat rates and found that the rates from the NW facing slopes in Longyeardalen where 100 % larger then the rates on the opposite valley side. Furthermore, we investigated in Paper 6 the erosional effect of cornices on the plateau edges.

This paper therefore aims to quantify the geomorphological significance of cornice fall avalanches by recording cornice fall activity and quantifying avalanche transported rock debris at the Nybyen and Larsbreen slope system. We studied data from overall 13 catchments over a time period of maximum 7 years, using time-lapse photography for cornice fall avalanche activity monitoring and a direct method of rock debris quantification by permanently installed sediment traps (Figure 12f) and snow inventories.

The results show annual avalanche fan-surface accretion rates ranging from 8.2 to 38.7 kg/m^2 at Nybyen and from 0.8 to 55.4 kg/m^2 at Larsbreen. Correspondingly, the avalanche fan-surfaces accreted annually in a range from 3.65 to 13.60 mm/yr at Nybyen and from 0.29 to 21.41 mm/yr at Larsbreen. We also calculated rockwall retreat rates with an annual maximum of 0.94 mm/yr at Nybyen and 1.13 mm/yr at Larsbreen, with catchment specific annual rockwall retreat rates as high as 1.40 mm/yr at Nybyen and 5 mm/yr at Larsbreen. The annual maximum rockwall retreat

rates are comparable to the Holocene rates calculated by Siewert et al. (2012). These high avalanche sedimentation and rockwall retreat rates are due to the cornices producing avalanches with high rock debris content throughout the entire winter. The calculated rates are maximum rates, as rockfall, that does not make it onto the avalanche fans by itself, is also transported downslope by the avalanches.

We conclude in this study, that this process of cornice fall avalanche sedimentation must prevail throughout large parts of the Holocene, as the cornice fall derived rock glacier at the Larsbreen slope system is presumably of late Holocene age (<5000 years). We further conclude, that as cornice fall avalanches are the most dominant avalanche type in the Longyearbyen area (Paper 2), they are likely to be the dominant mode of sediment transport on any leeward slope.

9. Discussion and conclusion

9.1 Characteristics of the avalanche regime in central Svalbard – present, future, and up-scaling

The following points are the main characteristics that discriminate the present-day avalanche regime in central Svalbard from other avalanche climates in Arctic and Alpine regions. However, due to the novelty of the research and the lack of previous studies, the conclusions should be treated with care, as they are a result of a short observation period:

- A dominance of cornice fall avalanches due to the sedimentary plateau mountain topography and a prevailing winter wind direction (Paper 2, 5).
- A clear seasonal pattern in avalanche activity with a maximum amount of releases from March until July (Paper 2, 5). The main reasons are the slow onset of snow cover, with its maximum depth in April and the almost complete absence of cornice fall and loose snow avalanches during the early part of the snow season.
- The existence of a persistent depth hoar base (Paper 1), underlying the majority of the snowpack has not been observed to cause natural dry slab avalanching due to a very stress-resistant, hard middle part of the snowpack, consisting of meltforms and ice layers (Paper 3).
- The existence of continuous permafrost influences the snowpack only to a minor extent, by keeping the bottom part cool, allowing for large temperature gradients to form, when air temperatures rise (Paper 1). However, a direct effect of permafrost on snowpack stability could not be determined, which was also not found in a study by Phillips and Schweizer (2007) in the Swiss Alps.
- A comparably steep starting zone inclination for all avalanche types with a mean of 45 °, as well as for slab avalanches with 40 °. The reason might be the rather hard, stress resistant snowpack in general (Paper 2).
- A likelihood of mid-winter slush avalanching due to high intensity, slow passing low-pressure systems, with air temperatures well above freezing and record monthly amounts of rain, resulting in extreme avalanche events (Paper 4).
- Cold, stable high-pressure periods, when cold polar air masses extend over Svalbard lead to a significant decrease in avalanche activity.

- Cornice fall avalanches produce “dirty” avalanches, which are avalanches with high rock debris content throughout the whole snow season as a result of the sediment weathering and plucking processes of cornices.

The main conclusions about the present-day avalanche regime in central Svalbard are drawn from a dataset collected over a short period of time. Therefore, some of the conclusions can be seen as rather hypothetical, given that tiny changes in meteorological conditions could have drastic changes. The future climate in Svalbard is thus of special interest for future avalanche research and forecasting. Svalbard’s regional climate is recently much debated, due to the area’s sensitivity to changes (Houghton et al., 2001; Rogers et al., 2005). One set of predictions indicates significant warming and increase in precipitation, especially in the winter, up to three times more in the coming 100 years compared to the last 100 years (Førland et al., 2011). Humlum et al. (2011) on the other hand claim, that the observed late 20th century warming will not be continued and the climate will be highly variable with quite stable average air temperatures at the present level, for at least the next 25 years. In any case, warmer and wetter winters would generally lead to increased avalanche activity, as snow deforms faster in warmer conditions and more snow adds more load and thus stress onto the snowpack. A stable climate would obviously result in no significant changes. Both scenarios, however, would most likely not change the frequency of mid -winter slush avalanche extreme events, as we did not find any relationship between mean annual and snow season air temperatures, and their observed and potential occurrence (Paper 4). Both scenarios apply, however, in general to any avalanche regime worldwide. Nevertheless, the avalanche regime in central Svalbard is significantly different, as described above. The primary difference is the dominance of cornice fall avalanches, which is to a large degree determined by the topography, and less by meteorology. A study by Zahn and von Storch (2010) showed that the frequency of low-pressure systems is likely to decrease in the North Atlantic in a warming climate. This scenario could effectively reduce the avalanche activity in central Svalbard, as 80 % of all avalanches release in cycles induced by low-pressure activity (Paper 2). Such a climate change scenario would lead to a further increased dominance of cornice fall avalanches.

This first basic study on the avalanche regime in central Svalbard is confined to a roughly 17-km^2 large study area around Longyearbyen. This area is the most used part of the landscape regarding infrastructure and travel and has year-round field accessibility. Nevertheless, an up- scaling of the study area, and thus an up- scaling of the avalanche regime and snow climate towards the south to the mining settlements Svea and Barentsburg or the west coast at Kapp Linné, with its touristic infrastructure, is both interesting from a scientific point of view, as well as from a geohazards perspective. In the Central Tertiary Basin, stretching roughly north- south in Nordenskiöldland, the dominant plateau mountain topography (Figure 4) certainly determines the dominance of cornice fall avalanches. This plateau mountain topography is not entirely unique, as it also occurs in north-western Iceland, producing a distinct avalanche hazard (Decaulne, 2007). Both on the west and east coast of Nordenskiöldland, older bedrock are shaped into more alpine topography, where widespread, high-lying snow source areas are limited. Humlum (2002) modeled the late 20th century precipitation in Nordenskiöldland, and his results show a precipitation gradient with high amounts in the coastal areas and lower amounts in the interior. A vertical precipitation gradient was also found, being again higher at the coast than in the central parts (Humlum, 2002). However, amounts of precipitation can influence, but do not necessarily control avalanche activity. Especially at the west coast of Nordenskiöldland compared to its interiors, a larger fraction of the winter precipitation can be expected to fall as rain, due to a warmer more maritime climate. Rain on snow, depending on its intensity, has usually first a destabilizing effect, by building up a water table in the snowpack, before, once the free water freezes inside the snowpack, it stabilizes it again. The hard, middle part of the snowpack, consisting of meltforms and ice layers prevents avalanches from releasing. High intensity rain on snow events can obviously cause extreme wet avalanche cycles. I therefore suspect higher avalanche activity in the high grounds of the interior, where more precipitation falls as snow. This claim is supported by a more extensive glaciation in the interiors of Nordenskiöldland, where large cirque glaciers are situated in snowdrift lee positions, partly also fed by avalanches (Humlum, 2002; Humlum et al., 2007).

9.2 Avalanche forecasting

"Avalanche forecasting is defined as the prediction of current and future snow instability in space and time relative to a given triggering level for avalanche initiation." (McClung, 2002). If the destructive potential or effects of avalanches on humans and infrastructure are integrated, the term avalanche hazard forecasting is applied (McClung and Schaerer, 2006). To date, no such avalanche forecasting is in place in Longyearbyen. Only a project between the company K-SAT and the Red Cross Longyearbyen aims to assess the avalanche hazard on a mountain road. Avalanche forecasting can be done both on a regional and local scale (McClung, 2002). As there is only avalanche forecasting on a local scale, central Svalbard is in need of a regional-scale forecasting program as well.

Two types of information are necessary for avalanche forecasting (McClung, 2002): singular and distributional data, where the first is specific information to a case in question, and the second is information about similar situations in the past. To avoid bias, both types of data need to be included in avalanche (hazard) forecasting. Singular data includes one's opinion about current and future snow instability when entering avalanche terrain (McClung, 2002). Such knowledge only comes from experience, often bound to a specific terrain type and snow climate. For the Longyearbyen area, now, detailed basic research on how the special topographical (Paper 2, 5) and snowpack conditions (Eckerstorfer et al., 2012) (Papers 1,3,4), as well as the high arctic climate (Papers 1,2,4) and latitude (Papers 1,2,3,4) control avalanche activity is available. Such data is distributional data and examples can be rule of thumbs or statistical analysis to compare similar situations from the past with current data (McClung, 2002).

Not all data is equally relevant in the forecasting process. Moreover, data is ranked according to their relevance and ease of interpretation with respect to estimating instability (McClung, 2002). Whether an avalanche can start or not is determined by the instability of the current snow conditions. While snow with good stability can support additional (rapid) loading, snow with poor stability can fail with only little additional load.

Three classes of factors, with the last being the most relevant, are needed for avalanche forecasting: (LaChapelle, 1985; McClung, 2002; McClung and Schaerer, 2006):

Class III: Meteorological factors (precipitation, wind, temperature, radiation): This type of data provides only indirect evidence of current or future snow instability. Examples are amounts of new snow, wind speed and direction and air temperature fluctuations.

We have shown that low-pressure system induced air temperature fluctuations and increased wind speeds cause avalanche cycles with direct-action avalanching (Paper 1). High intensity low-pressure system passages resulted in mid-winter slush avalanching, due to rain on snow (Paper 4). For natural dry slab avalanches, sums of precipitation and snowdrift prior to avalanching provide possible meteorological predictor variables (Paper 3).

Class II: Snowpack factors (snowpack weaknesses and loads on them): This type of data provides information about the presence of weak layers and their strength. Examples are the depth and distribution of weak layers and their structural characteristics.

We have shown that persistent and non-persistent weak layers are found in the snowpack. Depth hoar, occurring as a persistent weak layer, underlies almost the entire snowpack, varying only in amount and structure mainly due to ground conditions (Paper 1). Due to frequent mid-winter rain on snow events, faceted crystals around ice crusts are the dominating, non-persistent weak layer in the upper two third of the snowpack (Paper 1).

Class I: Stability factors (relationship between downslope load on a weakness and strength): This type of data includes the relationship of loads on a weak layer and its fracture propensities. Examples are direct avalanche observations and snow stability tests.

Papers 1 to 4 are analyses of direct avalanche observations, while Paper 1 focuses on stability tests. Both sets of data were essential for this PhD study and showed for example, that no natural slab avalanche fractured on the most dominant persistent weak layer depth hoar (Paper 3). The reason is that the strength of the overlying snow layers, mostly meltforms and ice layers, exceeds any natural stress increase.

We studied the spatial variability in snowpack stability on a wind-affected slope in Fardalen (Eckerstorfer et al., 2012; Eckerstorfer et al., submitted). Experience suggests that shallow, steep zones on slopes are likely spots for artificially slab avalanche

triggering. We could find, that snowpack stability decreased significantly with decreasing slab thickness, which correlates to how deeply a weak layer is buried. Therefore the weakest spots on the slope coincided with the shallowest and steepest spots, such as topographic heights or large rocks.

All factors in these three classes are dynamic just as avalanche forecasting itself is dynamic. However, the topography is an integral part of every factor, as terrain induces variations in snow deposition patterns and insolation, determines the slope-parallel component in fracture initiation and creates avalanche terrain traps (McClung, 2002). Specifically in central Svalbard, we show in Papers 2 and 5, that topography significantly determines the avalanche type distribution, with cornice fall avalanches being the dominant type.

Topography also determines potential avalanche sizes, their preferred paths and runouts. The majority of slopes in the study area have an overall concave slope profile, as they valleys are of glacial origin. In 90 % of natural dry slab avalanching (Paper 3), the starting zone in the upper slope third had a convex curvature, favouring their release. Protruding rock noses intersect many slopes, dividing them into natural avalanche paths, which confines the size of avalanches. Moreover, due to the mostly wide-open runout zones in the valley bottoms, avalanche debris depths are small. However, deeply incised river valleys, moraines and talus rock glaciers are natural terrain traps, where large amounts of avalanche debris can pile up. The most prone locations for artificial, high consequence slab avalanche release are therefore narrow, steep river-cut gorges and couloirs close to ridgelines, that terminate in any kind of V-shape profiled bottom valley. Additionally, if the location is only a couple of kilometers away from Longyearbyen, and thus outside the mobile phone range, professional search and rescue can be significantly delayed. Areas prone to avalanche hazard on infrastructure and people are primarily located on and underneath leeside slopes with cornices on top. Also, locations at the mouth of river valleys with an upper basin, where slush avalanches can occur during spring melt and mid-winter rain–on-snow events, are prone to avalanching (Eckerstorfer and Christiansen, 2010).

9.3 Snow and avalanche field monitoring setup. Standards and recommendations

Periglacial slope process monitoring depends on the following points:

- Easy year-round field accessibility to periglacial slopes, provided by UNIS' location in Longyearbyen and a field area around town, with the key sites in the valley Longyeardalen.
- Being permanently situated at UNIS as an internal PhD student, thus being able to conduct fieldwork year-round.
- Frequent avalanche and snowpack observations during the snow season, at least two times per week on snowmobile and skis.
- Avalanche and snowpack observations according to international standards, provided by the American Avalanche Association (Greene et al., 2004).
- A field technician and several MSc students for help with observations and instrumentation as well as for safety measures (avalanches, polar bears).
- A network of meteorological stations in a transect from the coast to the mountains further inland.
- A network of instrumentation like automatic time lapse cameras for avalanche activity and cornice dynamics observations, miniature temperature logger arrays for snowpack, ground surface and air temperature evolution and miniature shock loggers for avalanche activity recording at key sites.

Based on my 5 years experience in slope process monitoring in a periglacial environment, my recommendations for future basic research in this field are:

- Concentration on already identified key sites for cornice dynamics, slush avalanche, slope scale snowpack stability and avalanche sedimentation monitoring.
- Introduction of an additional study site, for comparison, in a different bedrock zone, with slightly different climate (e.g. Kapp Linné).
- Slope process monitoring with a higher frequency by installing more automatic time lapse cameras and miniature shock loggers or seismic sensors (van Herwijnen and Schweizer, 2011) and increase in manual field observations by an increase in manpower. A field technician, planning fieldwork and maintaining field instruments throughout the whole year would be valuable. Additionally, 1 – 2 UNIS

PhD students, permanently located in Svalbard would ensure monitoring with high temporal resolution.

- Use of new technology like Terrestrial Laser Scanning (TLS), Satellite Synthetic Aperture Radar (SAR) and Ground Penetration Radar (GPR). With the TLS method, the cornice dynamics could be monitored and quantified in great detailed. Within the last years, TLS has made it possible to measure snow surfaces with high spatial and temporal resolution, even in high complex alpine terrain (Bremer and Sass, 2012; Prokop, 2008; Wirz, 2011). It will therefore be possible to quantify the relationship between the collapsed cornice volume and the resulting avalanche debris volume, given the amount of snow on the slope. This will enable a calculation of maximum avalanche run-out scenarios, crucial for avalanche forecasting. As the cornices are also efficient erosion agents, using the TLS, will enable to access annual rock erosion rates and avalanche fan sedimentation rates in great detail, by comparing high-resolution digital elevation models of the slopes on a yearly basis.
- The use of InSAR (polarimetry and backscatter time series analysis) would enable a significantly improved understanding of periglacial landscape sensitivity to meteorological variables and a monitoring at landscape scale (Liu et al., 2012). Another challenge would be to monitor seasonal vertical change in ground, by avalanche sedimentation, using the InSAR technology.
- The physical characteristics of the snowpack, its spatial distribution and temporal evolution could be significantly better monitored than performed in this thesis, by the use of TLS as well as GPR (Schaffhauser et al., 2008). Especially upward-looking ground penetration radar could provide high temporal resolution data on snow stratigraphy, particularly in wet snow conditions during rain on snow events (Mitterer et al., 2011). With additional measurements of snow density and snow water equivalent, by the use of snow probes and snow tubes, the likelihood of slush avalanche releases could be determined.

By concentrating on key areas, increasing the scientific and technical personnel and improving the technical instrumentation, central Svalbard could become a model region for basic research on seasonal snow pack dynamics, avalanche activity and their geomorphological impact. Furthermore, improved knowledge on how snow controls periglacial slope processes like different types of avalanches, but also rock glaciers,

solifluction and rockslides, could be obtained. In the end, the response of snow dynamics and its interannual variability in a changing climate could be studied in great detail and taught in various highly specialized courses at UNIS. Moreover, a better understanding of all the process dynamics involved would form the basis needed for the development of any future regional avalanche warning in the Longyearbyen area.

9.4 Periglacial processes and paraglacial slope adjustment

Avalanches, especially dirty snow and slush avalanches, are recognized as important geomorphological agents in periglacial landscapes, where relief, climate and lithology are favourable. Therefore the studies of the avalanche dynamics in Longyeardalen adds to the understanding of classic concepts in periglacial geomorphology: rock weathering, erosion and transport, associated with periglacial landscape / landform evolution. Periglacial geomorphology deals with landscape evolution due to frost action (French, 2007). More refined, French and Thorn (2006) defined periglacial to be associated with seasonal and perennial ice. However, the definition of a landscape is a rather diffuse one (Berthling and Etzelmüller, 2011). In its most simple sense, the landscape is a grouping of individual landforms (Berthling and Etzelmüller, 2011). The importance of long term, large-scale landscape evolution by periglacial processes is questioned (André, 2003). While major glaciations determine landscape evolution on large time and spatial scales, periglacial processes act normally on a much smaller time and spatial scale (Berthling and Etzelmüller, 2011). Gullies and incisions, created under paraglacial conditions thus can be rather short-lived landforms, whose activity stops once the water source is extinct (André, 2003; Ballantyne and Benn, 1994). In northwest Spitsbergen rock glacier fronts show a decrease in clast size from their fronts to the supplying backwall (André, 2003). While the largest boulders have been delivered during rock glacier initiation about 3500 – 4000 yr BP, the smallest clasts were provided during the end of the Little Ice Age (André, 2003). Since then, many rock walls have been colonized by lichens, and undergo slow modern biogenic flacking, leading to a triple-rate increase in rockwall retreat (André, 1997). This is confirmed by Rapp (1960b), who found also a major discrepancy between very small contemporary rates, and significantly higher Holocene rates, inferred from the volume of the talus cones and associated rock glaciers in the Tempelfjorden area, Spitsbergen.

However, there are also examples of long time scale and large spatial scale periglacial landscape evolution for example from Siberia. The massive ground ice body, being of glacial origin at Yukorski Peninsula is preserved by the permafrost throughout several interglacials (Eemian and Holocene) as well as several Saalian and Weichselian interstadials (Ingólfsson and Lokrantz, 2003). Also the nivation landforms, both erosional niches and associated depositional fans of up to early Weichselian age, periglacially transformed the Saalian glacial landscape in southwestern Jutland, Denmark (Christiansen, 1997). The concept of nivation includes the different forms, processes and sediments associated with and intensified by the accumulation and melting of snow (Christiansen, 1998). Nivation is particularly effective at seasonal and perennial snowpatches and at avalanche sites with unconsolidated sediments. This nivation concept applies therefore for the process of cornice fall avalanche sedimentation in the Longyeardalen valley. Nivation is on a large scale controlled by a prevailing snow-bearing wind direction and a large fraction of precipitation falling as snow. The topographical conditions are the weathered sediments on the plateau edge and the gently sloping plateau edge topography, enabling large cornices to accrete. Applying the High Arctic nivation process-form-sediment model, established by Christiansen (1998) permits the quantification of all nivation process rates (Paper 7), and the reconstruction of palaeo wind directions and potential periods of snowdrift activity. Finally, applying the model could provide a better understanding of potential changes in snowfall and prevailing wind directions caused by a changing climate.

In central Svalbard, in paper 7, we concluded, that due to active backwall erosion of the plateau edge of leeward facing rock slopes by cornices, rockwall recession is larger there than on the opposite sides. The cornices favour the active weathering and erosion of the plateau edge bedrock. In the cornice environment an important interplay occurs between the cryotic surface, being snow covered by cornices, the subsurface permafrost affected thermal regime and the geomorphological process of plucking rock debris. Thus, the concept of cryo-conditioning, recently introduced by Berthling and Etzelmüller (2011), applies to the processes described above and studied in papers 6 and 7. Cryo-conditioning is the interaction of a cryotic surface with a subsurface thermal regime and geomorphological processes (Berthling and Etzelmüller, 2011). As these authors argue that cryo-conditioning bridges the gap between small-scale processes and large-scale landscape development, the geomorphological work of cornices is a good example. We could show in paper 7 that even after the early Holocene

deglaciation of the hill slopes in Longyeardalen (Svendsen and Mangerud, 1997), the present-day rockwall retreat rates are higher than the Holocene ones. This is in clear contrast to the conclusion of the studies by André (1997; 2003). Also Ballantyne (2002) argues, based on a literature review, that large volumes of rock fall accumulation are inconsistent with low present-day rates, inferring high rates right after deglaciation as part of the paraglacial adjustment right after deglaciation. However, he discusses that especially debris-mantled slopes are due to high erosion rates by avalanches and debris flow, reworking the slopes in a matter of decades or centuries (Ballantyne and Benn, 1994). These slope processes form paraglacial landforms of gullies, debris cones and valley infilling. Ballantyne and Benn (1994) find debris flows to be of greatest importance in reshaping the paraglacial landscape, and avalanches to have only minor importance.

Disregarding the importance of avalanches reshaping the landscape, and thinking landscape development on an even longer timescale, avalanches can take place on a landscape scale in relatively short time periods enabling debris to be available in the valleys for future glacial advances (Ballantyne, 2002). However, the exhaustion model of paraglacial activity does not only have one peak of maximum sediment availability shortly after deglaciation, but can also have secondary sediment transfer peaks (Ballantyne, 2002). The occurrence of secondary peaks of activity can be due to regional uplift, climate change, extreme climatic events or anthropogenic influence.

Periglacial landscape evolution might be especially sensible to climate change, more so then glacial landscape evolution. In central Svalbard, a shift in prevailing winter wind direction, creating cornices on mainly west, northwest facing slopes, could have activated these sediment storages, but would have also caused more backwall erosion. An example can be found in the valley Todalen (Figure 5), close to the Longyeardalen valley. Here several multi-genetic colluvial fans are found, consisting of an old body of avalanche deposits with old debris flow imprints, and with renewed overprinting of avalanche and rockfall deposits (see the geomorphological map of landforms and sediments by Rubensdotter et al. 2012, available in the Svalbard Museum). In addition the recent debris flow activity is superimposed from a slightly shifted source area (Rubensdotter et al., 2009). Fan development was consequently controlled possibly by a slight shift in climate induced wind direction. Due to the non-linearity of the geomorphological slope processes, an end product of valley evolution can only be assumed. However, periglacial landscape evolution can be seen in a long-term perspec-

tive, reworking the landscape on a large scale, still interacting with glacial processes. A good example is the cornice fall avalanche derived rock glacier that originates from the foot of the Larsbreen slope system, being of at least late Holocene age (Humlum et al., 2007).

10. References

Ackroyd, P, 1987. Erosion by snow avalanche and implications for geomorphic stability, Torlesse Range, New Zealand. *Arctic and Alpine Research*, **19**(1), 65-70.

Ahlmann, HW, 1953. Glacier variations and climatic fluctuations, American Geographical Society, New York.

Åkerman, HJ, 1984. Notes on talus morphology and processes in Spitsbergen. *Geografiska Annaler*, **66A**(4), pp. 17.

André, M-F, 1990. Geomorphic impact of spring avalanches in Northwest Spitsbergen (79°N). *Permafrost and Periglacial Processes*, **1**(2), 97-110. doi: 10.1002/ppp.3430010203.

André, M-F, 1995. Holocene climate fluctuations and geomorphic impact of extreme events in Svalbard. *Geografiska Annaler*, **77A**(4), 241-250.

André, M-F, 1997. Holocene rockwall retreat in Svalbard: A triple-rate evolution. *Earth Surface Processes and Landforms*, **22**(5), 423-440.

André, M-F, 2003. Do periglacial landscapes evolve under periglacial conditions? *Geomorphology*, **52**(1-2), 149-164. doi: 10.1016/s0169-555x(02)00255-6.

Arlov, TB, 1996. Svalbards historie, Oslo: Aschehoug.

Ballantyne, CK, 2002. Paraglacial geomorphology. *Quaternary Science Reviews*, **21**(18-19), 1935-2017. doi: 10.1016/S0277-3791(02)00005-7.

Ballantyne, CK, Benn, DI, 1994. Paraglacial slope adjustment and resedimentation following recent glacier retreat, Fåbergstøllsdalen, Norway. *Arctic and Alpine Research*, **26**(3), 255-269.

Balstad, L, 1956. Kvinna på Svalbard. *Forum, Stockholm*.

Barsch, D, Jakob, M, 1998. Mass transport by active rockglaciers in the Khumbu Himalaya. *Geomorphology*, **26**(1-3), 215-222.

Bell, I, Gardner, J, DeScally, F, 1990. An estimate of snow avalanche debris transport, Kaghan Valley, Himalaya, Pakistan. *Arctic, Antarctic, and Alpine Research*, **22**(3), 317-321.

Berthling, I, Etzelmüller, B, 2011. The concept of cryo-conditioning in landscape evolution. *Quaternary Research*, **75**(2), 378-384. doi: 10.1016/j.yqres.2010.12.011.

Bremer, M, Sass, O, 2012. Combining airborne and terrestrial laser scanning for quantifying erosion and deposition by a debris flow event. *Geomorphology*, **138**(1), 49-60. 10.1016/j.geomorph.2011.08.024.

Caine, N, 1976. A uniform measure of subaerial erosion. *Geological Society of America Bulletin*, **87**, 137-140.

Christiansen, HH, 1997. Periglacial sediments in an Eemian-Weichselian succession at Emmerlev Klev, southwestern Jutland, Denmark. *Palaeogeography, Palaeoclimatology, Palaeoecology*, **138**, 245-258.

Christiansen, HH, 1998. Nivation forms and processes in unconsolidated sediments, NE Greenland. *Earth Surface Processes and Landforms*, **23**(8), 751-760.

Christiansen, HH, 2001. Snow-cover depth, distribution and duration data from northeast Greenland obtained by continuous automatic digital camera. *Annals of Glaciology*, **32**, 102-108. doi: 10.3189/172756401781819355.

Christiansen, HH, Etzelmueller, B, Isaksen, K, Juliussen, H, Farbrot, H, Humlum, O, Johansson, M, Ingeman-Nielsen, T, Kristensen, L, Hjort, J, Holmlund, P, Sannel, ABK, Sigsgaard, C, Åkerman, HJ, Foged, N, Blikra, LH, Pernosky, MA, Ødegård, RS, 2010. The thermal state of permafrost in the nordic area during the international polar year 2007-2009. *Permafrost and Periglacial Processes*, **21**(2), 156-181. doi: 10.1002/ppp.687.

Christiansen, HH, Humlum, O, Eckerstorfer, M, in press. Central Svalbard 2000-2011 meteorological dynamics and periglacial landscape response. *Arctic Antarctic and Alpine Research*.

Cornell, SS, 1873. Cornell's Physical Geography. D. Appleton and Company, New York, NY. pp. 112.

Decaulne, A, Saemundsson, T, 2006. Geomorphic evidence for present-day snow-avalanche and debris-flow impact in the Icelandic Westfjords. *Geomorphology*, **80**(1-2), 80-93. doi: 10.1016/j.geomorph.2005.09.007.

Decaulne, A, 2007. Snow-avalanche and debris-flow hazards in the fjords of north-western Iceland, mitigation and prevention. *Natural Haards*, 41, 81-98. doi: 10.1007/s1 1069-006-9025-x.

Dickson, RR, Osborn, TJ, Hurrell, JW, Meincke, J, Blindheim, J, Adlandsvik, B, Vinje, T, Alekseev, G, Maslowski, W, Cattle, H, 2000. The Arctic ocean response to the North Atlantic Oscillation. *Journal of Climate*, **13**, 2671-2696.

Eckerstorfer, M, Christiansen, HH, 2010. An extreme slush and slab avalanche event in High Arctic maritime Svalbard, Proceedings of the International Snow Science Workshop 2010, Squaw Valley, USA, pp. 791-794.

Eckerstorfer, M, Farnsworth, RW, Birkeland, WK, 2012. Potential dry slab avalanche trigger zones on wind-affected slopes, Proceedings of the International Snow Science Workshop 2012, Anchorage, Alaska, USA. 462-466.

Eckerstorfer, M, Neumann, U, Christiansen, HH, 2008. High arctic avalanche monitoring in maritime Svalbard., Proceedings of the International Snow Science Workshop 2008, Whistler, Canada, pp. 784-790.

Eckerstorfer, M, Neumann, U, Christiansen, HH, 2009. Avalanches and snow mobile traffic around Longyearbyen, Proceedings of the International Snow Science Workshop 2009, Davos, Switzerland, pp. 44-47.

Eckerstorfer, M, Farnsworth, W.R, Birkeland, K.W, submitted. Potential dry slab avalanche trigger zones on wind-affected slopes in central Svalbard. *Cold Regions Science and Technology*.

Ellehauge, J, 2003. Influence of meteorological and topographic conditions on snow avalanches in central Spitsbergen, Svalbard. MSc, University Centre in Svalbard, Longyearbyen, pp. 65.

Førland, EJ, Benestad, RE, Hanssen-Bauer, I, Haugen, JE, Skaugen, TE, 2011. Temperature and precipitation development at Svalbard 1900-2100. *Advances in meteorology*, 2011, **14**. doi: 10.1155/2011/893790.

French, MH, 2007. The periglacial environment, **Third edition**. John Wiley & Sons. pp. 458.

French, MH, Thorn, CE, 2006. The changing nature of periglacial geomorphology. *Geomorphologie-Relief Processus Environnement*, **3**, 165-173.

Gauthier, D, Jamieson, B, 2010. On the sustainability and arrest of weak layer fracture in whumpfs and avalanches, Proceedings of the International Snow Science Workshop 2010, Squaw Valley, USA, pp. 224-231.

Greene, EM, Birkeland, KW, Elder, K, Johnson, G, Landry, C, McCammon, I, Moore, M, Sharaf, D, Sterbenz, C, Tremper, B, Willimas, K, 2004. Snow, weather, and avalanches: Observational guidelines for avalanche programs in the United States. American Avalanche Association, Pagosa Springs, Colorado. pp. 150.

Hanssen-Bauer, I, Kristensen Solås, M, Steffensen, EL, 1990. The climate of Spitsbergen, Norwegian Meteorological Institute. Klima-Rapport **39/90**. pp. 40.

Heckmann, T, Wichmann, V, Becht, M, 2005. Sediment transport by avalanches in the Bavarian Alps revisited - a perspective on modelling. *Zeitschrift für Geomorphologie, N.F.*, **138**, 11-25.

Heierli, J, Gumbsch, P, Zaiser, M, 2008. Anticrack nucleation as triggering mechanism for snow slab avalanches. *Science*, **321**(5886), 240-243. doi: 10.1126/science.1153948.

Hestnes, E, 1996a. Barnehage, Longeyarbyen. Vurdering av skredfaren mot aktuelle tomter for ny barnehage ved kirka, Oslo. pp. 45.

Hestnes, E, 1996b. Det gamle sykehuset, Longeyarbyen. Skredfarevurdering, Oslo. pp. 37.

Hestnes, E, 1998. Slushflow hazard - where, why and when? 25 years of experience with slushflow consulting and research. *Annals of Glaciology*, **26**, 370-376.

Hestnes, E, 1999. Permafrost response to environmental and industrial loads. Snø og snøskred på Svalbard. Registrering av snøforhold, snøskred og utløpslengder., Longyearbyen. pp. 40.

Hestnes, E, 2000. Impact of rapid mass movement and drifting snow on the infrastructure and development of Longyearbyen, Svalbard. In: K. Senneset (Ed.), International Workshop on Permafrost Engineering, Longyearbyen, Svalbard, Norway, pp. 328.

Houghton, JT, Ding, Y, Griggs, DJ, Noguer, M, van der Linden, PJ, Dai, X, Maskell, K, Johnson, CA, 2001. IPCC, 2001: Climate change 2001: The scientific basis. Contribution of Working Group 1 to the Third Assessment Report of the Intergovernmental Panel on Climate Change, Cambridge, United Kingdom and New York, NY, USA.

Humlum, O, 2002. Modelling late 20th-century precipitation in Nordenskiold Land, Svalbard, by geomorphic means. *Norsk Geografisk Tidsskrift - Norwegian Journal of Geography*, **56**(2), 96 - 103. doi: 10.1080/002919502760056413.

Humlum, O, Christiansen, HH, Juliussen, H, 2007. Avalanche-derived rock glaciers in Svalbard. *Permafrost and Periglacial Processes*, **18**(1), 75-88. doi: 10.1002/ppp.580.

Humlum, O, Instanes, A, Sollid, JL, 2003. Permafrost in Svalbard: a review of research history, climatic background and engineering challenges. *Polar Research*, **22**(2), 191-215.

Humlum, O, Solheim, J-E, Stordahl, K, 2011. Spectral analysis of the Svalbard temperature record 1912-2010. *Advances in meteorology*, **2011**, 14. doi: 10.1155/2011/175296.

Humlum, O, Vogel, S, Eckerstorfer, M, Christiansen, HH, 2010. Excursion to Gruvefjellet. EUCOP III Excursion Guidebook. The Geological Survey of Norway, Trondheim, Norway.

Ingólfsson, Ó, Lokrantz, H, 2003. Massive ground ice body of glacial origin at Yugorski Peninsula, arctic Russia. *Permafrost and Periglacial Processes*, **14**(3), 199-215.

Instanes, A, Lønne, I, Sandaker, K, 2004. Location of avalanche victims with ground-penetrating radar. *Cold Regions Science and Technology*, **38**(1), 55-61.

Jaedicke, C, 2001. Drifting snow and snow accumulation in complex Arctic terrain: field experiments and numerical modelling. Ph.D., University of Bergen, Bergen.

Jaedicke, C, 2002. Snow drift losses from an Arctic catchment on Spitsbergen: an additional process in the water balance. *Cold Regions Science and Technology*, **34**(1), 1-10.

Jahn, A, 1976. Contemporaneous geomorphological processes in Longyeardalen, Vestspitsbergen (Svalbard). *Biuletyn Peryglacjalny*, **26**, pp. 25.

Jamieson, B, 1999. The Compression test - after 25 years. *Avalanche Review*, pp. 9.

LaChapelle, E, R., 1985. The ABS of Avalanche Safety. 2nd edition. The Mountaineers, Seattle. pp. 112.

Larsson, S, 1982. Geomorphological effects on the slopes of Longyear valley, Spitsbergen, after a heavy rainstorm in July 1972. *Geografiska Annaler*, **64A**(2), 105-125.

Latham, J, Montagne, J, 1970. The possible importance of electrical forces in the development of snow cornices. *Journal of Glaciology*, **9**, 375-384.

Lewkowicz, AG, 2008. Evaluation of miniature temperature-loggers to monitor snowpack evolution at mountain permafrost sites, northwestern Canada. *Permafrost and Periglacial Processes*, **19**(3), 323-331. doi: 10.1002/ppp.625.

Lied, K, Bakkehøi, S, 2001. Skredulykken under Håbergnuten, Svalbard, Oslo.

Liu, L, Schaefer, K, Zhang, T, Wahr, J, 2012. Estimating 1992-2000 average active layer thickness on the Alaskan North Slope from remotely sensed surface subsidence. *J. Geophys. Res.*, **117**(F1), F01005. doi: 10.1029/2011jf002041.

Luckman, BH, 1977. The geomorphic activity of snow avalanches. *Geografisk Annaler. Series A, Physical Geography*, **59**, 31-48.

Luckman, BH, 1978a. Geomorphic work of snow avalanches in the Canadian Rocky Mountains. *Arctic and Alpine Research*, **10**(2), 261-276.

Luckman, BH, 1978b. The measurement of debris movement on alpine talus slopes. *Zeitschrift für Geomorphologie, N.F.*, **Suppl. Bd. 29**, 117-129.

Luckman, BH, 1988. Debris accumulation patterns on talus slopes in Surprise Valley, Alberta. *Geographie physique et Quaternaire*, **42**(3), 247-278.

Major, H, Haremo, P, Dallmann, W, Andresen, A, 2001. Geological map of Svalbard. 1:100 000. C9G Adventdalen. *Norsk Polarinst. Temakart 31/32*.

McCammon, I, Haegeli, P, 2006. Evaluation of a rule-based decision aid for recreational travelers in avalanche terrain, Proceedings of the International Snow Science Workshop 2006, Telluride, Colorado, 1-6.

McClung, DM, 2002. The elements of applied avalanche forecasting, Part II: The physical issues and the rules of applied avalanche forecasting. *Natural Hazards*, **26**, 131-146.

McClung, DM, Schaerer, P, 2006. The Avalanche Handbook. 3rd edition. The Mountaineers, Seattle. pp. 342.

Met.no, 2012. eklima. Free access to weather- and climate data from Norwegian Meteorological Institute form historical data to real time observations. http://www.eklima.no.

Mitterer, C, Heilig, A, Schweizer, J, Eisen, O, 2011. Upward-looking ground-penetrating radar for measuring wet-snow properties. *Cold Regions Science and Technology*, **69**(2-3), 129-138. doi: 10.1016/j.coldregions.2011.06.003.

Montagne, J, McPartland, JT, Super, AB, Townes, HW, 1968. The nature and control of snow cornices on the Bridger Range, southwestern Montana. pp. 16.

NGI, 2010. Snøskredulykker i Norge vinteren 2003/04. http://www.snoskred.no.

Paulcke, W, Welzenbach, W, 1928. Schnee, Wächten, Lawinen. *Zeitschrift für Gletscherkunde, Eiszeitforschung und Geschichte*, **16**, 49-69.

Phillips, M, Schweizer, J, 2007. Effect of mountain permafrost on snowpack stability. *Cold Regions Science and Technology*, **47**(1-2), 43-49.

Prokop, A, 2008. Assessing the applicability of terrestrial laser scanning for spatial snow depth measurements. *Cold Regions Science and Technology*, **54**(3), 155-163. doi: 10.1016/j.coldregions.2008.07.002.

Rapp, A, 1960a. Recent developments of mountain slopes in Kärkevagge and surroundings, northern Scandinavia. *Geografisk Annaler*, **XLII**, 71-200.

Rapp, A, 1960b. Talus slopes and mountain walls at Tempelfjorden, Spitsbergen. *Norsk Polarinstitut Skrifter*, pp. 119.

Rapp, A (Ed.), 1985. Extreme rainfall and rapid snowmelt as causes of mass movements in high latitude mountains. Field and Theory. University of British Columbia Press.

Rogers, JC, Yang, L, Li, L, 2005. The role of Fram Strait winter cyclones on sea ice flux and on Spitsbergen air temperatures. *Geophysical Research Letters*, **32**, 1-4. doi: 10.1029/2004gl022262.

Rubensdotter, L, Stalsberg, K, Christiansen, HH, Neumann, U, Eckerstorfer, M, Humlum, O, 2009. The potential of high arctic collovial fan development and process regeneration as palaeoclimate proxies; Collovial source area and sediment mapping within the CRYOSLOPE Svalbard framework., EGU General Assembly 2009. Geophysical Research Abstracts, Vienna.

Sass, O, Hoinkis, R, Wetzel, K-F, 2010. A six-year record of debris transport by avalanches on a wildfire slope (Arnspitze, Tyrol). *Zeitschrift für Geomorphologie, N.F.*, **54**(2), 181-193.

Schaerer, P, 1986. Weather patterns for major avalanches. *The Avalanche Review*, **4**(3), pp. 2.

Schaffhauser, A, Adams, M, Fromm, R, Joerg, P, Luzi, G, Noferini, L, Sailer, R, 2008. Remote sensing based retrieval of snow cover properties. *Cold Regions Science and Technology*, **54**(3), 164-175. doi: 10.1016/j.coldregions.2008.07.007.

Scherer, D, Gude, M, Gempeler, M, Parlow, E, 1998. Atmospheric and hydrological boundary conditions for slushflow initiation due to snowmelt. *Annals of Glaciology*, **26**, 377-380.

Scherler, D, Bookhagen, B, Strecker, MR, 2011. Hillslope-glacier coupling: The interplay of topography and glacial dynamics in High Asia. *Journal of Geophysical Research*, **116**(F02019), 21. doi: 10.1029/2010JF001751.

Schweizer, J, 2008. Snow avalanche formation and dynamics. *Cold Regions Science and Technology*, **54**(3), 153-154. doi: 10.1016/J.Coldregions.2008.08.005.

Schweizer, J, Jamieson, BJ, Schneebeli, M, 2003. Snow avalanche formation. *Reviews of Geophysics*, **41**(4), 1-25. doi: 10.1029/ 2002RG000123.

Selby, MJ, 1993. Hillslope Materials and Processes. Oxford University Press, Oxford, England. pp. 451.

Seligman, G, 1936. Snow cornices, Snow structure and ski fields, 237-269.

Sentralbyrå, S, 2011. Dette er Svalbard. Hva forteller tallene? Statistisk Sentralbyrå / Statistics Norway, Oslo.

Serreze, MC, Barrett, AP, 2008. The summer cyclone maximum over the Central Arctic Ocean. *Journal of Climate*, **21**(5), 1048-1065.

Siewert, MB, Krautblatter, M, Christiansen, HH, Eckerstorfer, M, 2012. Arctic rockwall retreat rates estimated using laboratory-calibrated ERT measurements of talus cones in Longyeardalen, Svalbard. *Earth Surface Processes and Landforms*. 10.1002/esp.3297.

Simenhois, R, Birkeland, KW, 2009. The Extended Column Test: Test effectiveness, spatial variability, and comparison with the Propagation Saw Test. *Cold Regions Science and Technology*, **59**(2-3), 210-216.

Sørbel, L, Tolgensbakk, J, Hagen, JO, Hogvard, K, 2001. Geomorphological and quaternary geological map of Svalbard. 1:100 000. C9G Adventdalen. *Norsk Polarinst. Temakart 31/32*.

Svendsen, JI, Mangerud, J, 1997. Holocene glacial and climatic variations on Spitsbergen, Svalbard. *The Holocene*, **7**(1), 45-57. doi: 10.1177/095968369700700105.

Sysselmannen, 1992. Snøskred i Liefdefjorden. 11.6.92.

Thiedig, F, Kresling, A, 1973. Meteorologische und geologische Bedingungen bei der Entstehung von Muren im Juli 1972 auf Spitzbergen. *Polarforschung*, **43**, pp. 10.

Thiedig, F, Lehmann, U, 1973. Die Entstehung von Muren als saekulares Ereignis auf Spitzbergen (Svalbard) und ihre Bedeutung fuer die Denudation in der Frostschutzzone. *Mitt. Geol. Inst. Univ. Hamburg*, pp. 42.

van Herwijnen, A, Schweizer, J, 2011. Monitoring avalanche activity using a seismic sensor. *Cold Regions Science and Technology*, **69**(2-3), 165-176. doi: 10.1016/j.coldregions.2011.06.008

Washburn, AL, Goldthwait, RP, 1958. Slushflows (Abstract). *Bulletin of the Geological Society of America*, **69**(1), 1657-1658.

Welzenbach, W, 1930. Untersuchungen über die Stratigraphie der Schneeablagerungen und die Mechanik der Schneebewegungen nebst Schlußfolgerungen auf die Methoden der Verbauung. *Wissenschaftliche Veröffentlichungen des Deutschen und Österreichischen Alpenvereins*, **9**, 1-105.

Winther, J-G, Bruland, O, Sand, K, Gerland, S, Marechal, D, Ivanov, B, Glowacki, P, Koenig, M, 2003. Snow research in Svalbard - an overview. *Polar Research*, **22**(2), 125-144.

Wirz, V, Schirmer, M., Gruber, S., Lehning, M., 2011. Spatio-temporal measurements and analysis of snow depth in a rock face. *The Cryosphere*, **5**, 893-905. doi: 10.5194/tc-5-893-2011.

Zahn, M, von Storch, H, 2010. Decreased frequency of North Atlantic polar lows associated with future climate warming. *Nature*, **467**(7313), 309-312. doi: 10.1038/nature09388.

11. Peer-reviewed articles

Paper 1:
Eckerstorfer, M., Christiansen, H.H. 2011. The "High Arctic maritime snow climate" in Central Svalbard. *Arctic, Antarctic and Alpine Research.* 41/1. 11-21. doi: 10.1657/1938-4246-43.1.11

Paper 2:
Eckerstorfer, M., Christiansen, H.H. 2011. Topographical and meteorological control on snow avalanching in the Longyearbyen area, central Svalbard 2006-2009. *Geomorphology.* 134. 186-196. doi:10.1016/j.geomorph.2011.07.001

Paper 3:
Eckerstorfer, M., Christiansen, H.H. 2011. Relating meteorological variables to the natural slab avalanche regime in High Arctic Svalbard. *Cold Regions Science and Technology.* 69. 184-193. doi:10.1016/j.coldregions.2011.08.008

Paper 4:
Eckerstorfer, M., Christiansen, H.H. 2012. Meteorology, topography and snowpack conditions causing two extreme mid-winter slush and wet slab avalanche periods in High Arctic maritime Svalbard. *Permafrost and Periglacial Processes.* 23. 15-25. doi:10.1002/ppp.734

Paper 5:
Vogel, S., **Eckerstorfer, M.,** Christiansen, H.H. 2012. Cornice dynamics and meteorological control at Gruvefjellet, Central Svalbard. *The Cryosphere.* 6. 157-171. doi:10.5194/tc-6-157-2012

Paper 6:
Eckerstorfer, M., Christiansen, H.H., Vogel, S., Rubensdotter, L. 2012. Snow cornice dynamics as a control on plateau edge erosion in central Svalbard. *Earth Surface Processes and Landforms.* doi: 10.1002/esp.3292

Paper 7:
Eckerstorfer, M., Christiansen, H.H., Rubensdotter, L., Vogel, S., Siewert, M. submitted. The role of cornice fall avalanche sedimentation (in the valley Longyeardalen, central Svalbard). *Journal of Geophysical Research – Earth Surface.* 20 p.

Paper 1

2 cm thick ice layer that formed during the rain on snow event in January 2010.

Arctic, Antarctic, and Alpine Research, Vol. 43, No. 1, 2011, pp. 11–21

The "High Arctic Maritime Snow Climate" in Central Svalbard

Markus Eckerstorfer† and Hanne H. Christiansen**

*Arctic Geology Department, The University Centre in Svalbard, Pb 156, 9171 Longyearbyen, Norway; Department of Geosciences, University of Oslo, Pb 1047, 0316 Oslo, Norway
†markus.eckerstorfer@unis.no

Abstract

In this first systematic classification of the snowpack in central Svalbard a new additional snow climate is presented. Based on field observations in the 2007–2009 period, 109 snow pits were quantitatively analyzed in terms of temperature gradients, grain shapes, grain sizes, and hardness of every snow layer. Emphasis was given to the occurrence of depth hoar, ice layers, the most observed weak layer–bed surface interfaces. These parameters in combination with meteorological observations define the "High Arctic maritime snow climate" as having a very thin and cold snowpack, a basal layer of depth hoar with winds labs and ice layers on top. The snowpack lasts for 8–10 months of the year, at higher grounds for the whole year. Snow climate classifications are an important part of improving the local avalanche characterization. This is timely, especially for the area around Svalbard's main settlement Longyearbyen, where avalanches represent a natural hazard. Also, climate models for the area predict changing meteorological conditions, especially more solid precipitation, thus a description of the snow climate as it is today is important. This "High Arctic maritime snow climate" characterization is based on the 16.8 km^2 mountainous area around Longyearbyen at 78°N, and does not fit any other High Arctic location. Svalbard has in comparison to other High Arctic locations milder climate due to an overall meteorological maritime influence.

DOI: 10.1657/1938-4246-43.1.11

Introduction

SNOW CLIMATE CLASSIFICATIONS

Over the past 50 years, numerous studies defined "snow climates" and analyzed their characteristics. The three main snow climate types are maritime, continental, and transitional (McClung and Schaerer, 2006). The analysis of a snow climate is mainly based on the combination of meteorological and snowpack factors, and builds the basis for characterizing avalanche types, frequencies, and patterns. LaChapelle (1966) was the first to describe dominant weather causing avalanches. The first quantitative analysis of snow climates was carried out by Armstrong and Armstrong (1987) in the Rocky Mountains in the western United States. Numerous other studies followed, mainly from the western United States (Fitzharris, 1987; Mock and Birkeland, 2000; Haegeli and McClung, 2003). Recently, Ikeda et al. (2009) added a new snow climate, the "rainy continental snow climate" to the common snow climate classification, and expanded the discussion to the Japanese Alps. Another snow climate classification was proposed by Sturm and Holmgren (1995). They defined each snow class in terms of snow layer sequences, grain shapes, and thickness. Sturm and Holmgren (1995) described the snow class "tundra," based on data collected in Alaska, as a thin, cold, wind-blown snow cover lasting 10 months of the year, with maximum depths of about 75 cm, consisting of a basal layer of depth hoar overlain by multiple wind slabs.

OBJECTIVES OF THE STUDY

There is no snow climate classification that provides a description of meteorological and snowpack characteristics determining avalanche activity currently operating for any Arctic area. Eckerstorfer and Christiansen (submitted) found in their study for central Svalbard that direct action avalanches are over 50% the dominant avalanche type, releasing during or immediately after snowstorms, involving only the newly fallen snow. Furthermore, extreme weather events cause extensive avalanching in the form of climax avalanches (Eckerstorfer and Christiansen, 2010), a type that results from a structural weakness in the snowpack. Thus, forecasting is, according to LaChapelle (1966), predominantly based on weather observations and the investigation of any structural weakness in the snowpack. The objective of this study is therefore to define a High Arctic snow climate and to test how it fits into traditional snow climate classifications. As climate and meteorology are well studied in central Svalbard (Hanssen-Bauer et al., 1990; Førland et al., 1997; Benestad et al., 2002), we focus in this paper on snowpack characteristics (depth, temperature, hardness, grain shapes) as well as stratigraphy of the snowpack, including detailed slab and weak layer combinations as primary indicators of avalanche formation (Schweizer et al., 2003). This study is based on field and meteorological observations in the 2007–2009 period. It represents the first systematic snowpack study from the 16.8 km^2 large mountainous area around Svalbard's main settlement Longyearbyen.

Study Area

The study area (16.8 km^2) is located around the main settlement Longyearbyen at 78°13′N (Fig. 1). Longyearbyen is situated in the center of the main island Spitsbergen (Nordenskioldland, Inlet Fig. 1) in the Svalbard archipelago, which covers 63,000 km^2 from 74° to 81°N and 10° to 35°E. In the study area, a 70-km-long snowmobile track through 7 valleys, called the "Little Round" (Fig. 1) represents the most used winter "road." The

1523-0430/11 $7.00

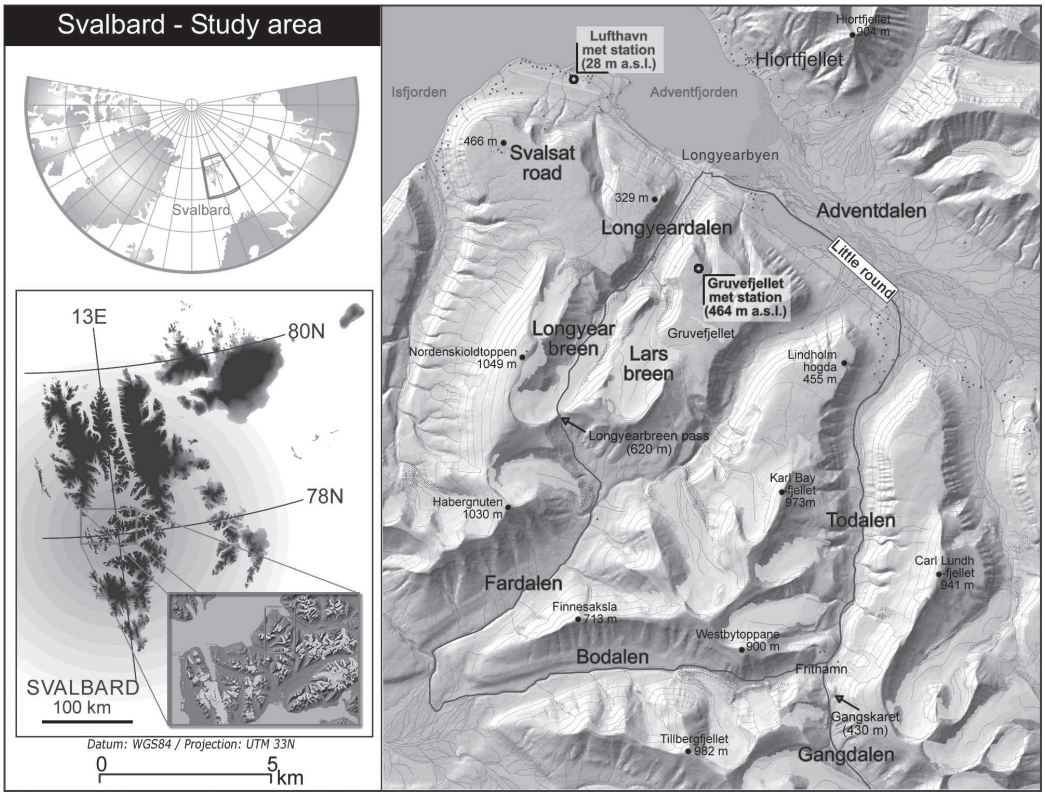

FIGURE 1. Study area in central Spitsbergen, main island of the Svalbard Archipelago. The small-scale map inlet shows Nordenskioldland where the study area is situated.

valleys display a concave curvature with the steepest parts close to the mountain crests (up to 60°). Moraines and rock glacier termini have a convex and steep curvature. At about 300–370 m a.s.l. a hard sandstone formation, in average 50–70 m in height, divides the slopes into narrow gullies on both sides of the outcrops. Continuous permafrost underlies the periglacial high-relief landscape (Humlum et al., 2003). Plateau-shaped mountain massifs dominate the landscape, with the highest peaks reaching 1000 m a.s.l.

CLIMATE AND METEOROLOGY IN CENTRAL SVALBARD

High Arctic climates are defined by French (2007) as distinct periglacial climates with extremely low winter temperatures for most of the year, and consequently the occurrence of continuous permafrost and temperatures above freezing only for 2–3 months a year. Precipitation amounts are low, winter snow cover is thin and often discontinuous because upland surfaces and exposed areas are windswept. French (2007) delimited the High Arctic climate in the northern hemisphere from the treeline or the 8–10 °C July air isotherm. The study area in central Svalbard is therefore located in the High Arctic. The climate in Svalbard is furthermore characterized as a polar tundra climate according to the Koeppen-Geiger climate classification (Kottek et al., 2006).

When comparing the mean annual air temperature (MAAT) of −3.8 °C and the mean annual precipitation of Longyearbyen (200 mm water equivalent [w.e.]) (Norwegian Meteorological Institute) in 2009 to other meteorological stations in the High Arctic between 70° and 80°N, it is obvious that Svalbard is significantly warmer (Fig. 2). The High Arctic MAATs otherwise range between −9 °C and −15 °C, and Eureka in the Canadian High Arctic is significantly cooler. Eureka is also the driest station, while Longyearbyen is close to the average. All stations except Hatonga in Siberia experience a certain maritime influence. But the significant difference with Longyearbyen is the influence of the warm Norwegian Current that flows partly along the west coast of Svalbard (Førland et al., 1997), causing mainly winter sea ice-free conditions. Likewise, Svalbard's location in the main North Atlantic cyclone track (Hanssen-Bauer et al., 1990) leads to relatively high temperatures, especially during the winter season. We therefore assume that the snowpack in other High Arctic locations show some similarities to the snowpack in our study area, with significant differences due to the warmer setting.

The study area is in the driest parts of Svalbard with an annual precipitation of 200 mm w.e. at sea level (Førland et al., 1997), but most likely with a systematic underestimation of especially the snow precipitation due to difficulties in measuring the amounts. Humlum (2002) suggested, therefore, based on modeling results, a 100% correction upwards. Large interannual variations in precipitation can be expected (Humlum, 2002). November–March may experience heavy snowfalls as well as mild spells, but snow may fall at any altitude in any month of the year and is thus the dominant type of precipitation. At sea level a snow cover exists usually from early

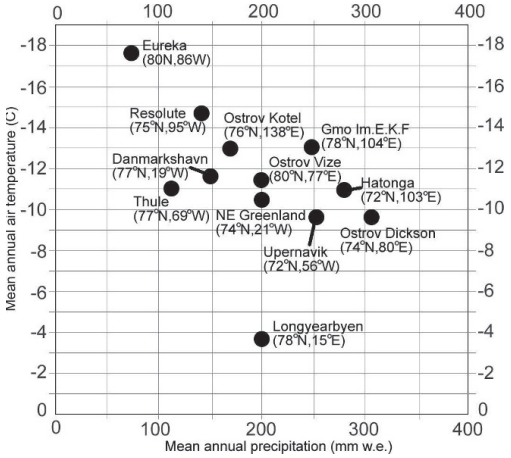

FIGURE 2. Mean annual air temperature (°C) and mean annual precipitation (mm water equivalent [w.e.]) for High Arctic meteorological stations in 2009. Data from http://www.climate-charts.com and http://www.wunderground.com. All stations are below 100 m a.s.l.

October to early June, higher altitudes tend to be covered continuously by snow. The snowpack is, however, very inhomogeneous, with snow-free areas on wind exposed slopes and mountaintops, while thick snowdrifts accumulate on lee slopes (Jaedicke and Gauer, 2005). The prevailing winter wind direction over the study area is from SE, but may locally vary due to channeling effects by topography (Humlum, 2002).

Highly fluctuating air temperatures on a daily or weekly basis are typical for Svalbard's winter weather (Humlum, 2002). A major meteorological controlling factor is the Siberian high-pressure system, a cold anticyclone that forms over eastern Siberia in winter, prevailing from late November to early March. If the Siberian High extends to the west, covering parts of Europe, but not Svalbard, it results in very cold winters in Europe (Humlum, 2002). Airflow over the Nordic seas is then strong and southerly with cyclones traveling up to Svalbard causing heavy snowfalls/rainfalls and/or snowmelt periods in mid-winter (Humlum et al., 2003). Svalbard is in general highly climatically sensitive due to its location near the confluence of ocean currents and air masses with different thermal regimes, and the rapid variations in sea-ice extent (Benestad et al., 2002).

Methods

One hundred thirty-two field trips following the "Little Round" were carried out during the two snow seasons 2007/2008 and 2008/2009 (Eckerstorfer et al., 2008). One hundred nine snow pits were dug in different valleys, aspects, and altitudes, 58 in the snow season 2007/2008 and 51 in the snow season 2008/2009. Meteorological and avalanche observations in both snow seasons were collected between mid-October and the end of May. The snow pit studies in the first observation year started not before February, thus data from autumn 2007 is missing. The timing of the field days was determined by the seasonal variation in sunlight. During the polar night, observations were difficult; therefore, the majority were carried out when light conditions allowed observations of both snow pits and avalanches (Fig. 3).

The most comprehensive snowpack study was carried out on a south-facing slope at the mountain col Gangskaret (430 m a.s.l.) (Fig. 1) where 32 pits were dug. From a climatic point of view, this location is more continental due to its inland, higher position, and it receives more snow precipitation due to orographic lifting. In general, most snow pits in both snow seasons were dug on south-facing slopes (33%). Also a NNE-facing slope on the Longyearbreen (Fig. 1) was studied more (24% of all pits) due to its easy access and representative snowpack for the area surrounding it. Both slopes are located in the 400–500 m a.s.l. elevation range, were 44% of all snow pits were dug. Favored snow pit locations were easy to access with a rather thin snowpack where higher temperature gradients in the snow enabled constructive metamorphism and thus the growth of potential weak layers. With the dominating plateau mountains reaching generally 500 m a.s.l., most snow pits were dug in the avalanche starting zone, and are therefore useful for slope stability evaluations.

Snow pits were analyzed according to the classification system of Fierz et al. (2009). All snow layers were classified quantitatively; grain shapes, grain sizes (mm), hand hardness liquid water content (by measuring snow temperature, visual observation of liquid water), thickness of each snow layer (cm), and snow temperature (every 10 cm, in °C) were recorded (Fierz et al., 2009). The weakest layers in the snowpack were identified by Compression test (Jamieson, 1999) and observed slab avalanche activity. Every snow pit was classified into one of the 10 hand hardness profiles, as presented by Schweizer and Wiesinger (2001).

The meteorological data were studied from two different meteorological stations in the study area, one located close to sea level (Lufthavn, 28 m a.s.l.), the official meteorological station of the Norwegian Meteorological Institute, and one on a mountain plateau (Gruvefjellet, 464 m a.s.l.), operated by the University Centre in Svalbard [UNIS] since 2001 (Fig. 1). The data were analyzed from 1 September until 31 May in the following year; consequently called snow seasons 2007/2008 and 2008/2009. From 1 September the snow cover usually starts to build up and begins to melt significantly by the end of May, making frequent field trips impossible.

Results

METEOROLOGY

The mean snow season air temperature (MSSAT) at sea level in 2007/20008 was −6.4 °C and in 2008/2009 −7.9 °C, both

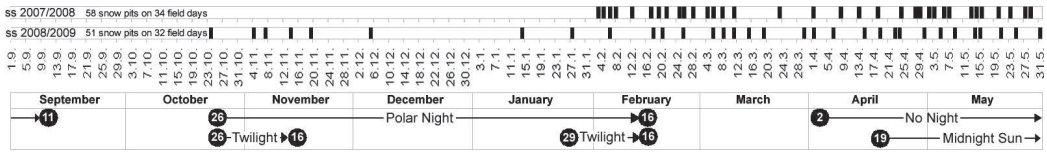

FIGURE 3. Timing of field days and snow pits dug during the two snow seasons 2007/2008 and 2008/2009. Field days are indicated as black columns with dates as vertical numbers. The polar night and the midnight sun period with their transition phases are indicated with dates.

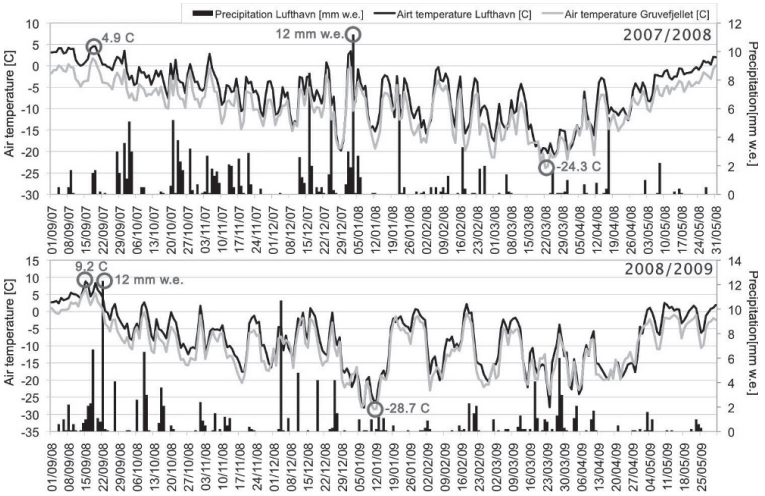

FIGURE 4. Daily average air temperatures from the two meteorological stations Gruvefjellet and Lufthavn for the snow seasons 2007/2008 and 2008/2009. Daily precipitation data is from Lufthavn in mm water equivalent (w.e.). The circles indicate the highest and lowest daily air temperatures, and highest daily precipitation rates in both snow seasons.

warmer than the 1980–2010 MSSAT average of −9.7 °C (Norwegian Meteorological Institute). The MSSAT has varied in the last 30 snow seasons between −14.1 °C in 1980/1981 and −4.7 °C in 2005/2006, with the MSSAT of the studied snow season being in the warmer quartile. Significant air temperature fluctuations on a daily and weekly base were found in both snow seasons, with very high (12.4 °C on 15 September 2008 at Lufthavn) and very low air temperatures (−32 °C on 7 January 2009 at Lufthavn) observed (Fig. 4).

Wind was almost constantly blowing over the study area (Figs. 5a, 5b). The mean wind speed during the snow seasons was 4.1 m/s in 2007/2008 and 6.6 m/s in 2008/2009 (Figs. 5a, 5b). In 2007/2008, the wind exceeded 10 m/s 22% of the time, in 2008/2009 16.5% of the time. This enabled significant snow redistribution as well as packing of the surface layers. The highest wind velocities during both snow seasons occurred in the autumn, when low pressures passed Svalbard, with a prevailing wind direction from the SE (Figs. 5a, 5b). In 2007/2008, high wind velocities were observed from the SSW, and in both snow seasons, almost no winds came from the N–E sector (Figs. 5a, 5b).

We observed snow precipitation in 81 days of both snow seasons (2007/2008 and 2008/2009). The largest amount of snowfall measured at snow stakes was 55 cm of accumulation (no water equivalent measurements carried out) in 3 days in mid-February 2008. Snow precipitation mostly came along with rising temperatures induced by passing low pressure systems. In total 144 mm w.e. (snow season 2007/2008) and 140 mm w.e. (snow season 2008/2009) were measured at sea level (Norwegian Meteorological Institute). The average snow depth of the snow pits in 2007/2008 was 143 cm, and in 2008/2009 it was 116 cm. The

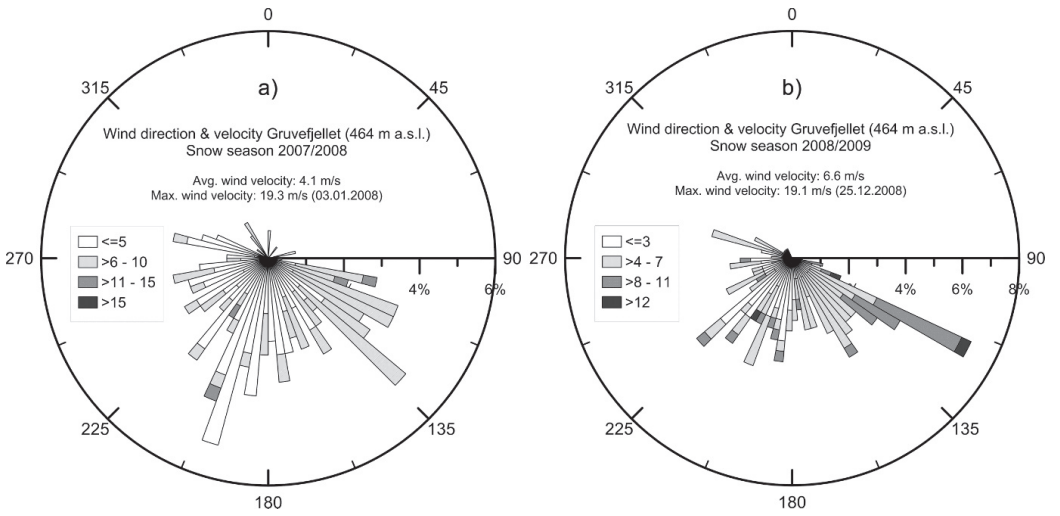

FIGURE 5. (a, b) Wind direction and velocity values from the meteorological station at Gruvefjellet for the snow seasons 2007/2008 and 2008/2009. The percentage on the *x*-axis represents the relative frequency of every wind velocity bin.

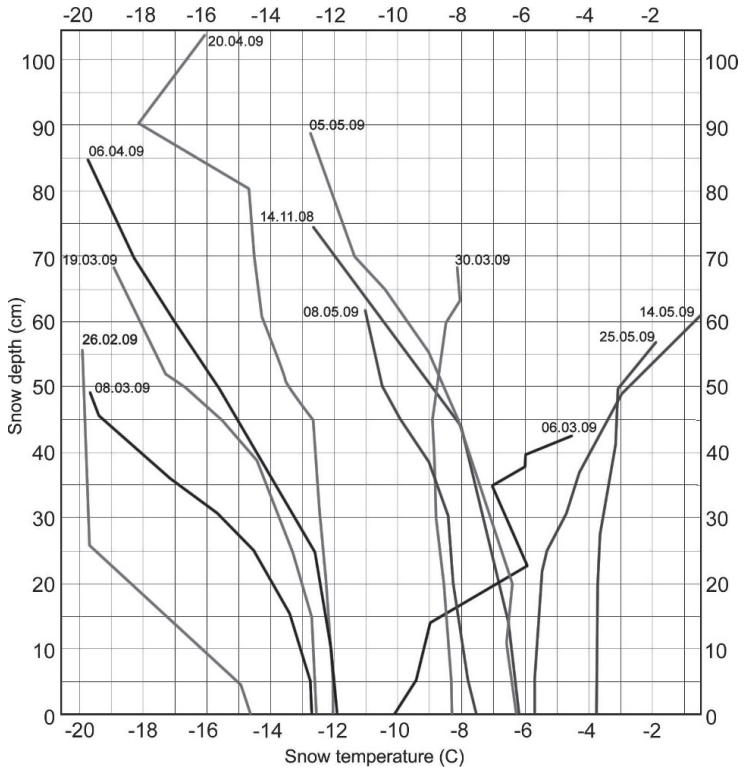

FIGURE 6. Snowpack temperature gradients (°C) at Gangskaret (464 m a.s.l.) in the snow season 2008/2009.

most shallow snowpack of 35 cm was studied at sea level, the thickest snow cover of 333 cm was investigated on a mountain col at 400 m a.s.l. The onset of the snow cover was very slow, and a more or less persistent snow cover built up by mid-October in both snow seasons. Maximum snow depths were then reached in April, and from mid-May the snow started to melt again, persisting only at higher altitudes. The extensive wind redistribution of snow causes a significant snowpack thickness variation from 0 cm on windswept landforms to a few meters of snow, mainly on glaciers and in other topographical lee positions. As a result of the SE-prevailing winter wind direction, the spatial snow distribution patterns were similar in both years.

SNOWPACK TEMPERATURES

In Figure 6 we show the typical temperature gradients of 12 snow pits dug at the south-facing slope of Gangskaret (430 m a.s.l.) (Fig. 1) in the snow season 2008/2009. Most pits were dug in March, while only 1 pit was analyzed before late December. The lowest temperatures at the surface of the snowpack were −20 °C in the coldest periods in the beginning of March 2008, and end of February until mid-March 2009 (Fig. 6). The lowest temperatures at the bottom of the snowpack reached −17 °C in a 62-cm-thick snowpack (15 January 2009). As the air temperature dropped rapidly to −28.7 °C on 12 January 2009 (Fig. 4), a fast response of the snowpack temperature down to the bottom could be observed. During this cooling process, high temperature gradients in the snowpack favored the formation of weak layers. The largest temperature gradients were observed in autumn (14 November 2008 with 7 °C/74 cm) and, for example, after significant cold spells (25 February 2009 with −23 °C air temperature resulting in a temperature gradient of 7.5 °C/48 cm) (Fig. 6). When these very cold periods persisted over longer periods, the snowpack turned isothermal, enabling only very slow snow metamorphism, and thus diminishing the probability of snow slope failures. Then, only already existing weak layers were preserved, which then failed following temperature increases, causing a decrease in the strength of the snowpack. Except for the snowpack temperature gradients from 26 February 2009 and 6 March 2009, all snow pits show a small temperature gradient in the lower 40 cm of the snowpack. The surface snow layers reached temperatures close to 0 °C by mid- to end of May, but still did not exceed −4 °C at the bottom layer due to the permafrost. The most distinctive and rapid warming events with air temperatures close to or above 0 °C, in combination with rain precipitation, created ice layers (2 January 2008 with 3 °C at sea level and 12 mm w.e. precipitation), which remained persistent over most of the snow season and built a bed surface on which avalanches released.

GRAIN TYPES

The relative number of grain types is quite similar in both snow seasons. The dominant grain type (23%) was mixed forms (rounded particles with few facets as well as faceted particles with recent rounding of facets) in both snow seasons (Fig. 7). These mixed forms were mostly found in the upper two-thirds of the snowpack. Of all grain-type layers found in the snowpack in 2007/2008 and 2008/2009, the 11–12% ice masses and the 8% mainly

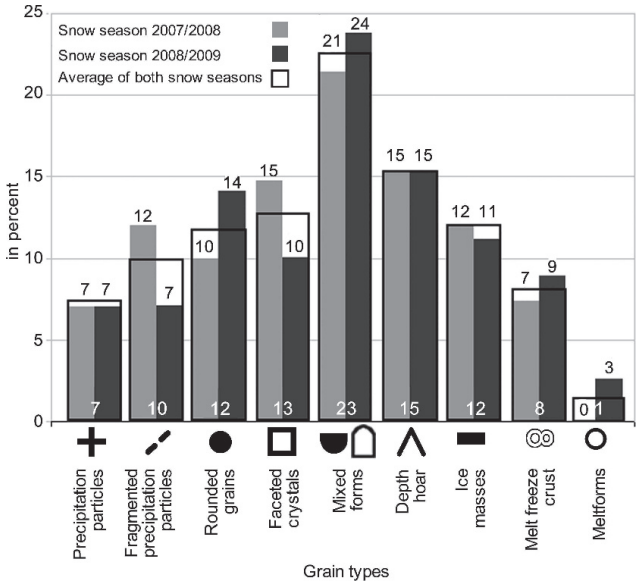

FIGURE 7. Relative amount (%) of grain types in the snowpack for the snow seasons 2007/2008 and 2008/2009 and the average of both snow seasons. Grain types are according to the classification by Fierz et al. (2009).

rain crusts are remarkable and unexpected in a cold High Arctic climate. These crusts formed after significant temperature increases during winter, when the water-saturated snow layer consequently refroze. Around these ice masses, faceted crystals were often observed due to near-crust faceting, as the ice masses are relatively impermeable to vapor transport (McClung and Schaerer, 2006). Rounded grains were mostly observed in wind slabs and less as a product of equilibrium metamorphism, which was less significant than kinetic growth. The reason for this is mainly due to fluctuating air temperature penetrating the snowpack, creating large temperature gradients. The significant effect of wind during snowfall explains also the low amount of precipitation particles found, with 7% average in both snow seasons. The small amount of wet grains is due to the limited access to the study area during the melting season. The 15% depth hoar was expected; differences in the amount of depth hoar throughout different snow pits seems to be controlled by the soil material. On coarse-grained talus slopes more depth hoar was found, most likely due to wind pumping and thus a warmer ground. Warmer ground seems to have resulted in a larger temperature gradient in the snowpack in early winter when the depth hoar developed. Still, more data needs to be collected from the early winter snowpack to verify this assumption.

HAND HARDNESS AND HAND HARDNESS PROFILES

The hand hardness (Fierz et al., 2009) of the studied pits (Fig. 8) clearly shows a dominance of hard layers. Winther et al. (2003) reported average snowpack density values of 374 kg/m^3 in Svalbard, which is comparable to our hand hardness results. The reasons are the numerous hard wind slabs in the snowpack and the low air temperatures that cool and harden the snowpack. Twenty-nine percent is referred to as ''high hardness'' represented by ''P,'' 25% as ''medium hardness'' represented by ''1F'', and 21% as ''very high hardness'' represented by ''K'' for both snow seasons 2007/2008 and 2008/2009. Both snow seasons are quite uniform in terms of hand hardness of the snowpack (Fig. 8) because of the also quite uniform distribution of grain shapes (Fig. 7). Both layers with mixed forms and rounded grains were in general rather hard. Precipitation particles, fragmented precipitation particles, facets, and depth hoar were found to be usually soft (F to 4F), although facets and depth hoar could be harder as well.

Figure 9 shows that hand hardness profile type 3, with a hard middle part and softer layers at the surface, as well as on the ground, was observed the most, uniformly over both snow seasons (19%). This profile type was typically found between February and April with cold temperatures and a low temperature gradient. Usually soft precipitation snow was found on top, a hard middle part consisting of hard mixed forms and surrounding ice layers, and a weak base of depth hoar and facets. The second most observed profile type was a ''staircase-like'' profile (profile 4) with increasing hardness towards the ground, but a weak base occurring 16% of the time (Fig. 9). This profile type was typically found also in early spring with again cold temperatures and low temperature gradients and mixed forms building hard layers in the lower part of the snowpack, underlain by a weaker depth hoar layer. Hand hardness profile 1, with a soft snowpack throughout the entire snowpack, was observed only in 2% of all snow pits (Fig. 9). This would be a typical isotherm snowpack at 0 °C in late spring when the snow got water saturated. An extension of the fieldwork period would have resulted in an increased amount of type 1 observed. There were also significant differences in the amount of certain profiles found between the two snow seasons (Fig. 9). Twenty percent of all snow profiles in 2008/2009 could be classified as profile 2, with a reversed ''staircase-like'' profile, which is an early season profile. The depth hoar base formed during the slow snow onset and consequent wind slabs accumulating on top, building up profile type 2. In the snow season 2007/2008 no snow pits were dug before late December (Fig. 3), thus this discrepancy in the data can be seen. Interseasonal differences were also observed in profile 7, with two ''staircase-like'' parts on top of each other, found in 20% of all pits in the snow season 2008/2009, while only in 7% of all pits in 2007/2008 (Fig. 9). This profile type shows the occurrence of an ice layer sandwich with faceted

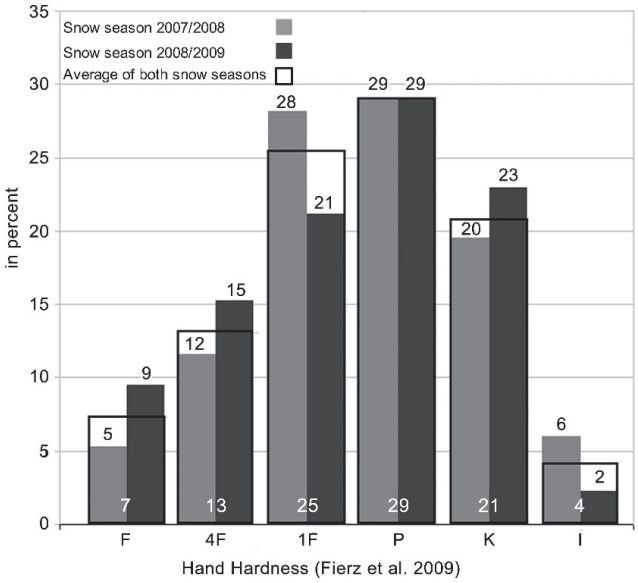

FIGURE 8. Average snow layer hand hardness of all studied snow pits. Hand hardness is used according to the classification by Fierz et al. (2009).

layers in between that formed due to the blockage of water vapor by the ice. In general large interseasonal variations in the hand hardness profiles were observed as a result of different timing of snow precipitation, rain on snow events creating ice layers, different physical properties of the snowpack in different stages of the snow season, and of course also the timing of the observations. Main characteristics of the snowpack in this High Arctic maritime setting are a persistent weakness at the bottom and an in general rather hard snowpack as a consequence of occurring ice layers and thaw/freeze cycles during the winter.

WEAK LAYER–BED SURFACE INTERFACE

Figure 10 illustrates the stratigraphy from the weakest layers to the underlying bed surface in all 109 snow pits studied. The release of a slab avalanche requires an initial failure in the weak layer induced by a triggering mechanism. This then propagates outwards to release a slab avalanche that slides down on a bed surface (Schweizer, 1999). Not all weak layer–bed surface combinations lead to avalanching. The potentially weakest combination of grain types in both seasons was depth hoar on the ground (Fig. 10) since it is the most frequently found and most persistent weak layer. Mixed forms on top of mixed forms follow this combination. Other frequent combinations were mixed forms on top of ice layers (19% in 2008/2009), and facets on top of mixed forms (18% in 2007/2008). Forty-two percent of all weakest layers in the snowpack had mixed forms, followed by facets (29%) and depth hoar (27%) (Fig. 10). Both snow seasons showed a quite similar picture with the depth hoar–ground combination dominating as well as mixed forms and facets as the dominant weak layers (Fig. 10). The kinetic growth of snow grains above ice masses is a common observed phenomena (McClung and Schaerer, 2006), and both mixed forms and facets might have comparable mechanical properties in terms of fracture initiation and propagation, with facets being more fragile. The average hand hardness of the weakest layers was "low" (= 4F [47%]), followed by "very low" (= F [32%]) and could be found in 36% in the lower third and 33% in the upper third of the snowpack (Fig. 11). Mixed forms were the most common weak layer found in the upper third of the snowpack, occurring in 22% of the analyzed profiles (Fig. 11), and facets most common in the second third of the snowpack (14%). In 37% of all analyzed snow pits, grain shapes other than depth hoar (27%), mixed forms (22%), and facets (14%) (Fig. 10) were interpreted as a weak layer. The dominance of depth hoar as a persistent weak layer is also reflected by the hand hardness profiles with a weak base in 89% of all studied pits

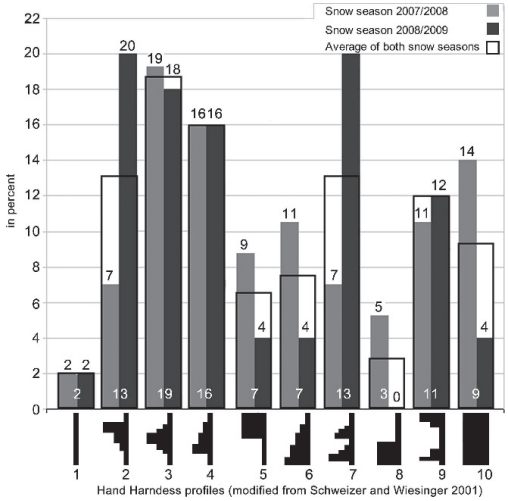

FIGURE 9. Hand hardness profiles of snow pits for the snow seasons 2007/2008 and 2008/2009 and the average of both snow seasons. The hand hardness profiles are based on the classification system by Schweizer and Wiesinger (2001). Types 7 and 9 are modified, displaying a weak base.

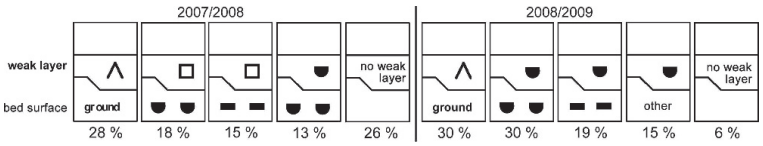

FIGURE 10. Relative amount of weak layer–bed surface combinations observed in the snowpack for the snow seasons 2007/2008 (5 snow pits on the left) and 2008/2009 (5 snow pits on the right). Grain shape symbols are explained in Figure 7.

(Fig. 9). When the weak layer was in the middle third of the snowpack, where facets were dominant (Fig. 11), hand hardness profiles 3, 7, and 9 were observed (Fig. 9). The weak mixed forms in the upper part of the snowpack were often overlain by wind slabs, building a weak old-new snow interface (Fig. 11).

Potential slab layers were in 30% of all snow pits two times and in 18% even four times harder than the weak layer on the hand hardness scale (Fierz et al., 2009), building very fragile weak layer–bed surface combinations (Fig. 12). Besides differences in grain shapes or grain sizes, hardness differences can account for weak bounding between the potential slab and the potential weak layer. Therefore, we analyzed also the hand hardness differences between potential weak layers, and the bed surfaces (Fig. 12). In 26% the potential weak layer were two steps harder on the hand hardness scale (Fierz et al., 2009) (Fig. 12). The 40% other cases take into account that the most found weak layer–bed surface interface was depth hoar on the ground (Fig. 10), thus no hand hardness difference could be taken.

DEPTH HOAR

In 2007/2008, in 81% of all snow pits, we found depth hoar with an average thickness of 10 cm. The thickest depth hoar layer was 40 cm thick on a coarse-grained talus slope. In 2008/2009, 82% of all snow pits had a depth hoar layer with an average thickness of 8 cm, reaching maximum depths of 30 cm in one pit in mid-March. The depth hoar layers did not grow significantly after late December in both snow seasons; moreover, the depth hoar got compressed by the weight of the overlying snow layers and therefore sometimes formed into columns of depth hoar, reducing the thickness of the layer. Again, also, Figure 6 shows that no significant temperature gradients were observed in the bottom part of the snowpack, partly due to the cooling influence of the permafrost. In general, thicker depth hoar layers were found on coarse-grained sediments due to enhanced conduction through blocks protruding into and through the snow and thereby acting as efficient heat bridges (Juliussen and Humlum, 2008).

Discussion

The central Spitsbergen snowpack has characteristics of an early winter snowpack (Phillips and Schweizer, 2007), with a persistent weak foundation, despite that it accumulates entirely through the winter. Depth hoar at the bottom of the snowpack persists over the entire snow season until the snowpack turns isothermal at 0 °C. The depth hoar layer accumulates during autumn and early winter due to a very slow onset of the snow cover; therefore the thin, early snow season snow cover leads to a significant temperature gradient favoring high snow crystal growth. For comparison, in the Columbia Mountains in Canada, low air temperatures and a shallow snowpack in early winter, resulting in depth hoar formation, is classified as abnormal (Haegeli and McClung, 2003). Later in the snow season as the snowpack accumulates, the minimum temperatures of the snowpack's surface layers decrease, particularly during the coldest periods of the year. Temperature gradients in the snowpack are large in the beginning of the coldest periods and then the snow turns isothermal due to the cold penetrating quickly into the relative dense and hard snowpack (Fig. 6). This hard snowpack enables efficient thermal conduction. Even when large temperature gradients exist in the snowpack, the lower 40 cm stay more or less isothermal in contrast to the upper part. Also when positive air temperatures penetrate through the snowpack in the same efficient way in spring, snow temperatures at the bottom of the snowpack respond only to a certain degree due to the influence of the cooling permafrost. This can be seen in Figure 6 when within 11 days in the beginning of March 2009, the ~50-cm-thick snowpack varied significantly in its surface temperature (15.5 °C variation) and less in its bottom temperature (4.5 °C). The air temperature influences efficiently the upper part of the snowpack and less the bottom part. And as large daily and weekly air temperature fluctuations occur very commonly in Svalbard (Fig. 4), these cycles of cold and warm air temperatures penetrating the snowpack to a certain depth happen frequently. This might explain the dominant occurrence of mixed forms and facets that were found in the upper two-thirds of the snowpack where temperature gradients were the highest (Fig. 11). The hard snowpack is a result of numerous wind slabs and ice masses.

A significant difference from the published snow class "tundra" by Sturm and Holmgren (1995), as well as already defined continental snowpacks to the Svalbard snowpack is the widespread occurrence of ice layers (Fig. 7). Warm and moist air from the south causes sudden temperature increases at any time during the winter, when low pressures reach Svalbard, leading to ice layer formation. Consequently buried ice masses favor growing of facets above and underneath, and can serve as bed surface layers, one of the prerequisites for slab avalanching. The wind slabs are a result of the significant snow redistribution over the landscape due to persistent winds with a prevailing SE wind direction for the snow season and the lack of high vegetation (Fig. 5). These observations correspond with the findings of Jaedicke and Gauer (2005), who observed higher wind speeds at mountain ridges and lower wind speeds in the valleys in Svalbard. Despite the hard and dense snowpack observed, the snow pit study shows that in 89% a substantial weakness was found somewhere in the snowpack (Fig. 11). Persistent weak layers can be found everywhere in the snowpack. The most commonly found weak

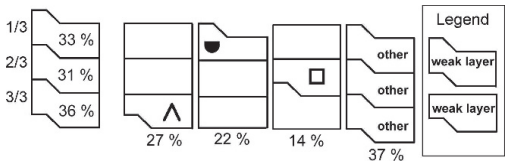

FIGURE 11. Weak layer stratigraphical position in each third of the snowpack. Four snow pits show the most weak layers for each third of the snowpack of all 109 snow pits. Grain shape symbols are explained in Figure 7.

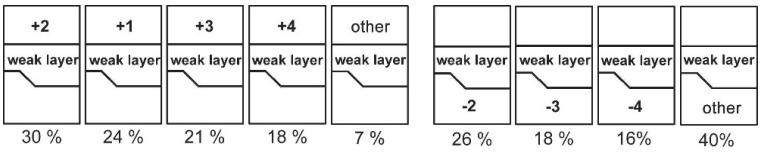

FIGURE 12. Hand hardness differences between the weak layer in the middle, the potential slab above (5 pits in the left part) and the potential bed surface beneath it (4 pits in the right part), for all 109 snow pits. Hand hardness according to Fierz et al. (2009).

layer–bed surface combination is a depth hoar layer lying on the ground (Fig. 10), where the above slab layer is two hand hardness levels harder than the weak layer (Fig. 12). This depth hoar layer undergoes no significant change during the snow season until melting starts. Nevertheless, not all weak layer–bed surface combinations lead to extensive avalanching during the snow season, since they might have been deeply buried in the snowpack and overlain by strong snow layers. On the other hand, avalanches released not only by fracture propagation in the weak layer (Schweizer et al., 2003) but also as a result of little cohesion in the new snow–old snow interface during or directly after snow loading.

Based on the presented 2-year snowpack analysis we propose to classify the central Svalbard snow climate as the ''High Arctic maritime snow climate,'' developed as a modification of the ''tundra'' snow class introduced by Sturm and Holmgren (1995) (Fig. 13). While it is similar with respect to low snowpack temperatures and a generally thin snowpack, the snowpack in Svalbard has more depth hoar and significantly more ice layers than what is standard for the tundra class. Therefore, the ''High Arctic maritime snow climate'' has characteristics of a continental snow climate (Armstrong and Armstrong, 1987; Mock and Birkeland, 2000) with low temperatures, clear skies in winter, a small amount of snowfall, and a weak snowpack. Mock and Birkeland (2000) also stated that in a typical continental snow climate, the base of the slab involved in an avalanche is often located below the old snow–new snow interface, which we find to be true also in our study area.

Mock and Birkeland (2000) furthermore identified six snow climate variables, which classify a certain snow climate to be continental, maritime, or transitional: minimum temperature, maximum temperature, total snow depth, daily snowfall, daily snow water equivalent, and daily rainfall. Adding values to these parameters, the authors state a seasonal air temperature threshold value for determining a continental climate of -7 °C. While the average air temperature at Lufthavn was around that value during the two snow seasons, it was lower on Gruvefjellet. The Gruvefjellet meteorological station is less disturbed by sea ice variations and, due to its elevated position at 464 m a.s.l., more representative for the avalanche release zone conditions. The MSSAT at sea level ranged in the last 30 years between -14.1 °C and -4.7 °C, making it hard to clearly determine a continental climate. The maximum threshold value for snow precipitation for a continental climate, stated by Mock and Birkeland (2000), is 560 cm, which is not reached in the study area. Official snow depth measurements have a large uncertainty and vary locally, which makes it hard to compare directly with results from other continental climates, and snow water equivalent was not measured. But rainfall during the winter is more likely to occur in a maritime climate.

Koeppen (1936) in his global climate classification located Svalbard in the polar climate class. Koeppen described a polar climate with an average air temperature of the warmest month below 10 °C, and rather mild maritime-influence winters for such a high latitude. Still, by comparing meteorological data from sea level with stations located further inland, a vertical temperature and precipitation gradient exists, showing a more continental climate. LaChapelle (1966) identified in his study four different snow climates for the Rocky Mountains in the western United States. He states that the snow climates are largely determined by the overall climate of the area. The snow climate in our study area has characteristics of the ''Pacific Coast'' snow climate in terms of large quantities of snowfall in snowstorms as well as the frequency of mid-winter rain events that create ice layers. Both meteorological conditions lead to dominating direct-action avalanching, found also by Eckerstorfer and Christiansen (2008) for the central Svalbard study area. A large amount of depth hoar is found in the central Rocky Mountains as in our study area, as well as the accumulation of deep wind drifts within a few hours. This leads to the sliding of wind drift snow on poorly consolidated snow in the Rocky Mountains (LaChapelle, 1966), as well as in central Svalbard. This first description of the snow climate in the Rocky Mountains was confirmed by Armstrong and Armstrong (1987), who also emphasized the relation between snow structure and

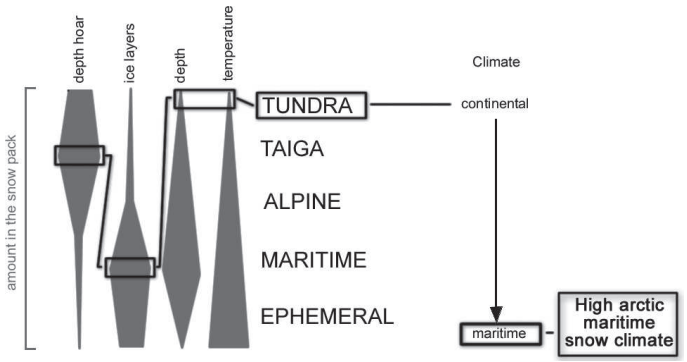

FIGURE 13. High Arctic maritime snow cover class modified after Sturm and Holmgren (1995). The black boxes indicate the amount of the certain snowpack characteristics found in the study area compared to different snow climates.

avalanche release. This was further developed by Haegeli and McClung (2003) in the Canadian Rocky Mountains, providing the term "avalanche climate" that contains also information about snowpack characteristics like weak layers. The authors found that natural avalanche activity on persistent weak layers in maritime-influenced winters was close to 0%, but up to 40% in continental winters. Still, avalanches seldom released in the Rocky Mountains on depth hoar or ice crusts. On the other hand Mock and Birkeland (2000) reported in a snow avalanche climatology study in the western United States mountain ranges that especially dangerous avalanche scenarios were caused by meager early season snowfalls and abnormally cold temperatures, favoring depth hoar growth. Also, Ikeda et al. (2009) found in a study of snow climates in the central Japanese Alps a significant amount of depth hoar, and characterized the snowpack as of the continental type with maritime influence. Our study area was maritime influenced but no natural avalanche released on depth hoar (Eckerstorfer and Christiansen, submitted). The reason for this is on one hand the domination of direct-action avalanches releasing at the new snow–old snow interface, and on the other hand the almost equal presence of weak layers in the entire snowpack. Weak layers in the upper part of the snowpack are more prone to failure, when stress on the snowpack is increased since the magnitude of this stress increase does not have to be very big. Therefore, climax avalanches more often release on facets as well as on facet-crust interfaces.

Conclusion

This study shows that the snow cover in central Spitsbergen, in a High Arctic meteorological setting with a strong maritime influence, has similarities with the snow class "tundra" proposed by Sturm and Holmgren (1995), but needs important additions and changes to fully classify it. We therefore suggest adding to the actual snow climate classification an additional snow climate: the "High Arctic maritime snow climate." This climate is characterized by a relatively thin and cold snowpack with a persistent structural weakness caused by depth hoar, as well as a significant amount of ice layering due to the overall meteorological maritime influence during the entire snow season. The snowpack lasts for 8–10 months of the year, and at higher ground parts of it for the whole year.

We propose this additional snow climate due to the fact that avalanches present a natural hazard in the mountainous area around Longyearbyen and infrastructure and because winter traffic and recreational activities are highly affected by snow avalanches. Therefore, a snow climate classification provides useful information for the establishment of modern avalanche forecasting; Haegeli and McClung (2007) emphasized the importance of snowpack observations for process-oriented avalanche forecasting. In detail, persistent weak layers especially determine the characteristics of an avalanche winter regime; Schweizer et al. (2003) showed that the primary indicator of avalanche formation is the snowpack stratigraphy. In particular, climax avalanches, a result of specific sequences of meteorological events (McClung and Schaerer, 2006) can be better predicted by including any weak layer information into the snow climate classification of an area. The three snow climates (maritime, continental, and transitional) (McClung and Schaerer, 2006) are well established and used in many studies to describe snow and avalanche characteristics on a regional scale. Despite Haegeli and McClung's (2007) warning that a snow climate classification should only be applied at full mountain range scale, we here establish a first classification of the snowpack in a smaller area, covering the full mountain landscape around Svalbard's main settlement Longyearbyen. As we have shown, even within a relatively small mountainous area, meteorological conditions and consequently snowpack characteristics—as the key factors for understanding avalanche activity patterns—can vary significantly. It therefore makes more sense to apply a snow climate classification to a smaller area.

Acknowledgments

This study was carried out as part of the CRYOSLOPE Svalbard research project (Climate change effects on High Arctic mountain slope processes and their impacts on traffic in Svalbard), funded by the Norwegian Research Councils Norklima program 2007–2009. Support for fieldwork was also received from the Svalbard Science Forum. Thanks to Ulli Neumann for brilliantly organizing and conducting the fieldwork, and to the other CRYOSLOPE Svalbard colleagues for stimulating discussions. Thanks also to editor Anne Jennings and two anonymous reviewers for very useful comments and suggestions that improved the manuscript significantly.

References Cited

Armstrong, L. R., and Armstrong, B. R., 1987: Snow and avalanche climates of the western United States: a comparison of maritime, intermountain and continental conditions. *Proceedings of the Davos Symposium, IAHS Publication*, 162: 281–294.

Benestad, R. E., Hanssen-Bauer, I., Skaugen, T. E., and Førland, E. J., 2002: Associations between sea-ice and the local climate on Svalbard. *07/02 Klima–Report Series of the Norwegian Meteorological Institute*, 1–13.

Eckerstorfer, M., and Christiansen, H. H., submitted: Characteristics of the "High Arctic avalanche climate" of the Longyearbyen area 2006–2009, central Svalbard. *Geomorphology*.

Eckerstorfer, M., and Christiansen, H. H., 2010: An extreme slush and slab avalanche event in High Arctic maritime Svalbard. Proceedings of the International Snow Science Workshop 2010 Squaw Valley, USA: 791–794.

Eckerstorfer, M., Neumann, U., and Christiansen, H. H., 2008: High Arctic avalanche monitoring in maritime Svalbard. *Proceedings of the International Snow Science Workshop 2008 Whistler, Canada*, 7: 784–790.

Fierz, C., Armstrong, R. L., Durand, Y., Etchevers, P., Greene, E. M., McClung, D. M., Nishimura, K., Satyawali, P. K., and Sokratov, S. A., 2009: *The International Classification for Seasonal Snow on the Ground*. Paris: IHP-VII Technical Documents in Hydrology No. 83, IACS Contribution No. 1, UNESCO-IHP: 90 pp.

Fitzharris, B. B., 1987: A climatology of major avalanche winters in western Canada. *Atmosphere-Ocean*, 25: 115–136.

Førland, E. J., Hanssen-Bauer, I., and Nordli, P. Ø., 1997: Climate statistics and longterm series of temperature and precipitation at Svalbard and Jan Mayen. *Rapport 21/97 - Report Series of the Norwegian Meteorological Institute*, 92 pp.

French, M. H., 2007: *The Periglacial Environment.* Third edition. Chichester, U.K. and Hoboken, New Jersey: John Wiley & Sons, 458 pp.

Haegeli, P., and McClung, D. M., 2003: Avalanche characteristics of a transitional snow climate—Columbia Mountains, British Columbia, Canada. *Cold Regions Science and Technology*, 37: 255–276.

Haegeli, P., and McClung, D. M., 2007: Expanding the snow-climate classification with avalanche-relevant information: initial description of avalanche winter regimes for southwestern Canada. *Journal of Glaciology*, 53: 266–276.

Hanssen-Bauer, I., Kristensen Solås, M., and Steffensen, E. L., 1990: The climate of Spitsbergen. 39/90 Klima –Report Series of the Norwegian Meteorological Institute: 40 pp.

Humlum, O., 2002: Modelling late 20th-century precipitation in Nordenskiold Land, Svalbard, by geomorphic means. *Norsk Geografisk Tidsskrift–Norwegian Journal of Geography*, 56: 96–103.

Humlum, O., Instanes, A., and Sollid, J. L., 2003: Permafrost in Svalbard: a review of research history, climatic background and engineering challenges. *Polar Research*, 22: 191–215.

Ikeda, S., Wakabayashi, R., Izumi, K., and Kawashima, K., 2009: Study of snow climate in the Japanese Alps: Comparison to snow climate in North America. *Cold Regions Science and Technology*, 59: 119–125.

Jaedicke, C., and Gauer, P., 2005: The influence of drifting snow on the location of glaciers on western Spitsbergen, Svalbard. *Annals of Glaciology*, 42: 237–242.

Jamieson, B., 1999: The Compression test—After 25 years. *Avalanche Review*: 1–9.

Juliussen, H., and Humlum, O., 2008: Thermal regime of openwork block fields on the mountains Elgåhogna and Sølen, central-eastern Norway. *Permafrost and Periglacial Processes*, 19: 1–18.

Koeppen, W., 1936: *Das geographische System der Klimate*. Handbuch der Klimatologie. Bd.1, Teil C, Berlin, Borntraeger: 1–44.

Kottek, M., Grieser, J., Beck, C., Rudolf, B., and Rubel, F., 2006: World map of the Koeppen-Geiger climate classification updated. *Meteorologische Zeitschrift*, 15/3: 259–263.

LaChapelle, E. R., 1966: Avalanche forecasting—A modern synthesis. *International Symposium on the Scientific Aspects of Snow and Ice Avalanches - IAHS Publication*, 69: 350–357.

McClung, D. M., and Schaerer, P., 2006: *The Avalanche Handbook*. 3rd edition. Seattle: The Mountaineers, 342 pp.

Mock, C. J., and Birkeland, K. W., 2000: Snow avalanche climatology of the western United States mountain ranges. *Bulletin of the American Meteorological Society*, 81: 2367–2392.

Phillips, M., and Schweizer, J., 2007: Effect of mountain permafrost on snowpack stability. *Cold Regions Science and Technology*, 47: 43–49.

Schweizer, J., 1999: Review of dry snow slab avalanche release. *Cold Regions Science and Technology*, 30: 43–57.

Schweizer, J., and Wiesinger, T., 2001: Snow profile interpretation for stability evaluation. *Cold Regions Science and Technology*, 33: 179–188.

Schweizer, J., Jamieson, B. J., and Schneebeli, M., 2003: Snow avalanche formation. *Reviews of Geophysics*, 41: 1–25.

Sturm, M., and Holmgren, J., 1995: A seasonal snow cover classification system for local to global applications. *Journal of Climate*, 8: 1261–1283.

Winther, J.-G., Bruland, O., Sand, K., Gerland, S., Marechal, D., Ivanov, B., Glowacki, P., and Koenig, M., 2003. Snow research in Svalbard - an overview. *Polar Research*, 22: 125–144.

MS accepted September 2010

Paper 2

Natural cornice fall avalanche that released in April 2009 in the valley Todalen. I am standing on a collapsed piece of cornice. Photo by Ulli Neumann.

Paper 3

Fracture line of a natural dry slab avalanche on Sukkertoppen in December 2010. The fracture crown has a maximum height of 150 cm.

Paper 4

Slush avalanche that released in March 2011 in Todalen. The slush avalanche has a maximum slide distance of 200 m.

Paper 5

A cornice that detached from the plateau by opening a tension fracture on Gruvefjellet in April 2008. I am investigating the crack. Photograph by Ulli Neumann.

The Cryosphere, 6, 1–15, 2012
www.the-cryosphere.net/6/1/2012/
doi:10.5194/tc-6-1-2012

The Cryosphere

Cornice dynamics and meteorological control at Gruvefjellet, Central Svalbard

S. Vogel[1,2], **M. Eckerstorfer**[1,2], **and H. H. Christiansen**[1,2]

[1]Arctic Geology Department, The University Centre in Svalbard, UNIS, Norway
[2]Department of Geosciences, University of Oslo, Norway

Correspondence to: S. Vogel (stephancvogel@googlemail.com)

Received: 29 June 2011 – Published in The Cryosphere Discuss.: 25 August 2011
Revised: 13 January 2012 – Accepted: 18 January 2012 – Published:

Abstract. Cornice fall avalanches endanger life and infrastructure in Nybyen, a part of Svalbard's main settlement Longyearbyen, located at 78° N in the High Arctic. Thus, cornice dynamics – accretion, cracking and eventual failure – and their controlling meteorological factors were studied along the ridgeline of the Gruvefjellet plateau mountain above Nybyen in the period 2008–2010. Using two automatic time-lapse cameras and hourly meteorological data in combination with intensive field observations on the Gruvefjellet plateau, cornice process dynamics were investigated in larger detail than previously possible. Cornice accretion starts directly following the first snowfall in late September and October, and proceeds throughout the entire snow season under a wide range of air temperature conditions that the maritime winter climate of Svalbard provides. Cornice accretion is particularly controlled by distinct storm events, with a prevailing wind direction perpendicular to the ridge line and average wind speeds from $12\,\mathrm{m\,s^{-1}}$. Particularly high wind speeds in excess of $30\,\mathrm{m\,s^{-1}}$ towards the plateau ridgeline lead to cornice scouring and reduce the cornice mass both vertically and horizontally. Induced by pronounced air temperature fluctuations which might reach above freezing and lead to midwinter rainfall events, tension cracks develop between the cornice mass and the plateau. Our measurements indicate a linear crack opening due to snow creep and tilt of the cornice around a pivot point. Four to five weeks elapsed between the first observations of a cornice crack until cornice failure. Throughout the two snow seasons studied, 180 cornice failures were recorded, of which 70 failures were categorized as distinctive cornice fall avalanches. A clear temporal pattern with the majority of cornice failures in June was found. Thus only daily air temperature could determine avalanche from non-avalanche days. Seven large cornice fall avalanches reached the avalanche fans on which the Nybyen settlement is located. The size of the avalanches was primarily determined by the size of the cornice that detached. The improved process understanding of the cornice dynamics provides a first step towards a better predictability of this natural hazard, but also highlights that any type of warning based on meteorological factors is not an adequate measure to ensure safety of the housing at risk.

1 Introduction

1.1 Motivation and scope of the study

Cornices are broadly defined as wedge-like projections of snow formed by wind deposition on the lee side of a ridgeline or slope inflection (Latham and Montagne, 1970; Montagne et al., 1968). Cornices and their dynamics have attracted the curiosity and concern of both scientists and mountaineers in the past, due to their particular shapes and their ability to trigger avalanches when breaking off (Latham and Montagne, 1970). However, there has been surprisingly little modern research on cornices and their dynamics. By developing and running a full year observation programme, we have been able to study the processes leading to cornice failures in great detail. In the study area in Svalbard, cornices form every winter along the lee edges of extensive plateau mountains. We have chosen to study the cornices along the plateau

mountain Gruvefjellet bordering the valley Longyeardalen, where Longyearbyen, Svalbard's main settlement, is located, and most people live in this archipelago.

Cracks develop between the plateau and the main cornice mass, leading to a detachment and eventually failure of the cornices as cornice fall avalanches. This process causes a natural hazard to the infrastructure and people living right underneath the slope. Today, there is no protection measure in place in the Nybyen study area. Cornice fall avalanches have destroyed cultural heritage on the slopes in the Longyeardalen valley in recent years. We have thus monitored and analysed cornice accretion, cracking and failure along the edge of the plateau mountain, and their controlling meteorological and topographical factors in the 2008–2010 period. This study forms the first comprehensive investigation of cornice formation and failure carried out in a High Arctic landscape. Our goal is to provide increased geomorphological understanding of cornice dynamics, and thereby also improving the predictability of cornice fall avalanches.

1.2 Earlier cornice studies

Due to the general scarcity of studies on cornice formation and failure, no comprehensive overview exists. There are, however, a few very detailed basic studies on different parts of the cornice formation process. Major fundamental work on cornices was carried out by Paulcke and Welzenbach in the 1920's in the European Alps (Paulcke and Welzenbach, 1928; Welzenbach, 1930), where they trenched cornices to accurately define the stratigraphy, as well as to distinguish between different kinds of cornices due to their formation (suction vs. pressure cornices), duration (permanent vs. temporary), topographical position (ridge vs. plateau), as well as the topographical control on cornice development. Furthermore they described the process of involution, and thereby the formation of roll cavities (Fig. 1) inside the cornices – a term later introduced by Montagne et al. (1968). Seligman (1936) translated the most technical terms invented by Paulcke and Welzenbach into English, and found varying cornice development depending on the inclination of the lee slope. Montagne et al. (1968) focussed on deformation processes inside the cornice mass, attributing creep and glide processes to the opening of tension fractures between the cornice mass and the ridgeline bedrock. Their studies followed work mainly on cornice accretion processes. Besides initial binding of the snow crystals by mechanical interlocking, the refreezing of a liquid water layer due to frictional contact and pressure melting at temperature close to 0 °C as well as the importance of electrical forces in the adhesion process were investigated by Latham and Montagne (1970). These authors concluded that all three suggested mechanisms might contribute to the development of snow cornices. Naruse et al. (1985) compared mean grain diameter, bulk density and hardness of the surface layer (0.05–0.15 m) along the cornice root and roof as well as the scarp (Fig. 1). These were found to be largest at the cornice root and roof as a result of sorting of snow particles in the deposition-erosion process. Smaller particles are more likely to be transported over the face by wind or collide with falling particles and redeposit at the scarp. McCarty et al. (1986) monitored a particular cornice during a one-month period and conducted density, strength, temperature, and physical properties profiles. Irrespective of the short observation period, the study demonstrated the quick response of the cornice to changes in meteorological conditions. Kobayashi et al. (1988) analyzed the formation processes of snow cornices in an experimental trench and calculated collection coefficients in the range of 2 % to 50 % of windblown snow particles at the newly forming cornice as well as along a mountain ridge. Burrows and McClung (2006) identified key meteorologically-related triggers of cornice failure: loading of the cornice by additional snow (precipitation or wind), distinctive temperature changes due to air temperature changes and rain-on-snow events or direct insolation.

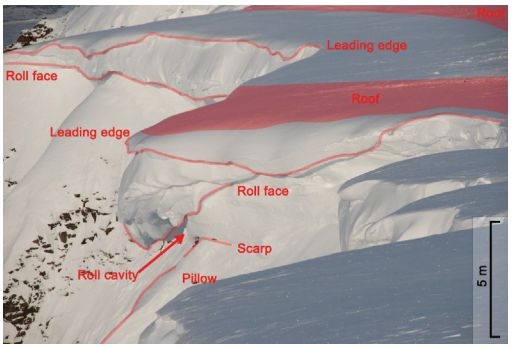

Fig. 1. Cornice profile showing the used cornice terminology, exemplified on a cornice from the study site at Gruvefjellet, Longyeardalen valley, Svalbard. Photo from 31 March 2010.

2 Study area

2.1 Geology and geomorphology

Longyearbyen (78° N, 15° E), Svalbard's main settlement is situated in the valley Longyeardalen, in the central part of the archipelagos main island Spitsbergen in the High Arctic (Fig. 2). Longyeardalen extends NE–SW, delimited by two large plateau mountains, Platåberget and Gruvefjellet to the W and E respectively (Fig. 2). The extensive plateaus consists of close to horizontal bedded Tertiary sedimentary rock (Major et al., 2001), into which Quaternary glaciations have eroded Longyeardalen. Svalbard lies in the continuous permafrost zone, with thicknesses ranging from approximately 100 m in valley bottoms and up to 400–500 m in mountain

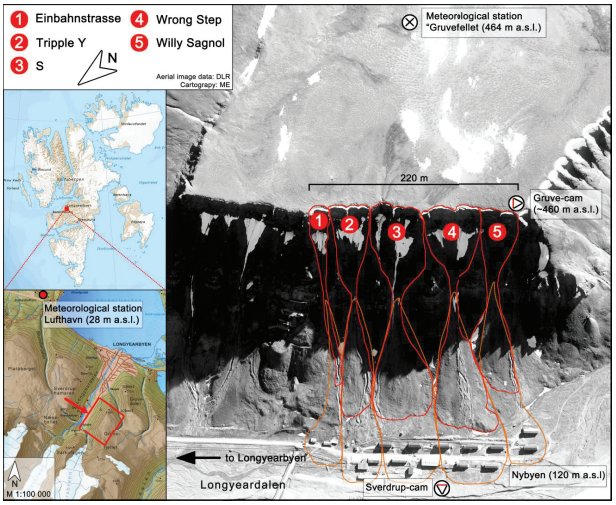

Fig. 2. Location of the study area in Svalbard and the detailed study site of the Gruvefjellet mountain slope above Nybyen in the valley Longyeardalen. The cornice site along the edge of the plateau mountain Gruvefjellet is 220 m long and subdivided into 5 larger funnels that narrow into gullies, intersected by hard rock noses. The red lines indicate the outline of the largest cornice fall avalanches observed in each of the 5 gullies during the 2008–2010 observation period, the orange line delimits the avalanche fans. The location of the meteorological stations Gruvefjellet and Lufthavn are indicated as well as the two automatic time-lapse cameras Gruve-cam on the plateau ridgeline and Sverdrup-cam on an artificial stockpile. The Sverdrup-cam real location is on the other side of the valley floor, about 1100 m away from the Gruvefjellet ridgeline.

areas (Humlum et al., 2003). The cornice study site contains a 220 m relatively sharp plateau ridgeline (about 460 m a.s.l) dividing the extensive three kilometre wide blockfields of the Gruvefjellet plateau from the steep underlying slope of Gruvefjellet (Fig. 2). The slope section below the ridgeline consists of an about 50–70 m high vertical free rock face, which below continues into a 55–60° steep slope at the upper part with a basal concavity. Rock outcrops in the middle part of the slope subdivide the cornice funnels into five distinctive avalanche paths, which reach down to the foot of the slope. The lower part of the valley side/slope consists of talus fans derived from rock fall but mainly from avalanche sedimentation, and are reworked by debris flows (Larsson, 1982) (Fig. 2). Seventeen houses accommodating more than 200 people are located on the basal concavity on the avalanche fans (Fig. 2).

2.2 Climate and meteorology

The climate of Svalbard is characterized as an ET polar tundra climate according to the Köppen-Geiger climate classification (Kottek et al., 2006). Svalbard is situated in a pathway of heat and moisture transport to the Arctic, thus the climate is sensitive to changes and is warmer than generally expected for the high latitude (Førland et al., 1997; Rogers et al., 2005). Svalbard's climate is mainly influenced by the interaction of the Icelandic Low with a high pressure over Greenland (Hanssen-Bauer et al., 1990). Thus typically in winter cold anti-cyclonic air masses extend to Svalbard from the north, alternating with low-pressure systems bringing warm and moist air masses due to meridional moisture transport along the North Atlantic cyclone track (Dickson et al., 2000).

The 1912–2010 annual air temperature average in Longyearbyen close to sea level is −6 °C, being almost 2 °C colder than the mean annual air temperature (MAAT) of −4.1 °C in 2010 (Met.no, 2011) recorded at the official meteorological station Lufthavn at 28 m a.s.l. (Fig. 2). 2008 with −4 °C and 2009 with −3.7 °C MAAT were also both warmer. At the Gruvefjellet meteorological station at 464 m a.s.l. on the central part of the Gruvefjellet plateau, 300 m from the study site (Fig. 2), the MAAT in 2010 was −6.7 °C, with almost the same values in 2008 −6.7 °C and in 2009 −6.1 °C. The mean snow season air temperature (MSSAT, 1 October–31 July) at Gruvefjellet was −8.7 °C in 2008/2009 and −6.8 °C in 2009/2010, while it was −6.2 °C in 2008/2009 and − 4.2 °C in 2009/2010 at the Lufthavn meteorological station.

Mean annual precipitation (MAP) at sea level (Lufthavn) in 2010 was 187 mm water equivalent (w.e.), the average of

1912–2010 was 196 mm w.e. (Met.no, 2011). MAP in 2008 was 200 mm and 153 mm in 2009 at the same site. Precipitation data from higher grounds do not exist. However, modelling results from Humlum (2002) suggest a vertical precipitation gradient with a 100 % upward correction factor. Since most of the precipitation falls as snow, accurate measurements in a landscape devoid of high vegetation are challenging.

Average snow season wind speed at Gruvefjellet was $4\,m\,s^{-1}$ in 2008/2009 and $3.9\,m\,s^{-1}$ in 2009/2010, with maximum wind speeds in both seasons exceeding $25\,m\,s^{-1}$ for shorter periods. Due to its constancy and the landscape being devoid of almost any vegetation, the wind freely redistributes snow in the landscape. While exposed parts of the landscape remain snow free for most of the winter, lee sides accumulate up to several meters of snow (Jaedicke and Gauer, 2005). The snowpack in the study area is generally thin and hard, characterised by wind slabs and ice layers (Eckerstorfer and Christiansen, 2011a). The prevailing winter wind direction in the 2008–2010 periods was from the SE on Gruvefjellet. Local wind directions vary due to topographical channelling effects (Humlum, 2002). However, on the study site the overall regional wind is dominating due to the wide Gruvefjellet plateau area, which enables extensive snow drifting and thus allowing cornice accretion.

3 Methods

The cornice development was studied during the two consecutive snow seasons 2008/2009 and 2009/2010. "Snow season" here refers to the duration of cornices along the Gruvefjellet plateau edge, lasting from the beginning of October until the end of July typically. During both snow seasons, 45 field trips up to the cornice site on the Gruvefjellet plateau were carried out (Fig. 3), as well as very frequent field investigations of the Gruvefjellet slope/valley side underneath the ridge. The majority of the fieldwork was conducted from mid January and onwards, when the snow cover of the Gruvefjellet slope was becoming continuous. Furthermore the beginning of the twilight period at the end of the polar night allows good enough detailed visual observations and measurements.

The magnitude of each cornice failure was determined by two values – the destructiveness (D) and the size relative to the given slope (R) (Greene et al., 2004). The D value describes the destructive potential of an avalanche from the mass of deposited snow, applied to an object (person, car, trees) located in the avalanche track or at the beginning of the runout zone. The R value estimates the size of an avalanche relative to the particular avalanche path length. R1 and R2 avalanches display small failures that ran out just below the free face and reaching down between the rock noses, respectively. R3 avalanches ran down below the rock noses to the upper part of the avalanche fans. R4 avalanches represent large cornice fall avalanches that reached the low inclined terrain on the lower part of the avalanche fans, indicated by the red lines in Fig. 2. As in particular the avalanches categorized as D2.5 and larger showed significant amounts of snow deposits in addition to the broken cornice blocks in the runout zone, we used the term "cornice fall avalanches". This also applied to the cornice failures in the very beginning and towards the end of the each snow season, when the snow cover on the slope beneath the cornices was shallow or even discontinuous and hence the amount of entrainable snow limited.

3.1 Automatic time-lapse photography observations

Two automatic digital time-lapse cameras were used to monitor directly, on an at least daily basis, cornice development and failure. Both cameras were standard digital cameras, equipped with a time-lapse controller (Harbortronics DigiSnap 2000 and similar custom-built) and a solar panel mounted on top of a weather-proof box, in which the camera and the entire set up was stored. A plastic window in front of the camera allowed the photographing from inside the box. Solar panels recharged a 12 V battery, which provided energy during the entire polar night and twilight period without charging. The photographs were stored as jpg-files on regular memory-SD cards, which were checked and changed at least every 2–4 weeks. Christiansen (2001) pointed out that automatic cameras provide additionally general weather information useful for understanding the process dynamics investigated specifically.

One camera "Gruve-cam" was placed perpendicular to the edge at the end of the cornice site (Fig. 2), photographing accretion, scouring and cracking as well as snow depth and general snow distribution, twice a day. As a consequence of the camera position and resolution, the most detailed observations were restricted to a short range of about 50–100 m, thus representing only a portion of the cornice site. To quantify changes in snow depth, snow stakes with a 5 cm scale were located along the ridge at the transition of the plateau to the cornice root; one of these as reference about 15 m in front of the camera. Snow stakes were first installed 11 February 2009, and readings could be done until 8 June 2009, with an accuracy of ± 5 cm. After the reinstallation of the reference snow stake, less than 10 m away from the "Gruve-cam", snow depth readings could be done with an increased accuracy of ± 2 cm in the snow season 2009/2010. Furthermore nine stakes were installed in a line on a prominent rock nose towards the cornice root perpendicular to the ridgeline, as suggested by Montagne et al. (1968). The stakes covered about 25 m, to visually determine the nature of deformation by a tilting of the stakes due to snow creep. Photographs were unfortunately not obtained between 28 April–16 May, 2 June–9 June and 6 September–1 November in 2009 due to technical operational camera problems (Fig. 3). In 2010, the period 18 March–6 May a malfunction of the battery, not

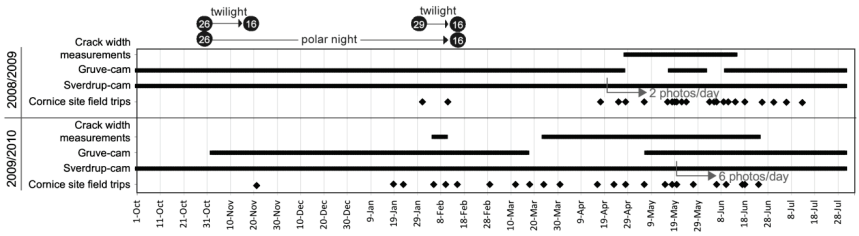

Fig. 3. Timing of field observations of the cornice study site for all the different observation methods used in the field during the snow seasons 2008/2009 and 2009/2010. Indicated is also the polar night period with start and end dates and both twilight periods.

being recharged by the solar panel, prevented collection of photographs (Fig. 3).

The other camera "Sverdrup-cam" was placed on the opposite side of Longyeardalen on an artificial stockpile, taking up to six daily photographs during the main avalanche season of the entire Gruvefjellet slope above Nybyen from 1100 m distance (Fig. 2). The high resolution of the DSLR camera enabled monitoring of all cornice failures of the study site in great detail, for improved directly linking to the meteorological conditions. The failures were assigned to one of the five major gullies (Fig. 2), and the recorded picture time of the automatic camera was taken as event timing, if there were no eyewitnesses to give directly the time of the avalanche. In general, light conditions during the polar night, snowstorms or very temporary snow accumulation in front of the camera lens affected this method negatively.

3.2 Cornice crack width measurements

Cornice crack measurements were conducted during the field visits once cracks started to open between the plateau and the cornice mass. Three series of cornice crack measurements with a total number of 29 readings were carried out in both snow seasons (Fig. 3). As a consequence of the appearance of cornice cracks, the three series of measurements were not conducted at the same cornice section. The setup consisted of two stakes, one installed on the plateau as the reference point, and one in the cornice mass, approximately 0.5 m away from the crack on the cornice side. Since the reference stake was installed on close to horizontal terrain and the snow cover on the plateau is particular dense, we considered the stake's position as constant. Furthermore the coverage by automatic time-lapse photography proved that the positions of snow stakes along the plateau edge were stable throughout the snow season. By repeated distance measurements stretching a rope permanently attached to the tip of the cornice stake, the relative opening of the cornice cracks was determined. This enabled easy manual recordings not causing any surface disturbance to the cornice root and roof except for the first installation. In the third series of measurements, the two stakes were also equipped with a scale to determine local relative variations in snow depth, and thus to investigate the influence of periods of cornice accretion and scouring on the cornice crack opening.

4 Results

Using the presented combination of methods we have been able to collect data that describe the complete cornice development process from accretion and scouring, to cracking, tilting of the cornice mass and eventual failure.

4.1 Cornice accretion and scouring

Periods of cornice accretion and scouring were identified by quantitative comparison of the time-lapse photographs in combination with the hourly meteorological data and direct field observations. The automatic camera data and direct field observations indicate that cornices grow to a significant size within a short time after the first snowfall. But at this stage we are unable to quantify this observation due to the lack of visibility during the polar night and the missing automatic photographs. Overall the first half of the snow season is characterized only by a shallow or even discontinuous snow cover until December. Cornice accretion proceeded during both entire snow seasons, when wind speeds averaged $12\,\mathrm{m\,s^{-1}}$, with a minimum of at least $10\,\mathrm{m\,s^{-1}}$, marking the lower limit of cornice accretion (Fig. 4). On average storm durations were about 46 h in the snow season 2008/2009 and 54 h in 2009/2010, with minimum periods in excess of 10 h in both seasons.

The prevailing wind direction during cornice accretion was very narrow at 120°, ± 5° (Fig. 4), almost perpendicular to the NNE-SSW orientated ridgeline (Fig. 2), whereas it varied much more 125–250° for non-accretion periods. Cornice accretion events were not influenced by air temperature. Figure 4 shows that even at air temperatures slightly above freezing, cornice accretion took place. This happened as a direct response to new snowfall on top of the cornice, even though the snow cover on the main plateau was already discontinuous close to the end of the snow season. In both snow seasons the last cornice remnants melted away along

the Gruvefjellet plateau edge towards the end of July. Thus, the cornices on Gruvefjellet are an annual and temporary phenomena with a clear seasonal cycle (Paulcke and Welzenbach, 1928; Welzenbach, 1930; Seligman, 1936).

Despite the lack of direct precipitation data the increased measured wind speed, and bad visibility due to snow drifting in front of the automatic camera during accretion events, clearly show that snowstorms largely accounted for accretion. Each accretion event added one or more snow layers onto the cornice mass. These wedge-like layers were initially bedded horizontally with a steeply inclined accretion face. Gradually the leading edge (Fig. 1) and consequently the entire cornice crept downwards, particularly under the load of successive accretion layers or air temperatures close to or above freezing, enabling fast snow creep/deformation (McClung and Schaerer, 2006). The formation of roll cavities (Montagne et al., 1968; Paulcke and Welzenbach, 1928) "Hohlkehle" was observed as this downward folding proceeded (Fig. 1). The roll cavities in general remained weak spots within the cornice mass and many partial failures have been observed along them.

Besides involution of the cornice and general snow settlement of the cornice mass, cornice scouring accounted for observable horizontal and vertical shrinking. Only two scouring events were identified, both occurred in the second snow season in the beginning of March (Fig. 5). During a snowstorm on 7 March 2010, cornice scouring was observed over a period of three hours with maximum wind gusts up to $32.4\,\mathrm{m\,s^{-1}}$, however, with winds from the S to SW. With this wind direction the strong winds blew almost straight towards the plateau edge, thus enabling scouring and not accretion. A total vertical reduction of 4 cm was recorded at the cornice root. With our study set-up it was not possible to quantify the variations in the horizontal extent of the cornices. Though, by comparison of the automatic photographs, significant shortening was determined as a consequence of the scouring events. The second scouring period occurred just one day later, lasting more than 7 h, reducing the cornice mass again by 4 cm vertically. The hourly maximum wind gusts were between 15–19 $\mathrm{m\,s^{-1}}$, and thus significantly lower than the previous event. Similarly, the wind direction was towards the plateau edge varying from WNW and NW. Both events took place during very different, but negative air temperature conditions (Fig. 5), which then does not seem to affect the scouring process.

4.2 Cornice cracking and tilting

Several cornice tension cracks between the plateau and the main cornice mass were observed in both snow seasons at the study site and the adjacent areas. Our time-lapse photography showed that a slight depression in connection with a bulge in the cornice root, followed by initial tilting of the cornice mass occurred in most cases before tension cracks appeared (Fig. 6a, b). These cornice cracks formed mostly at the transition from the shallow snowpack on the plateau to the inner part of the thicker cornice snow mass, where stresses due to tension were highest (Fig. 6c). We observed cornice cracks appearing very rapidly with a loud "bang" sound, as we unintentionally stepped onto the cornice root one time, adding load onto the cornice. With further opening of the cracks, lateral tension cracks developed at an obtuse angle to the initial cracking, forming a pronounced C-shape. This was contemporaneous with an upwards lifting of the inner and upper cornice mass (Fig. 6d). The cornice tilted around a fixed pivot point (Fig. 6e), which caused an even opening of the crack until the cornice mass displayed a very steep, close to vertical position (Fig. 6e). Thereby, parts of the cornice were lifted above its initial position along the plateau edge. Small failures progressively rounded the former leading edge and roll face, the majority of which occurred particularly along the roll cavities (Figs. 1 and 6d, e). These small failures also eroded the cornice scarp and pillow successively (Fig. 6e). The central cornice mass detached from the ridgeline in some cases, exposing cracks up to 3–4 m wide.

The most comprehensive cornice crack width distance measurements lasted from 24 March 2010 until 23 June 2010 (Fig. 7). At this site we combined the crack width distance measurements with the relative variation in snow depth, obtained from the two measurement stakes on the plateau and on the cornice (Fig. 7). The cornice crack was already open when the instrumentation was installed; we thus only monitored the relative opening of the cornice crack. Therefore 0 refers to the initial distance between the two stakes when the instrumentation was installed and the y-values in Fig. 7 do not express absolute crack distances. The first two measurements indicated a reduction of the crack by 20 cm over 22 days. Since we did not observe any actual closing of the crack, we explain this as a slight backward tilting of the cracked cornice mass. The measuring rope was permanently attached to the cornice stakes' tip to avoid being buried, so the slight backward tilting caused a reduction in the measured distance between the cornice stake and the plateau stake without actually reducing the cornice crack width (Fig. 6b). The onset of melting affected the position of both measurement stakes inserted into the snow during the last measurements, leading to stagnant width measurements. In the period between 16 April and 6 June 2010, a total cornice opening distance of 22 cm was measured, resulting in an average crack widening of $0.43\,\mathrm{cm\,day^{-1}}$. Regardless of air temperature fluctuations, the crack widening was almost linear (Fig. 7). Relative variation in snow depths on each site of the crack influenced the crack opening to some extent. For example, between 23 and 28 April 2010 the highest cornice crack opening rate of this series of $0.8\,\mathrm{cm\,day^{-1}}$ was recorded together with a pronounced increase in snow depth on the cracked cornice of 19 cm. However, in mid to end of May, no variations in snow depths were recorded, but the cornice crack still opened linearly (Fig. 7). The linear opening

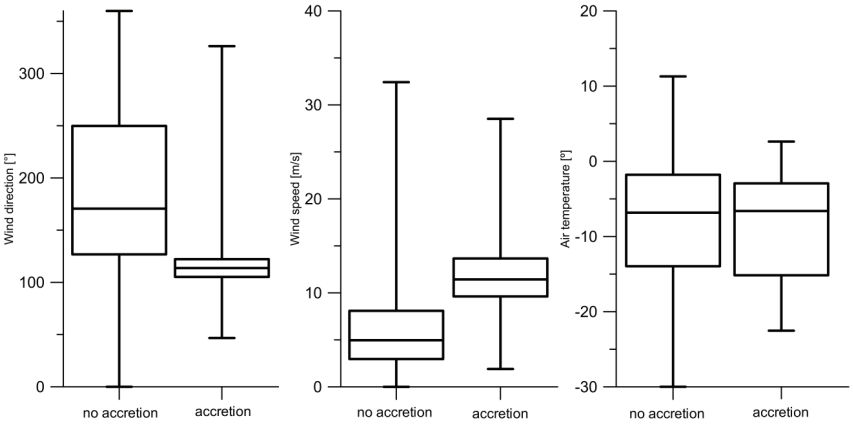

Fig. 4. Daily meteorological values recorded at the Gruvefjellet meteorological station for observed cornice accretion days ($N = 26$) and no accretion days (579) from both snow seasons.

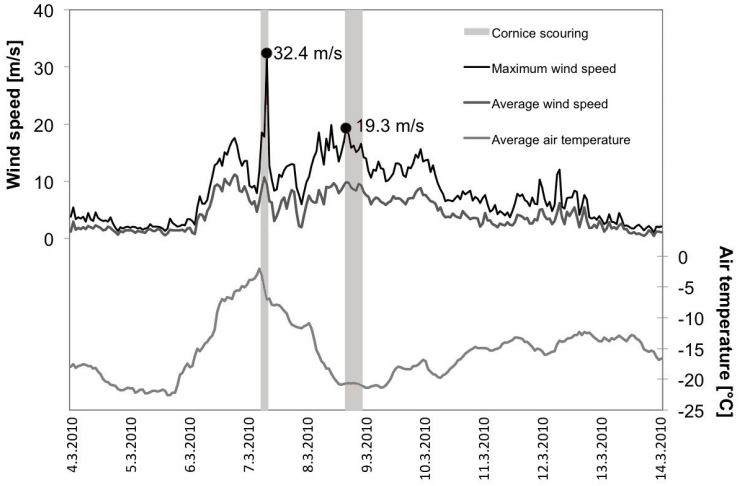

Fig. 5. Maximum and average wind speeds and air temperature recorded at Gruvefjellet meteorological station during the two observed cornice-scouring events.

rate, independently of snow depth and air temperature conditions clearly indicate, that after crack opening, the cornice mass was tilting around a fixed pivot point due to constant snow creep and deformation of the cornice.

The first series of measurements in the snow season 2008/2009 also showed a pronounced linear cornice crack opening (Fig. 8). During the period between 28 April and 6 June 2009, a cornice crack opened 105 cm after the crack was observed and the setup installed. Therefore the y-value 0 refers again to this initial distance between the two stakes. The average cornice crack opening of this period was 2.76 cm day^{-1} (Fig. 8). On 19 May 2009 a reduction of 21 cm to the previous day was measured. This was caused by a surface perturbation, where we observed the upper most layer of the cracked cornice part to be crept slightly towards the plateau, which affected the measurement stake. The following measurements indicated the same opening rate as prior to the perturbation.

The highest cornice crack opening rate of 8.6 cm day^{-1} was measured in a short series between 5 and 10 February

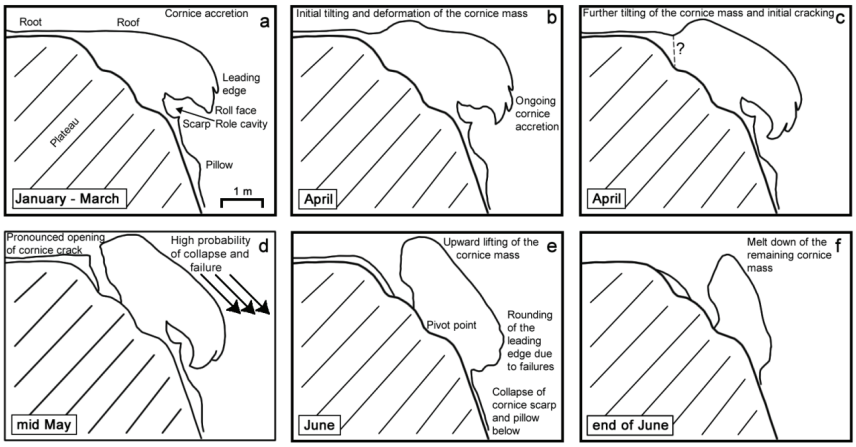

Fig. 6. Model of the seasonal stages of the annual cornice dynamics cycle from initial crack development, crack opening, upward lifting of the cornice mass to eventual failure or meltdown.

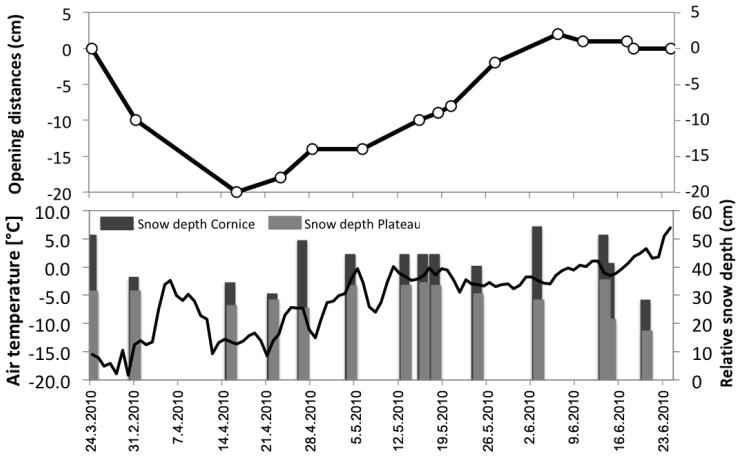

Fig. 7. Cornice crack width measurements, air temperature and relative snow depth from the snow season 2009/2010. The y-value 0 refers to the initial distance between the two stakes when the instrumentation was installed, so the y-values do not express absolute crack distances. Please observe that the crack width measurements indicate a reduction in the two first recordings, therefore the negative values.

2010. The series ended with an entire cornice failure. This was in contrast to the long lasting series of measurements, when melting conditions towards the end of the snow season prevented further accurate measurements. So crack opening rates of this size seem to lead to cornice failure.

In the snow season 2009/2010 the development of four cornice cracks until failure was observed in the "Gruve-cam" field of view. Thus using the time-lapse photographs, we were able to follow the entire cornice development from cracking and widening, to downward folding of the entire cornice mass (Fig. 6d) and eventually cornice failure (Fig. 9). In two of these failures we also observed initial cornice tilting (Fig. 6b), prior to the initial opening of the cornice cracks. Both initial tilting and crack opening occurred as a consequence of low-pressure systems passing Svalbard, causing snowstorms with increasing air temperatures (Fig. 9) close to or even above freezing, allowing significant deformation. After two weeks of initial tilting, the cornice cracks appeared open and a constant widening was observed for three and six weeks respectively, under varying meteorological conditions

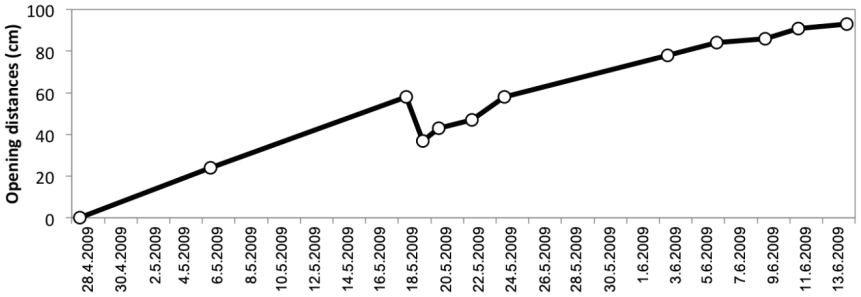

Fig. 8. Cornice crack width measurements from the snow season 2008/2009. The y-value 0 refers to the initial distance between the two stakes when the instrumentation was installed, so the y-values do not express absolute crack distances.

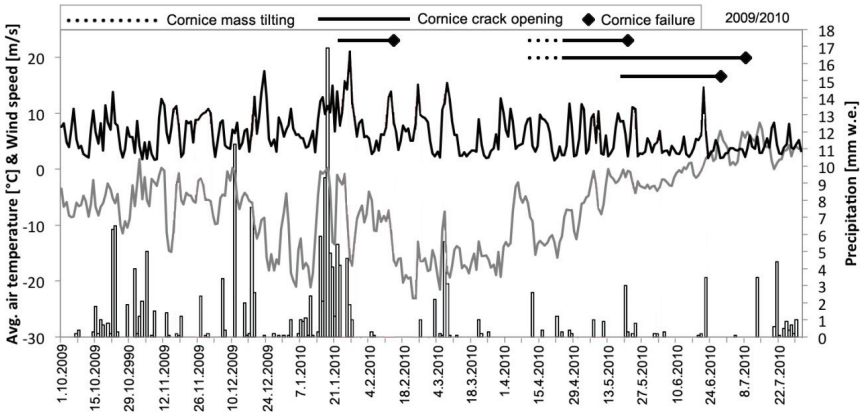

Fig. 9. Timing of cornice mass tilting, cornice crack opening and failure of 4 entire cornices in the camera's field of view in the snow season 2009/2010. Average daily air temperature (grey line) and average daily wind speed (black line) are recorded at the Gruvefjellet meteorological station. The precipitation data (columns) is from the Lufthavn meteorological station.

(Fig. 9). Also the time-lapse photographs of the the first snow season 2008/2009 and fieldwork observations outside the camera's field of view revealed very similar time periods for the cornice development. The data indicate that the period between crack development and eventual failure by reaching the particular cornice break over point can be variable. The observed periods averaged between four to five weeks. But the formation of cornice cracks did not necessarily lead to cornice failure and vice versa.

4.3 Cornice failure

In total 180 cornice failures were observed in the two snow seasons that were investigated (Fig. 10). There is a clear temporal pattern with the majority releasing between May to the end of June (Fig. 10). By then, full-developed cornices were able to crack and tilt through a period of time before failure. Besides entire cornice fall avalanches, the majority of the late season failures were mostly only collapses of cornice parts, like scarps or pillows, (Fig. 6c–e), or the release of lateral remnants of cracked cornices. Additionally the leading edge and accretion face of cracked and tilted cornices failed in relatively small pieces, leading to a rounding of the cornice mass (Fig. 6e). The temporal distribution of cornice failures differed somewhat between the two investigated snow seasons. No cornice failures occurred before May in the first snow season 2008/2009, while in particularly large failures were observed in the early part of the second snow season in December and February (Fig. 10). In the course of the two snow seasons, we did not observe any sizeable avalanches in our study area, which were not attributed to cornice failure.

On 13.7 % of all days in both snow seasons, cornice failures were observed. The temporal pattern of increasing cornice failures towards the end of the snow season is reflected

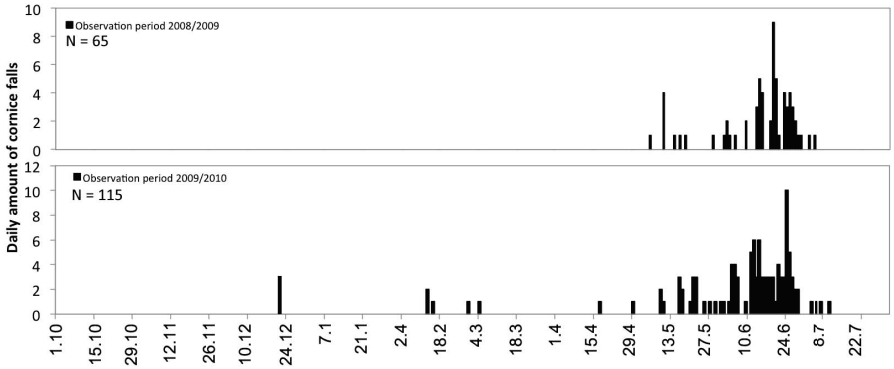

Fig. 10. Chronology of cornice failures for the Gruvefjellet study area in the two investigated snow seasons 2008/2009 and 2009/2010.

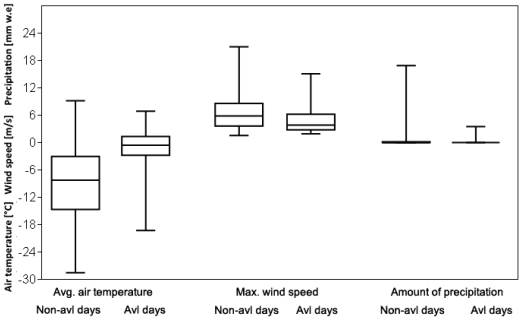

Fig. 11. Variation of daily meteorological values from the Lufthavn meteorological station during avalanche days (avl days) ($N = 73$) and non-avalanche days (non-avl days) ($N = 532$) from both snow seasons.

in the clear air temperature differences between avalanche and non-avalanche days (Fig. 11). The mean air temperature on avalanche days was −1.4 °C, which is significantly higher than on non-avalanche days with −8.9 °C (Fig. 11). However, error bars suggest that also on colder days, with air temperatures lower than the non-avalanche days mean, cornice fall avalanches occurred (Fig. 11). Both maximum wind speed as well as precipitation measurements from sea level cannot depict avalanche from non-avalanche days. This generally means, that at least in case of entire cornice failures, the meteorological conditions, except air temperature, concurrent with cornice failure are of less significance. Additionally direct insolation might contribute to this also, as we observed a trend of increased partial failures towards the late afternoon, when the sun hits the cornices.

Thirty-two percent of all 180 cornice failures were "D2R2" avalanches, capable of burying a person (Fig. 12). "D3R2" avalanches that ran out below the rock noses onto the upper avalanche fans, accounted for 22 % (Fig. 12). Seven cornice fall avalanches were categorized as "D3R4" avalanches, running close to infrastructure and capable of destroying it (Fig. 12). These avalanches had the longest run-out in each gully, indicated by the red outline on the avalanche fans in Fig. 2. Avalanche sizes were mostly correlated to the size of the failing cornice. The seven largest cornice fall avalanches were entire cornice falls that broke off right at the headwall. Thus the amount of entrainable snow in the avalanche path as well as the trigger of a secondary slab avalanche by the falling cornice, were of minor influence for the actual avalanche size. For these reasons, we also observed the largest cornice fall avalanches categorized as "D3R4" and "D3R3" avalanches in different parts of the snow seasons (Fig. 13), independent of the concurrent snow cover of the Gruvefjellet slope beneath. Generally the onset of the snow seasons was quite slow in both seasons, with only a shallow or even discontinuous snow cover by December (Eckerstorfer and Christiansen, 2011a). Similar snow conditions characterize the late part of the snow season in July, under the influence of melting. Despite this, both in December and June high magnitude events took place. There were some differences between the snow seasons. In 2008/2009 the first high magnitude (D3R4) failure was recorded on 3 June 2009, whereas in 2009/2010, the first "D3R4" cornice fall avalanche released already on 22 December 2009.

The size of cornice fall avalanches was also controlled by the size of the particular avalanche path as well as the size of the source area or starting zone along the ridgeline. The five avalanche paths (Fig. 2) differ considerably in their geomorphology along the plateau ridge. The spacing of major rock noses determines the horizontal width of the cornices along the plateau edge and consequently the size of the failures. The gullies "S" and "Wrong Step" are comparably wide and display continuous parts along the ridgeline. In contrast,

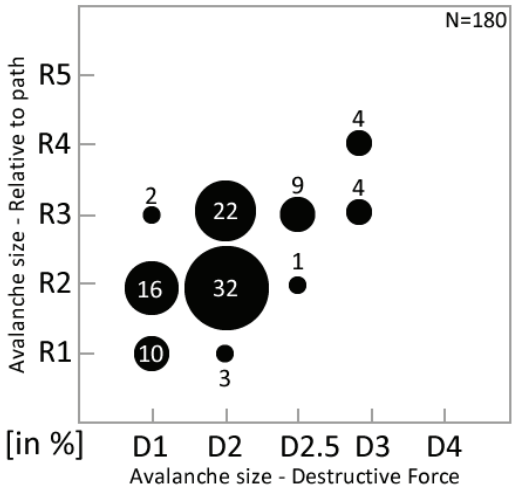

Fig. 12. Size distribution in % of all recorded cornice failures and their destructive potential (D) as well as size relative to path (R), according to the classification system by the American Avalanche Association (Greene et al., 2004), for both observed snow seasons.

in the most narrow avalanche gully path, "Einbahnstrasse", no large cornice fall avalanche released (Fig. 14) explaining the much smaller avalanche deposits extending below this (Fig. 2). On the other hand, 40 % of all cornice fall avalanches released in the avalanche gulley "Wrong step" were categorized as large "D3R4" failures (Fig. 14). The broad starting zone of this gully is only intersected by one rock nose (Fig. 2), thus enabling the built up of large continuous cornices. All but the confined avalanche path "Einbahnstrasse" had an almost similar amount of cornice failures with around 20 % of the total. The avalanche fans below "S" and "Wrong Step" are the largest in size (Fig. 2), most likely due to the highest cornice fall avalanche activity.

5 Discussion

5.1 Cornice accretion and scouring

26 cornice accretion days were identified, with a mean prevailing wind direction from SE and a mean wind speed of $12\,\mathrm{m\,s^{-1}}$ (Fig. 4). In turn, no difference was found in air temperature during accretion and non-accretion days. The somewhat higher mean accretion wind speed observed for the Gruvefjellet site compared to the $5–10\,\mathrm{m\,s^{-1}}$ stated by McClung and Schaerer (2006), can be explained by a commonly hard snow surface for the High Arctic setting (Eckerstorfer and Christiansen, 2011a). On a hard snow surface, the mean saltation lengths of drifting snow are generally larger (Kosugi et al., 2004), reducing the effective contacts of snow particles with the cornice mass and thus reducing cornices accretion. The entire snow season's average hourly maximum wind speed of $6\,\mathrm{m\,s^{-1}}$ is in the range, when snow particles are broken to smaller fragments (McClung and Schaerer, 2006). Also mechanical wind pressure leads to a densification of the near-surface part of the snowpack (Sokratov and Sato, 2001). Thus significant cornice accretion occurs during storm events with significantly higher wind speeds than the snow season's average.

Data on cornice scouring threshold wind speeds are sparse. Montagne et al. (1968) found wind speeds in excess of $27\,\mathrm{m\,s^{-1}}$ for cornice scouring, a value that was temporarily only reached twice during the entire observation period in Svalbard, and where scouring was observed during one of them. McClung and Schaerer (2006) stated that surface conditions, air temperature, humidity and other factors may cause variations in the cornice scouring threshold. Cornice scouring also highly depends on the concurrent snow surface hardness. A hard surface snow layer, due to persistent cold air temperatures or a surface ice layer, would probably alter the scouring effect. We observed only two cornice scouring events, both in the snow season 2009/2010 (Fig. 5). While the first event reached a record hourly maximum wind speed of 32.4 m the second event happened when the hourly maximum wind speeds varied between 19 and $15\,\mathrm{m\,s^{-1}}$. In contrast to cornice accretion, the wind direction during both events was almost perpendicular towards the ridgeline, and therefore against the rather frail cornice face and scarp below. Hourly maximum wind speeds similar to the latter scouring event were recorded several times in both snow seasons. But in contrast, these followed the prevailing wind direction from SE over the plateau and lead to cornice accretion.

Due to the time resolution of two pictures a day of the "Gruve-cam", short scouring events could have been missed. Still, we did not observe further significant shifts in the hourly meteorological data that we could associate with cornice scouring events. Despite their comparably low duration of only a few hours, both identified scouring events reduced the cornice mass significantly – vertically by 4 cm and also in the horizontal direction, but with our study set-up it was not possible to quantify these variations. In general due to the scarcity of scouring events visually observed by the Gruvefjellet automatic camera, and the absence of scouring events during the entire snow season 2008/2009, their general impact on cornice development cannot be discussed in more detail.

5.2 Cornice cracking and tilting

We observed numerous cornice cracks between the plateau and the main cornice mass in both snow seasons. Six of these were in the visual field of the "Gruve-cam" automatic camera, which additionally enabled detailed analysis. A very close relationship between the opening of these cornice tension cracks in connection with a prior tilting of the cornice

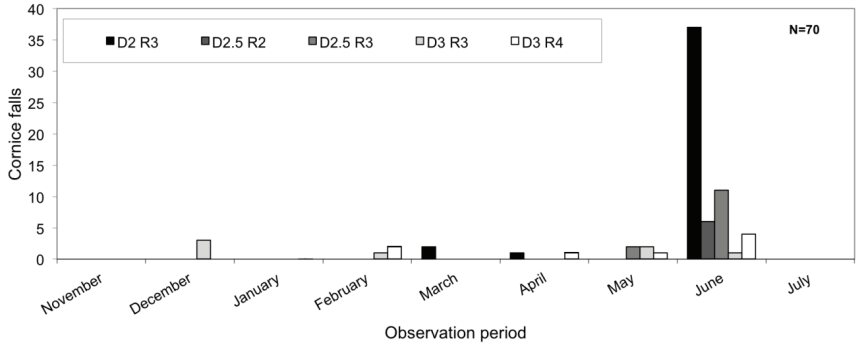

Fig. 13. The monthly distribution of the 70 cornice fall avalanches categorized as "D2R3" or larger for both observed snow seasons. Classification according to Greene et al. (2004).

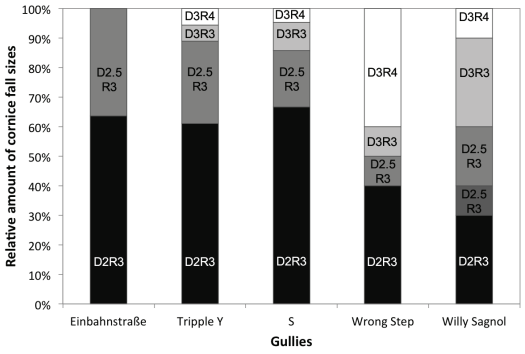

Fig. 14. Relative amount of cornice fall avalanche types per gully for both snow seasons along the 220 m long Gruvefjellet study area.

mass and very pronounced air temperature fluctuations appeared. Significant air temperature increases were caused by low-pressure systems reaching Svalbard, resulting in relatively warm and moist air masses and high wind speeds during snowstorms. Very pronounced was the appearance of a cornice crack observed on 23 January 2010 after a distinct warming period of 3 days (13–15 January 2010) with maximum air temperatures of 3.5 °C at Gruvefjellet and 34 mm of rain at sea level. As a consequence, slush and wet slab avalanches released in an extreme avalanche cycle in the Longyearbyen area, even at higher elevations than the Gruvefjellet study site (Eckerstorfer and Christiansen, 2012). Thus, the meteorological conditions that lead to extensive other type avalanching, also significantly influenced the cornices development. Conway (1998) found an immediate increase in the surface layer creep rate as a consequence of rain-on-snow events, which thus led to a decrease in slab stability. Observations of slab fracture mechanics may also account for cornice stability due to their particular cantilevered slab structure (Burrows and McClung, 2006).

Besides the early season processes, cornice tension cracks appeared also later in the snow seasons under the influence of solar radiation and generally higher temperatures. Schweizer and Jamieson (2010) investigated the effect of surface warming on snowpack stability. They suggest that increased deformation within the near-surface layer of a slab accounted for the instability in the case of dry-snow slab avalanches. Surface layer stiffness can be effectively reduced by surface penetrating solar radiation, which in turn directly affects snow stability (Schweizer and Jamieson, 2010) also affecting cornices. We found a trend of increased cornice failures during the late afternoon, when the sun hits the cornices. Still, these cornice failures were mostly partial failures of comparable lower magnitude. The meteorological station situated on the Gruvefjellet plateau does not record solar radiation, but it might be useful to analyze the relationship of solar radiation and cornice activity in greater detail.

Generally, Montagne et al. (1968) attributed the development of cornice cracks to on-going creep and glide processes. These deformation/creep processes also lead to the linear opening of the cornice cracks independent of variation in air temperature observed in the two longer series of cornice crack measurements, and the downward folding of the entire cornice mass around a pivot point.

The particular site and the nature of cornices demonstrate some crucial limitations for any kind of more sophisticated cornice crack installations as the sudden collapse of a cracked cornice could destroy the installations and impede collection of data. We observed a geomorphological determined sedimentary step approximately 3 m below the plateau surface in the upper free face that most likely acts as the pivot point. Here at the cornice foot, temperatures presumably remain constantly low due to efficient isolation by the thick

cornice mass from air temperature fluctuations recorded also after crack initiation. The isolation character of the snowpack became apparent on 23 April 2010, when widespread surface hoar was observed in the close surrounding of the most recently opened cornice cracks being exposed to the cold air. Thus the cornice might actually freeze onto the free face, as melt water that forms in the open exposed parts of the crack will percolate down towards the pivot point where temperatures will be constantly lower. This freezing might be the reason why numerous cornice failures do not involve the cornice roots, which often remains at the plateau edge and only melt down at the very end of the snow season in late July.

5.3 Cornice failure

We observed a total of 180 cornice failures during the two snow seasons, with a clear temporal pattern of increased cornice fall activity towards the end of both snow seasons (Fig. 10). 70 of these were categorized as "D2R3" avalanches and larger. To the authors' knowledge, this represents the first, comprehensive cornice failure monitoring performed. Likewise the literature is in general sparse on rates of cornice failure. Burrows and McClung (2006) described meteorological-related triggers, similar to those of slab avalanches. McCarty et al. (1986) monitored cornice strength using, among other methods, ram profiles, stating that cornices and their internal temperature variability respond quickly to their meteorological environment. In particular, the most exposed overhanging cornice roof indicated variations in cornice strength. However, analysing the success of explosives for dislodging cornices, McCarty et al. (1986) concluded that the strength of cornices may often be unpredictable.

In both snow seasons, we did not observe one single complete cornice failure as a direct response to snow loading and increasing air temperatures caused by a snowstorm. Snowstorms and associated air temperature fluctuations caused the initial cracking, which was observed in all except one case of complete cornice failure. Therefore the meteorological conditions leading up to the complete cornice failures are of less direct importance than the length of time since crack initiation and proximate tilting. For the cornice cracks that were studied, the length of time between crack initiation and failure varied between four to five weeks. The duration until eventual failure seemed to be primarily controlled by the micro-topography along the ridgeline, where the cornice foot was resting, and thus the particular break over point of the cornice. In many cases, the delimiting rock noses at the Gruvefjellet cornice site largely supported the cornice laterally (Fig. 2), preventing it from breaking off completely. In comparison, at an adjacent site further south, these rock outcrops are less pronounced and the headwall below the ridge is vertical, giving significantly less support to the cornice mass. Here, cracked cornices reached their break over point evidently faster, resulting also in more entire cornice failures. Thus in general, the size of the cornice, the micro topography along the plateau edge and the size of the avalanche path determined the cornice fall avalanche magnitude.

The amount of entrainable snow was of less importance as we observed high magnitude failures in different parts of the snow season. Despite of maximum snow depth on the slope around April, cornice fall avalanches categorized as "D3R4" avalanches occurred both in the very beginning and towards the end of the snow season, when the snow cover on the slope was shallow or even discontinuous. The timing of cornice fall avalanches at the study site is comparable to the overall timing of releases in the Longyearbyen area, with maximum activity between April and June (Eckerstorfer and Christiansen, 2011b). Seven cornice fall avalanches observed reached the "D3R4" size, capable of destroying infrastructure (Fig. 12). None of them actually reached the infrastructure. Earlier observations of cornice fall avalanches (Vogel, 2010), beginning in 2005/2006, confirm an annual return period of cornice fall avalanches categorized as "D3R4" avalanches at the study site, with housing infrastructure at the foot of the slope.

Despite the high frequency of cornice fall avalanches in our study area, we did not observe slab avalanches triggered by cornice failures, which involved substantial amounts of snow. Irrespective the actual size of the cornice fall avalanche, single cornice blocks reached significant longer runout length than the main avalanche mass. The avalanche fans that the Nybyen houses stand on the outer part of (Fig. 2) indicate higher magnitude avalanches in the past. Thus a large magnitude failure could be highly destructive, but the return period is unknown. The only evidence of such a size avalanche is from a cornice fall on the Gruvefjellet slope immediately north of the study area in March 2009. This cornice fall avalanche ran across the street and destroyed an old mining transport tower situated in its avalanche path on the valley side. This tower was built in 1938, and has not been destroyed in its roughly 70 yr period, which allows for some vague estimation of the return period of these extremely large cornice falls. Today there is no protective measure in place and a temporary closure of the slope has been proving to be ineffective. Thus, giving the potential of a destructive cornice fall avalanche, the forecasting accuracy based on meteorological factors is not adequate to ensure safety of life and infrastructure in Nybyen. An overview of mitigation measures, their application and effectiveness is given in Chaudhary and Singh (2006). Possible mitigation measures for a very comparable site in western Iceland are discussed by Hákonardóttir et al. (2008) and focus on a combination of snow fences in multiple rows on the plateau normal to the prevailing wind direction and a series of wind baffles along the plateau edge. McCarty et al. (1986) reviews the effectiveness of cornice control using explosives.

6 Conclusions

This study most likely represents the first and most comprehensive full season cornice process observations of its kind from the High Arctic landscape. During the course of the two snow seasons 2008/2009 and 2009/2010 we investigated the cornice development from accretion to cracking and eventual failure, and delimited their meteorological controls, along the ridgeline of the plateau shaped mountain Gruvefjellet in central Svalbard. Using automatic time-lapse photography in combination with manual fieldwork observations and hourly meteorological data enabled us to document the entire cornice development, identifying the period of cornice accretion and scouring as well as observing cornice failures with high time resolution, thus improving the geomorphological cornice process understanding. A conceptual annual model including the seasonal cornice dynamics has been established (Fig. 6). It shows that the cornices are seasonal and existed during the two observed snow seasons from the beginning of October to the end of July, when the last cornice remnants melted away along the plateau edge.

The extensive plateau mountain Gruvefjellet with the very distinct western edge located almost perpendicular to the prevailing winter wind direction, are the key factors controlling significant cornice development that was studied. The 26 days of cornice accretion occurred throughout the entire snow season under a wide range of air temperatures, with a mean hourly maximum wind speed of $12\,\mathrm{m\,s^{-1}}$ and the average duration of the storms lasting 46 h in the snow season 2008/2009 and 54 h in the snow season 2009/2010. Only in the second snow season, two periods of cornice scouring could be identified, which both reduced the cornice mass vertically by 4 cm, but also somewhat horizontally. The cornice scouring events indicate that strong winds towards the leading edge can erode the cornices and thus have a significant effect of the cornice development.

Pronounced air temperature fluctuation induced by low-pressure system reaching Svalbard, causing snowstorms, led to the opening of the cornice tension cracks detaching the cornice main mass from the plateau edge due to additional loading of the cornices. In some cases initial tilting of the cornice mass due to deformation prior to the appearance of cornice cracks was observed. Despite large air temperature variations the cornice crack opening revealed a linear opening distance, which we attribute to constant snow creep at the cornice foot, where the temperature conditions remain steady due to thick snow covering insulation and thus enabling the freezing onto the backwall in the permafrost environment. Thus the entire cornice mass was bending downwards around a pivot point. In some cases the central cornice mass detached from the ridgeline exposing cracks up to 3–4 m wide. The three conducted series of crack widening measurements indicate varying average opening rates of 0.43, 2.76 and $8.6\,\mathrm{cm\,day^{-1}}$. Only the highest rate from the short series of measurements led to a complete cornice failure. The micro-topography of the ridgeline presumably controls the cornice crack opening rate as well as the particular break over point of the cornice. The installation of tiltmeters at an early stage of cornice development might give deeper insights into the processes leading up to the appearance of cornice cracks, but certainly pose a high risk of losing the equipment due to complete failure. The duration from initial cracking to eventual failure of the cornices was on average four to five weeks, but not all cornices failed completely. In the cases of entire cornice fall avalanches, the meteorological conditions leading directly up to the cornice failures were of less significance than the duration since crack initiation. Distinct air temperature variations and significant snow loading/growth of the cornices mainly associated with storm events, however, are found to account for initial cracking of the cornices, which thus may lead to eventual failure after a period of time.

In the snow seasons that were studied, 180 cornice failures were observed, of which 70 were categorized as "D2R3" and larger cornice fall avalanches. 80 % of the cornice failures occurred towards the end of the snow season in June. However, cornice fall avalanches in the early part of the snow seasons were in particular entire cornice failures displaying the brittle behaviour of cornices. The seven largest cornice fall avalanches were classified as "D3R4" avalanches, which reached relatively close to inhabited housing infrastructure without permanent protective measures. Comparing these results with avalanche field observations since 2005/2006 revealed an annual return period of "D3R4" size cornice fall avalanches in the studied slope section. Therefore cornice fall avalanches represent a recurrent natural hazard for the residents and infrastructure in the Nybyen area. Continuous observations might be useful to develop more sophisticated models for large-scale cornice avalanche failures, and to refine the forecasting accuracy. However, our results also highlight that cornice fall avalanches are in particular hard to forecast and that any type of warning is not an adequate measure to take to ensure safety of the housing at risk. Permanent protective measures either on the plateau, along the plateau edge or located on the basal concavity of the slope would without doubt increase the safety for life and infrastructure.

Acknowledgements. This project was financed partly by the University Centre in Svalbard, UNIS and the CRYOSLOPE Svalbard Norklima research project 2006–2009, coordinated from the University Centre in Svalbard. Researchers in the project are thanked for valuable scientific discussions, especially Ole Humlum. We also want to acknowledge Ulrich Neumann for brilliantly helping with fieldwork and field instrument maintenance. The aerial image and DEM in Fig. 1 are kindly provided by Ernst Hauber from the German Aerospace Center, Institute of Planetary Research. Comments from reviewers K. Kronholm and B. Glude assisted us in clarifying our results.

Edited by: D. Hall

References

Burrows, R. and McClung, D. M.: Snow Cornice Development and Failure Monitoring, International Snow Science Workshop, Telluride Colorado, 2006.

Chaudhary, V. and Singh, G.: Structural Measures for Controlling Avalanches in Formation Zone, Defence Sci. J., 56, 791–799, 2006.

Christiansen, H. H.: Snow-cover depth, distribution and duration data from northeast Greenland obtained by continuous automatic digital camera, Ann. Glaciol., 32, 102–108, 2001.

Conway, H.: The impact of surface perturbations on snow-slope stability, Ann. Glaciol., 26, 307–312, 1998.

Dickson, R. R., Osborn, T. J., Hurrell, J. W., Meincke, J., Blindheim, J., Adlandsvik, B., Vinje, T., Alekseev, G., and Maslowski, W.: The Arctic ocean response to the North Atlantic Oscillation, J. Climate, 13, 2671–2696, 2000.

Eckerstorfer, M. and Christiansen, H.: The "High Arctic Maritime Snow Climate" in Central Svalbard, Arctic. Alpine Res., 43, 11–21, 2011a.

Eckerstorfer, M. and Christiansen, H.: Topography and meteorological control on snow avalanching in the Longyearbyen area, central Svalbard 2006–2009, Geomorphology, 134, 186–196, 2011b.

Eckerstorfer, M. and Christiansen, H. H.: Meteorology, topography and snowpack conditions causing extreme mid-winter slush and wet slab avalanches in High Arctic maritime Svalbard, Permafrost Periglac., in press.

Førland, E. J., Hanssen-Bauer, I., and Nordli, P.Ø.: Climate statistics and longterm series of temperature and precipitation at Svalbard and Jan Mayen, Norwegian Meteorological Institute, Klima, 21, 1–72, 1997.

Greene, E. M., Birkeland, K. W., Elder, K., Johnson, G., Landry, C., McCammon, I., Moore, M., Sharaf, D., Sterbenz, C., Tremper, B. and Willimas, K.: Snow, Weather, and Avalanches: Observational Guidelines for Avalanche Programs in the United States, American Avalanche Association, Pagosa Springs, Colorado, 150, 2004.

Hákonardóttir, K. M., Margreth, S., Tómasson, G. G., Indriłdason, H. D., and Þórðarson, S.: Snow drift measures as protection against snow avalanches in Iceland, International Symposium on Mitigative Measures against Snow Avalanches, Egilsstaldir, Iceland, 2008.

Hanssen-Bauer, I., Kristensen Solås, M., and Steffensen, E. L.: The climate of Spitsbergen, Norwegian Meteorological Institute, 1990.

Humlum, O.: Modelling late 20th-century precipitation in Nordenskiold Land, Svalbard, by geomorphic means, Norsk Geogr. Tidsskr., 56, 96–103, 2002.

Humlum, O., Instanes, A., and Sollid, J. L.: Permafrost in Svalbard: a review of research history, climatic background and engineering challanges, Polar Res., 22, 191–215, 2003.

Jaedicke, C. and Gauer, P.: The influence of drifting snow on the location of glaciers on western Spitsbergen, Svalbard, Ann. Glaciol., 42, 237–242, 2005.

Kobayashi, D., Ishikawa, N., and Nishio, F.: Formation process and direction distribution of snow cornices, Cold Reg. Sci. Technol., 15, 131–136, 1988.

Kosugi, K., Sato, T., and Sato, A.: Dependence of drifting snow saltation length on snow surface hardness, Cold Reg. Sci. Technol., 39, 133–139, 2004.

Kottek, M., Grieser, J., Beck, C., Rudolf, B., and Rubel, F.: World Map of the Koeppen-Geiger climate classification updated, Meteorol. Z., 15, 259–263, 2006.

Larsson, S.: Geomorphological effects on the slopes of Longyear valley, Spitsbergen, after a heavy rainstorm in July 1972, Geogr. Ann., 64, 105–125, 1982.

Latham, J. and Montagne, J.: The possible importance of electrical forces in the development of snow cornices, J. Glaciol., 9, 375–384, 1970.

Major, H., Haremo, P., Dallmann, W., and Andresen, A.: Geological map of Svalbard. 1:100 000, C9G Adventdalen, Norsk Polarinst, Temakart, 31–32, 2001.

McCarty, D., Brown, R. L., and Montagne, J.: Cornices: Their Growth, Properties, and Control, International Snow Science Workshop, Lake Tahoe, 1986.

McClung, D. M. and Schaerer, P.: The Avalanche Handbook, 3rd Edition, The Mountaineers, Seattle, 342 pp., 2006.

Met.no, eklima: Free access to weather- and climate data from Norwegian Meteorological Institute form historical data to real time observations, www.eklima.no, last access: Mai 2011, 2011.

Montagne, J., McPartland, J. T., Super, A. B., and Townes, H. W.: The Nature and control of snow cornices on the Bridger Range, Southwestern Montana, Alta Avalanche Study Center, Miscellaneous Report No. 14, 1968.

Naruse, R., Nishimaru, H., and Maeno, N.: Structural Characteristics of Snow Drifts and Cornices, Ann. Glaciol., 6, 287–288, 1985.

Paulcke, W. and Welzenbach, W.: Schnee, Wächten, Lawinen, Zeitschrift für Gletscherkunde, Eiszeitforschung und Geschichte, 16, 49–69, 1928.

Rogers, J. C., Yang, L., and Li, L.: The role of Fram Strait winter cyclones on sea ice flux and on Spitsbergen air temperatures, Geophys. Res. Lett., 32, L06709, doi:10.1029/2004GL022262, 2005.

Schweizer, J. and Jamieson, B.: On surface warming and snow instability, International Snow Science Workshop, Squaw Valley, 2010.

Seligman, G. L: Snow structures and ski fields, Macmillian, London, 555 pp., 1936.

Sokratov, S. A. and Sato, A.: The effect of wind on the snow cover, Ann. Glaciol., 32, 116–120, 2001.

Vogel, S.: Cornice accretion, cracking and failure along with their meteorological controls at Gruvefjellet, Central Svalbard, UiO/UNIS, Oslo/Longyearbyen, 102 pp., 2010.

Welzenbach, W.: Untersuchungen über die Stratigraphie der Schneeablagerungen und die Mechanik der Schneebewegungen nebst Schlußfolgerungen auf die Methoden der Verbauung, Wissenschaftliche Veröffentlichungen des Deutschen und Österreichischen Alpenvereins, 9, 1930.

Paper 6

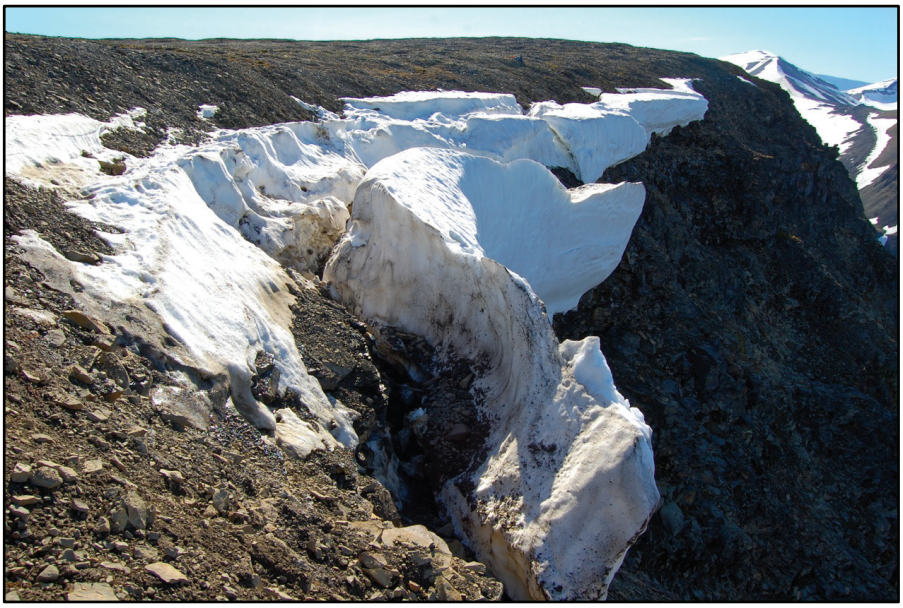

Remains of a cornice on Gruvefjellet in July 2010, with large amounts of plucked rock debris in the cornice tension crack. The tension crack has a maximum width of 3 m.

Paper 7

Rock debris transported by a cornice fall avalanche on Gruvefjellet in June 2010.

THE ROLE OF CORNICE FALL AVALANCHE SEDIMENTATION (IN THE VALLEY LONGYEARDALEN, CENTRAL SVALBARD)

*M. Eckerstorfer[1,2] , H. H. Christiansen[1,2], L. Rubensdotter[3], S. Vogel[1,2], M. Siewert[1,4]
[1]Arctic Geology Department, University Centre in Svalbard, P.O. Box 156, 9171 Longyearbyen, Norway
[2]Department of Geosciences, University of Oslo, 1047 Blindern, 0316 Oslo, Norway
[3]Geological Survey of Norway, P.O. Box 6315, Sluppen, 7491 Trondheim, Norway
[4]Department of Geography, University of Bonn, Meckenheimer Allee 166, 53115 Bonn, Germany

Abstract
In high relief landscapes snow avalanches can be important sediment erosion, transport and accumulation agents. However, traditionally most studies rank avalanches behind rockfall and debris flows in terms of their significance for rock slope sedimentation. Cornice fall activity and rock debris deposition on avalanche fans was recorded in 13 catchments at two slope systems, called Nybyen and Larsbreen, in the valley Longyeardalen in central Svalbard. Both slope systems are situated on NW-facing lee slopes underneath large summit plateau, where cornices form annually, and high frequency and magnitude cornice fall avalanching is observed. Avalanche activity was observed by daily automatic time-lapse photography. Avalanche sedimentation onto the avalanche fans was measured directly in either permanent sediment traps or by summer snow inventories. The results from a maximum of 7 years of measurements show avalanche sedimentation rates ranging from 8.2 to 38.7 kg/m^2 at Nybyen and from 0.8 to 55.4 kg/m^2 at Larsbreen. Correspondingly, the avalanche fan-surfaces accreted annually in a range from 3.7 to 13. mm/yr at Nybyen and from 0.3 to 21.4 mm/yr at Larsbreen. These comparably high avalanche sedimentation rates are due to collapsing cornices producing avalanches with high rock content throughout the whole winter. These avalanches effectively transport cornice plucked sediment, as well as rockfall deposits downslope. This causes distinct avalanche fans to be accumulated on the foot of slopes below cornices in the valley Longyeardalen, central Svalbard.

Introduction
The role of snow avalanches (hereafter called avalanches) as sediment erosion, transportation and accumulation agents is often underrated, but they can be of significance in the alpine sediment cascade (Sass et al., 2010). Their geomorphological importance depends highly on the slope relief, the lithology and the climate favorable for avalanche release (Caine, 1976; Decaulne and Saemundsson, 2006; French, 2007; Luckman, 1977). As a result of avalanche sedimentation, the formation of avalanche fans exhibits a morphologically distinguishable talus slope type (Luckman, 1988). Avalanche sedimentation rates are the quantification of rock debris transported and deposited by avalanches on avalanche fans, and are thus the most direct measure of the geomorphological work of avalanches (Blikra and Selvik, 1998; Christiansen et al., 2007). As avalanche erosion and accumulation contributes to backweathering of a rock slope, rockwall retreat rates are also an important parameter to quantify the geomorphological work of avalanches (Krautblatter and Dikau, 2007). Such quantification is done either by indirect methods using talus slopes as an inventory of long-term deposition (Schrott et al., 2002), or by direct measurements quantifying debris deposition (Luckman, 1978b). Both approaches were pioneered by Rapp in the 1950s (Rapp, 1960a; Rapp, 1960b). A comprehensive review of the methodologies is given by Krautblatter and Dikau (2007).
Until now, in studies worldwide, avalanches are primarily considered as subsidiary sediment transport agents, with rockfall and debris flows being more dominant (Luckman, 1978a). The longest slope monitoring was carried out in the Canadian Rocky Mountains. Both a 8 year and a 13 year record of sediment transport and accumulation showed significant geomorphological work by avalanches, quantified

by direct measurements (Luckman, 1978a; Luckman, 1988). Debris accumulation by avalanches averaged 0.6 to 4.8 mm/yr over the 8 year period and up to 5 mm/yr during the 13 year period. However, in both cases, rockfall was the dominant debris transport agent. Also in other studies, rockfalls of different magnitude and frequency have been ascribed as the most significant agent of rockwall retreat (Matsuoka and Sakai, 1999; Whalley, 1984) and talus cone formation (Krautblatter and Moser, 2009).
Studies focusing solely on avalanche sedimentation are sparse. Rapp (1960a) quantified avalanche sedimentation in Kärkevagge, Northern Sweden, which originated from a series of extreme events. He noted that the quantification of the particular importance of such events is rare. Furthermore he ranked sediment transport by avalanches second after debris flows, but emphasized that for both types of mass movement, frequency and magnitude mostly govern their geomorphological significance (Rapp, 1960b). Ackroyd (1987) in the New Zealand Alps and Bell et al. (1990) in the Himalayas quantified sedimentation of single avalanche events. Ackroyd observed the redeposition of large boulders by avalanches, and Bell et al. estimated a deposition area accretion of 0.74 and 0.21 mm after two avalanches. Heckmann et al. (2002; 2005) quantified and modeled the contribution of avalanches to the sediment balance of two alpine catchment areas for two years in the Bavarian Alps. They concluded that avalanches contributed significantly to the sediment balance and relief development of high mountain areas. Most recently, Sass et al. (2010) calculated rockwall retreat rates by avalanches based on a six-year record in the Tyrolean Alps. They documented that avalanches eroded 4-5 mm of debris since a wildfire cleared the catchment.

High Arctic Svalbard perspective

In Svalbard the dynamics of rockwall weathering, talus formation and avalanche sedimentation have been studied by Rapp (1960b), Jahn (1967; 1976; 1984), Åkerman (1984; 2005), André (1990; 1995; 1996; 1997) and most recently by Humlum et al. (2007) and Siewert et al. (2012). Åkerman (1984) and André (1990) assigned full-depth, slush avalanches and dirty spring avalanches high erosional significance. André (1990; 1996), however, did not find evidence for significant avalanche sediment erosion in schist and gneissic bedrock, as she observed avalanches only slightly reshaping the talus slopes. Also Jahn (1976), working on periglacial slope processes in the valley Longyeardalen ascribed avalanches only minor importance for the overall slope denudation. However, Humlum et al. (2007) studied a rock glacier in the Longyeardalen valley, and found that rock debris transport by avalanches was primarily responsible for the considerable amount of sedimentation that enabled the development of a rock glacier during the Holocene. Rock debris accumulation rates, quantified by direct measurements through 2 years ranged from 0 to 50.4 kg/m^2/yr, averaging 13 kg/m^2/yr on this NW facing slope (Humlum et al., 2007). The assumption that avalanche sedimentation is of high significance in the sedimentary bedrock of central Svalbard was confirmed by Siewert et al. (2012) in their study also from Longyeardalen. They estimated rockwall retreat rates using ERT measurements to quantify the volume of the talus deposits. Their results showed that rockwall retreat was 100 % higher on NW facing slopes compared to SE facing slopes. This is due to significant higher cornice fall avalanche activity on these NW facing slopes, due to a prevailing winter wind direction from the SE (Eckerstorfer and Christiansen, 2011b; Humlum et al., 2007). Snow cornices have been found to largely control plateau edge erosion likewise in the Longyeardalen valley by favouring rock weathering by ice segregation. As the cornices grow over the plateau edge, they keep it in the frost cracking window of -3 to -8 °C for large parts of the year (Eckerstorfer et al., 2012). When the cornice accretes in autumn, the weathered sediment is incorporated and later plucked out of the cornice rockwall by the downslope growing and deforming cornice. Sediment is either transported downslope by a collapsing cornice, inducing a cornice fall avalanche (Vogel et al., 2012) or by *in situ* melting of the cornice in late spring (Eckerstorfer et al., 2012).

Scope of the study

The geomorphological work of cornices and cornice fall avalanches on NW facing slopes in Longyeardalen seems to be of significance for rock slope sedimentation at present. This assumption is based on previous studies on these slopes (Eckerstorfer et al., 2012; Humlum et al., 2007; Siewert et al., 2012). Thus, a detailed quantification of avalanche sedimentation, causing the formation of well-defined ava-

lanche fans is still lacking. With its frost weathering susceptible sedimentary bedrock and its active cornice fall avalanching, the Longyeardalen valley is offering good conditions fur such quantification work. We have therefore combined monitoring of cornice fall activity with automatic time-lapse photography and field observations and direct measurements of annual avalanche sedimentation rates to quantify the geomorphological work of cornice fall avalanches. We define avalanche sedimentation as the transport and deposition of rock debris by avalanches forming distinct avalanche fans. The rock debris being transported this way can have its origin from erosion by cornices and / or cornice fall avalanches, as well as rockfall, but has been transported by an avalanche, contributing to avalanche fan deposition (Sass et al., 2010). The dataset was collected at two slope systems, Nybyen and Larsbreen (named after the Larsbreen glacier flowing on its foot) about 700 m apart below the same plateau edge on the NW facing slope of Gruvefjellet, delimiting the valley Longyeardalen on its east side (Figure 1). Data from a total of 13 catchments (5 at Nybyen, 7 at Larsbreen) with a record of maximum 7 years is presented.

Study area and slope systems

Large parts of the landscape in central Svalbard are periglacial, with only minor glaciers. In 2011 the mean annual air temperature (MAAT) was -3.4°C, and the 2011 annual precipitation (MAP) was 199 mm water equivalent (w.e.) at sea level in Longyearbyen (Met.no, 2012). This present-day MAAT is 2.6°C warmer than the entire 1912-2011 average, while MAP is close to the almost 100 year long record average of 196 mm (Met.no, 2012). The largest fraction of precipitation falls as snow, but due to the low amounts and the barren, windswept landscape, the snow cover is generally thin and discontinuous (Eckerstorfer and Christiansen, 2011a).

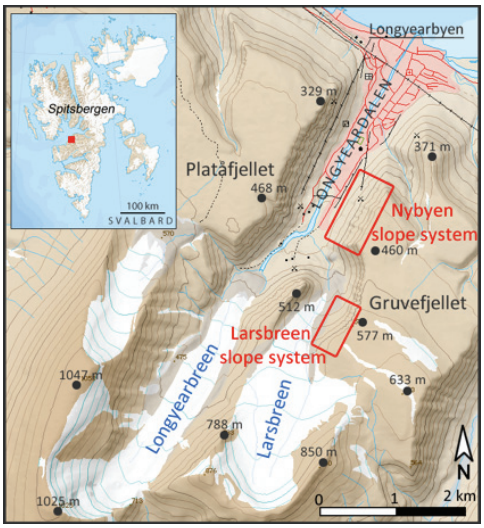

Figure 1: Topographic map of the location of the two slope systems (red squares) in the valley Longyeardalen in central Spitsbergen (inlet map). Svalbard's main settlement Longyearbyen is located at the northern end of Longyeardalen. Note the large summit plateau of the Gruvefjellet Mountain.

Both the Nybyen and the Larsbreen slope systems (hereafter called Nybyen and Larsbreen) are situated within the same bedrock region of near horizontal sedimentary layers of sandstones and shales in the Van Mijenfjorden Group; lower Tertiary age (Hjelle, 1993). This geological setting with horizontal bedrock structures forms the basis for the extensive plateau mountain topography in central Svalbard. This large-scale plateau topography (Figure 1), in combination with snow transport by wind, with a prevailing regional winter wind direction from the SE, favours cornice formation on lee-side slopes (Eckerstorfer and Christiansen, 2011b; Eckerstorfer et al., 2012; Vogel et al., 2012). Into this plateau

topography large V or U-shaped valleys are incised, primarily eroded by either fluvial/periglacial and/or glacial processes. The valley sides of these large valleys are, however, shaped by a combination of gravitational periglacial processes mainly avalanches and rockfalls. Additionally smaller V-shaped gullies or ravines are cut into the plateau edges. These ravines are then located between protruding bedrock-noses in the more resilient bedrock formations. The detailed morphology of these ravines varies depending somewhat on the bedrock setting, but they are in many places funnel-shaped, with one or more contributing couloirs that run from the funnel-shaped upper part down to the lower less steep rock slope areas of the avalanche fans...

Methods

Geomorphological mapping

To determine past and present slope activity, sediment cover and landforms, detailed geomorphological mapping was carried out. The area was first studied using infrared-composite aerial photographs to assess the general setting, and to determine the most prominent landforms and slope processes. After the production of a first raw map, fieldwork was conducted to verify the aerial photograph interpretation and to determine sediment compositions and geomorphological processes. Fieldwork observations were directly integrated into the map in the field, using ArcGIS 10. The final geomorphological maps for both slope systems were constructed using stereo analysis of aerial photographs from 1990 (courtesy of the Norwegian Polar Institute).

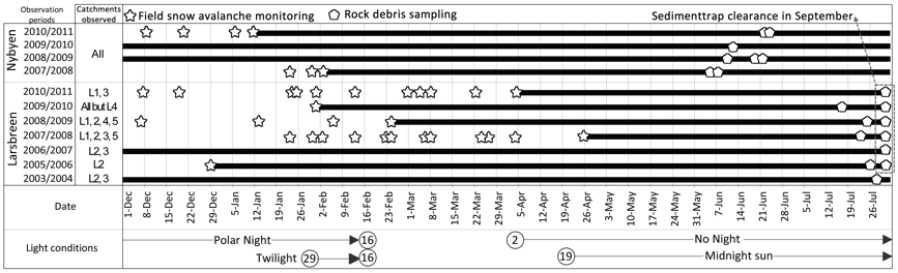

Figure 2: Annual avalanche monitoring and rock sediment collection for each slope system. The black lines indicate periods with daily automatic time-lapse photography .The stars indicate field avalanche monitoring on site, and the pentagons indicate rock sediment collection in avalanche snow deposits. The sediment traps at the Larsbreen catchments were between 2005/2006 and 2010/2011 all emptied in early September. The daylight conditions are indicated with the date (number in circle) when seasonal changes occur.

Avalanche activity monitoring

Seasonal avalanche activity was monitored by field observations and automatic time-lapse photography (Christiansen, 2001; Vogel et al., 2012) (Figure 2, Figure 3). Time periods without photo coverage were mainly due to technical problems with the camera, bad visibility, or darkness during the Polar Night (Figure 2). Up to six, but at least one daily photograph was taken of the Nybyen and Larsbreen slope system. Additionally, one daily photograph was taken of the catchments L1-L3 at Larsbreen (Lars-cam). All Nybyen catchments were monitored between 2007/2008 and 2010/2011. At Larsbreen, avalanche monitoring started in 2003/2004 in catchments L2 and L3, both having the longest records, with 7 years at L2 and 6 years at L3. No observation and sampling took place in 2004/2005 on Larsbreen (Figure 2). Therefore, rock debris sampled in catchment L3 in 2006/2007 is from two years of debris deposition.

Each avalanche release was stored in a database with date and time of release, location of release (number of catchment) and extent. The extents of the avalanche snow-deposits (m^2) were calculated by digitizing the outlines of each avalanche in ArcGIS 10. Only avalanches that reached the primary fan were included in the calculations. The visible rock debris content, estimated *in situ*, or from the time-

lapse photographs was classified into three classes; “no visible rock debris”, “some visible rock debris” and “high amounts of visible rock debris”.

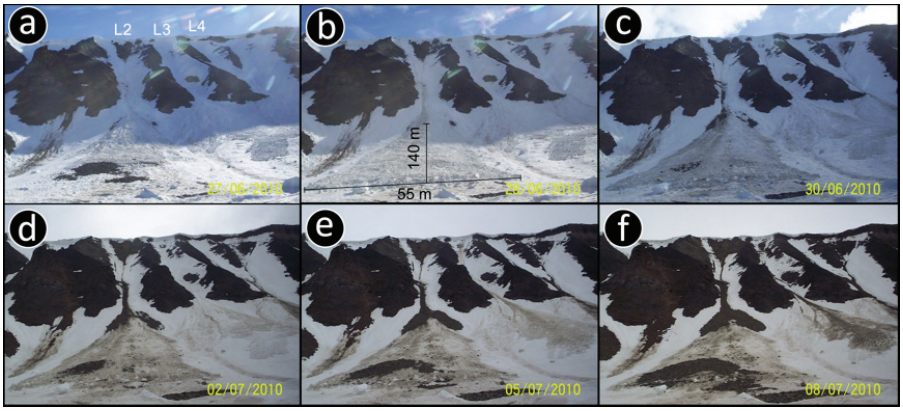

Figure 3: Time lapse photography series from the camera (Lars-cam) overlooking catchments L1-L3. The time series shows a late spring cornice fall avalanche, followed by the progressional melt out of rock debris through summer on the avalanche fan in catchment L2 at Larsbreen. Note that visible rock debris content becomes more apparent as the avalanche debris melts.

Rock sediment collection

We used a direct approach to measure rock debris deposition by avalanches, following Luckman (1978a). In two catchments (L2 and L3) at Larsbreen, four 16 m^2 large polyethylene squares were installed in 2003/2004 (T1 to T4 in Figure 4a, b). These squares were anchored along the entire periphery with a line of boulders and emptied each year in September (Figure 2). Only at this time of the summer, the avalanche debris' had melted enough to make the plastic sheets partly visible. In some years, the plastic sheets had to be replaced due to holes in them, and the sediment traps needed to be slightly moved. In catchment L2, additionally a large, flat-topped boulder (T5 in Figure 4a, c) was used as another sediment trap, also only cleared in September each year.

Rock debris quantification based on snow surface inventories (Luckman, 1978a) were carried out in all catchments at both sites since 2007/2008. These were done when the rock debris, due to melting of the snow, had concentrated on the snow surface, with a still intact boundary to the avalanche fan-surface of the previous year below (Figure 4d). These snow inventories, in average 4-8 m^2 parcels (Figure 4e), were taken at the furthest possible downslope locations on the avalanche fans. All catchments at Nybyen were sampled in June each year (Figure 2) as the snow melts earlier at this lower slope system. At Larsbreen some sampling took place either end of July or in September each year. In all cases the rock debris transported downslope by all avalanches in a particular year and catchment was sampled. The rock debris in each sampling parcel or in the permanent sediment traps were weighed in a cotton bag using a hand scale. The weight of small fragments was estimated and the sum of all rock debris rounded to the next kg. Large, heavy boulders were hammered into smaller pieces for weighing.

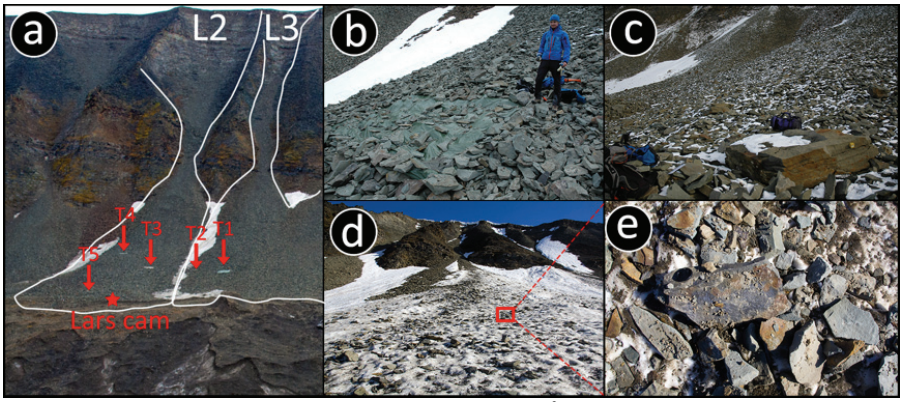

Figure 4: a) Locations of all four permanently deployed, 16 m^2 large polyethylene sheets (T1-T4) and one large, flat-topped boulder (T5) in catchments L2 and L3 at Larsbreen. The Larsbreen glaciers ice-cored moraine is visible in the foreground. The location of Lars-cam is marked with a star. b) A 16-m^2 large polyethylene sheet (T4) with a border of lined up stones, containing rock debris to be weighed at the end of summer 2009. c) The large flat-topped boulder (T5), acting as sediment trap in catchment L2. d) Avalanche deposited rock debris, concentrating at the surface in catchment L7 in September 2010. e) Close-up of avalanche deposited rock debris with rocks of different clast sizes (from boulders to fines) in catchment L7 in September 2010.

Avalanche fan-surface accretion and rockwall retreat rates

To quantify the geomorphological work of cornice fall avalanches, avalanche sedimentation rates (kg/yr), avalanche fan-surface accretion rates (mm/yr) and rockwall retreat rates (mm/yr) were calculated for each catchment annually. These rates were only calculated for a particular catchment and year, if avalanche activity was recorded and rock debris deposition was directly measured (Figure 2). We first defined the annual maximum extent of avalanche snow-deposits (m^2) per catchment, by calculating it in ArcGIS 10, based on the outlines of all avalanches observed.

The total amounts of avalanche deposited rock debris (kg), directly measured in the sediment traps or in the snow inventories were calculated by summing the amounts of rock debris weighed in each sampling parcel. Mean annual avalanche sedimentation (kg/m^2) was obtained by dividing the total amount of rock debris (kg) by the total area of permanent sediment traps or snow inventories (m^2). Annual total avalanche sedimentation (kg/yr) was calculated by multiplying the annual maximum area of avalanche snow deposition (m^2) with the mean annual rock debris sedimentation rate (kg/m^2). To receive avalanche fan-surface accretion rates (mm/yr), and rockwall retreat rates (mm/yr), the volume was calculated by dividing the total avalanche sedimentation rate (kg/yr) by the mean rock density of ~2,250 kg/m^3 measured by Siewert et al. (2012) in the laboratory on sandstone rock samples from the study area. Dividing the total sediment volumes (m^3) by the area of the avalanche fans (m^2) (depositional areas) enabled avalanche fan-surface accretion rates (mm/yr) to be calculated. Likewise by dividing the total sediment volumes (m^3) by the area of the rockwall (source areas) (m^2), rockwall retreat rates (mm/yr.) could be determined assuming all debris comes directly from the backwall (see later discussion for more details on this). The source and depositional areas are marked in Figure 5b with a white outline, separated by the green stabled line. In Figure 6b the source and depositional areas are also marked with a white outline, separated by the yellow stabled line.

The source, depositional areas and the area of the annual maximum extent of avalanche snow-deposits (m^2) were mapped in ArcGIS 10 using the '3D analyst' tool 'interpolate polygon to multipatch', to receive the area of the three dimensionally delimited landform (as opposite to a planimetric area). A DEM with a spatial resolution of 2 m was used for the calculations.

Results

The geomorphology of the Nybyen and Larsbreen slope systems

The Nybyen slope system consists of a multi-stepped erosion, transport and sedimentation system with a vertical relief of 300 m, and a 1000 m long horizontal ridgeline (Figure 5). The detailed geomorphological description of the Nybyen slope system is presented in Table 1.

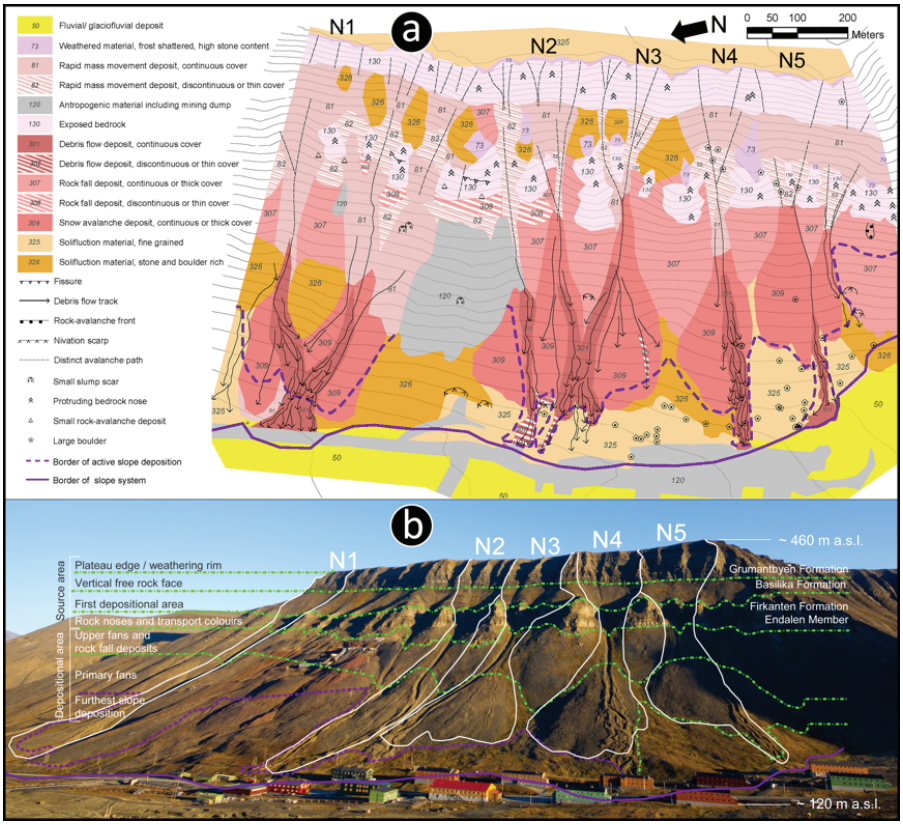

Figure 5: a) Geomorphology and sediments of the Nybyen slope system based on detailed geomorphological field mapping and 3D aerial photogrammetry. b) Nybyen with the five investigated catchments (N1-N5) (white line). The white line indicates the maximum modern runout distance of cornice fall avalanche sedimentation observed. The green stabled lines indicate different parts of the source and depositional areas or delimit the geological formations. The debris flow channels located in the overall depositional area are, however, erosional features.

The Larsbreen slope system is between 130-160 m high, and about 600 m long. The varying height is due to some variation in plateau height but primarily because the foot of the slope system is based at the lateral moraine of Larsbreen glacier (Figure 6,), which acts as a topographical barrier. Hence, the slope deposits extend onto the ice-cored moraines (Etzelmueller et al., 2000). The slope system is relatively simple with avalanches and rockfall and as the predominant transport processes, and a clear connection between erosional and depositional areas, with no long-term intermediate storage (Table 1).

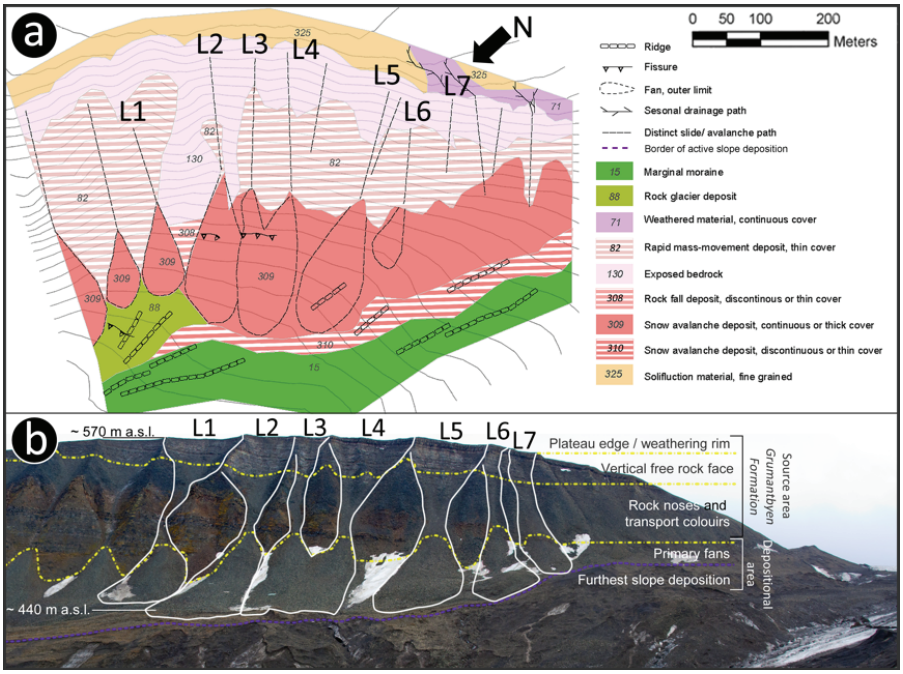

Figure 6 a) Geomorphology and sediments of the Larsbreen slope system based on detailed geomorphological field mapping and 3D aerial photogrammetry. b) Larsbreen with the seven catchments (L1-L7) (white line). The white lines indicate the maximum runout distance of cornice fall avalanches observed. The yellow dashed lines indicate different parts of the source and depositional areas or delimit the geological formations.

Table 1: Geomorphology of the Nybyen (N) and Larsbreen (L) slope systems The number codes for each sedimentological unit in Figure 5 and Figure 6 are given.

	Landform	Slope	Characteristics
N	Plateau edge and weathering rim	15-85°	Thin rim of frost-shattered bedrock of Grumantbyen sandstone (code 73), transitioning into free rock face (code 130). The plateau edge consist of highly weathered rock debris without lichen-cover, unlike the rocks of the summit plateau blockfield and the plateau edges facing other directions than NW (Eckerstorfer et al., 2012)
L			Slightly more resilient Grumantbyen sandstone than at Nybyen. Above catchments N4-N7, the rim is vertical (code 130).
N	Vertical free rock face	85-90°	Undulating lateral morphology, forming the upper part of the funnel-shaped gullies below. Primary source area for slope deposits
L			In the southern part, the cliff is laterally almost vertical, while couloirs are developed in the northern part, increasing in depth towards north.
N	First depositional area	40-45°	Covered by a layer of rockfall and avalanche deposits (code 81, 82), in the Basilika shale formation. Large parts are lichen covered, showing slow rates of deposition (code 326) (N1-N3).
L	Not existing at Larsbreen		
N	Rock noses and transport couloirs	35-45°	Primarily erosional landforms, with only little sediment between the rock noses, developed in the Firkanten Formation. The rock noses are rockfall source areas (code 130). The couloirs act as transport funnels. The thin sediment cover consists of fines and sandstones and shales from rockfall and avalanche deposits (code 82).
L		45-55°	The free rock face gradually declines in steepness downwards, but the general steepness of the slope prevents any long-term storage (code 82). The thin sediment cover is a mix of in-situ weathered material, rockfall deposits and to some smaller degree avalanche deposits.
N	Upper fans and rockfall deposits	40-50°	The upper fans and the areas in between mainly consist of rockfall deposits (code 307), accounting for a steep, relatively homogenous slope (vertical grain-size distribution).
L	Not existing at Larsbreen		
N	Primary fans	45–20°	Almost coalescing, large avalanche fans, with concave curvature. Grain size varies from silt/sand to boulders. The bimodal rock composition in the source areas, with sandstones and black and grey shales cause the almost bimodal grain size distribution.
L		45-15°	The avalanche fans are visibly highly intermixed with snow and ice at depth in the active layer. The fans have a concave curvature. The morphology and development of this section of the slope system is very uneven along the slope itself. In the southernmost part (L6-7) there are no real individual fans distinguishable morphologically. The fans in the north (L5 and north) are well-developed avalanche fans, with a concave cross-profile. The avalanche fans have clear apex and fan-foots, connected to well distinguishable couloirs. The northernmost fans (L1 –L4) continue directly into the upper end of a rock glacier (code 88) that is located north of the large ice-cored frontal moraine of Larsbreen.
N	Furthest slope deposition	15-5°	Consisting of debris and slush flow levees on both sides of distinct erosional channels (Debris flow track arrows), recently periglacially reworked by frost sorting and solifluction (code 325, 326). The weathering of stones, lichen and the general vegetation cover of these landforms the degree of periglacial reworking show that they have not been active recently.
L		0-15°	The lowermost part of the avalanche deposition is a thin sediment cover (code 310), with larger grain sizes then the glacial till (code 15), on top of the ice-cored lateral moraine ridges

Cornice fall avalanche activity and rock debris quantification

Table 2: All calculations of avalanche sedimentation rates (kg/yr) for each catchment at the Nybyen (N1-N5) and Larsbreen (L1-L7) slope systems. The annual averages or sums for Nybyen and Larsbreen are given in bold. The highest values and rates for each calculation step are given in italic. The values and rates marked with a star are from 2 years of observations.

	2007/2008	2008/2009	2009/2010	2010/2011		2003/2004	2005/2006	2006/2007	2007/2008	2008/2009	2009/2010	2010/2011
Annual amount of avalanche per catchment (N)												
N1	2	2			**L1**				5	4	7	5
N2			6	3	**L2**	2	4	5	4	5	*10*	8
N3				2	**L3**	2		5	4	7	*10*	7
N4		4		2	**L4**					3		
N5	4		*7*		**L5**				5		3	
					L6						7	
					L7						3	
	6	**6**	**13**	**7**		**4**	**4**	**10**	**18**	**19**	**40**	**20**

Annual maximum area of avalanche snow deposition (m^2)												
N1	26,894	*27,508*			**L1**				6,989	6,168	6,884	7,106
N2			9,482	13,948	**L2**	7,209	7,490	6,811	6,186	7,241	7,932	*8,567*
N3				18,822	**L3**	4,564		4,877	4,088	6,487	5,698	7,653
N4		14,955		21,844	**L4**					5,123		
N5	15,944		11,640		**L5**				8,183		2,685	
					L6						4,896	
					L7						3,218	
	42,838	**42,463**	**21,122**	**54,614**		**11,773**	**7,490**	**11,688**	**25,446**	**25,019**	**31,313**	**23,326**
Annual amount of avalanche deposited rock debris, directly measured (kg)												
N1	290	*1,801*			**L1**				160	147	225	587
N2			619	467	**L2**	209	368	74	544	651	*11,135*	717
N3				669	**L3**	144		*328	73	207	632	530
N4		201		967	**L4**					443		
N5	298		685		**L5**				98		120	
					L6						370	
					L7						220	
	588	**2,002**	**1,304**	**2,103**		**352**	**368**	**402**	**875**	**1,448**	**12,702**	**1,834**
Annual sums of rock debris collection area (m^2)												
N1	32	*220*			**L1**				8	11	16	16
N2			16	25	**L2**	54	36	90	44	26	*543*	36
N3				25	**L3**	36		*90	8	18	34	32
N4		12		30	**L4**					8		
N5	20		28		**L5**				8		4	
					L6						12	
					L7						16	
	58	**232**	**44**	**80**		**90**	**36**	**180**	**68**	**63**	**625**	**84**
Annual amount of avalanche deposited rock debris (kg) / Annual sums of rock debris collection area (m^2) = Mean rock debris sedimentation rate (kg/m^2)												
N1	9.1	8.2			**L1**				20.0	13.4	14.1	*36.7*
N2			*38.7*	18.7	**L2**	3.9	10.2	0.8	12.4	25.0	20.5	19.9
N3				26.8	**L3**	4.0		*3.6	9.1	11.5	18.6	16.6
N4		16.8		32.2	**L4**					*55.4*		
N5	14.9		24.5		**L5**				12.3		30.0	
					L6						30.8	
					L7						13.8	
	11.3	**8.6**	**29.6**	**26.3**		**3.9**	**10.2**	**2.2**	**12.9**	**23.0**	**20.3**	**21.8**
Annual maximum area of avalanche snow deposition (m^2) * Mean rock debris sedimentation rate (kg/m^2)= Avalanche sedimentation (kg/yr)												
N1	243,727	225,190			**L1**				139,780	82,427	96,806	260,701
N2			366,835	260,549	**L2**	27,835	76,502	5,615	76,481	181,304	162,651	170,626
N3				503,677	**L3**	18,218		*17,755	37,303	74,601	105,916	126,753
N4		250,496		*704,105*	**L4**					*283,686*		
N5	237,566		284,764		**L5**				100,242		80,550	
					L6						150,960	
					L7						44,248	
	484,399	**366,426**	**625,979**	**1,435,666**		**46,072**	**76,502**	**26,093**	**327,430**	**575,040**	**636,360**	**509,284**

At both slope systems, all avalanches were exclusively cornice fall avalanches. Only avalanches at the very end of the winter were full depth avalanches, incorporating rock debris in the transport couloirs, when sweeping through. The peak activity of avalanches at both slope systems was from May to July (Figure 7b, Figure 8b), which is late compared to the overall registration of avalanche activity in the Longyearbyen area, with an activity maximum between April and June (Eckerstorfer and Christiansen, 2011b). However, at both slope systems, cornice fall avalanches were registered throughout the entire snow season, as early as December at Larsbreen (Figure 8b). At least one avalanche released annually in each of the 13 catchments at both slope systems, however, not all of them were sampled for rock debris deposition.

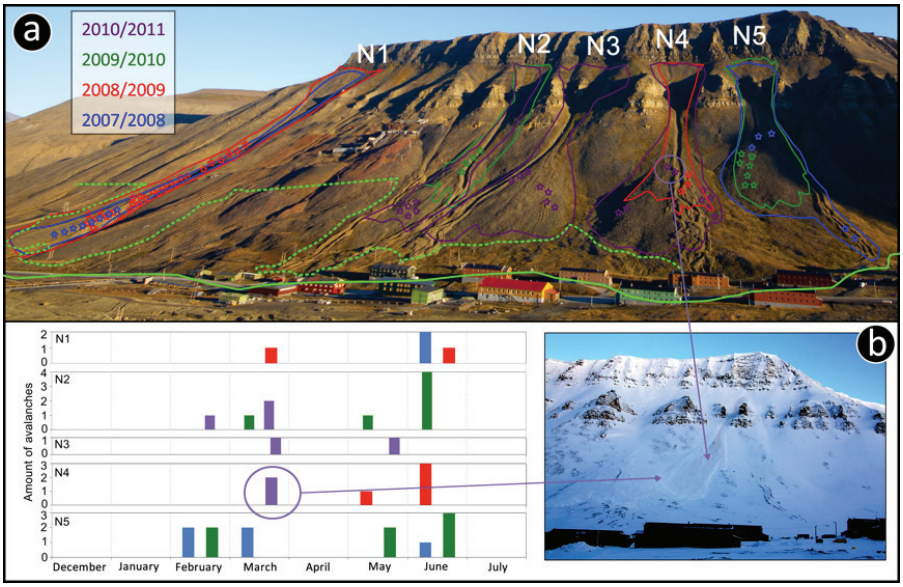

Figure 7: a) Outlines of the outermost annual extent of avalanche snow-deposits in the Nybyen slope system. The stars indicate the snow inventory rock debris sampling sites. b) Annual number of avalanches that released in each catchment. The picture shows an avalanche that released in March 2011 in catchment N4 and from which rock debris was sampled in June 2011. Note the high visible rock debris content in the avalanche that originated directly from the plateau edge and the free rock face, as the avalanche was not a full-depth release.

At Nybyen, 77 avalanches were recorded during the observation period 2007/2008 – 2010/2011. Rock debris was quantified in 41.5 % (32 avalanches) of the total. In 60 % of the 32 avalanches analyzed, the debris terminus reached the lower third of the primary fans, 37 % reached the middle third and 3 % stopped in the upper third of the maximum runout zone (white line, Figure 5b). Rock sediment was visible in 97 % of the avalanche deposits, with 68 % of them having "high amounts of visible rock debris". This underlines that not only "dirty" spring avalanches contribute to the avalanche fan accumulation. It furthermore stresses that rock debris, plucked from the backwall by cornices (Eckerstorfer et al., 2012) as well as rockfall deposited in the source area is transported downslope by avalanches during the entire avalanche season, as we recorded cornice fall avalanches in every month of the winter (Figure 7b, Figure 8b). The picture in Figure 7b exemplifies a cornice fall that released in March 2011 in catchment L4. The high visible rock content, covering the majority of the avalanche debris is clearly visible. With an almost continuous snow cover on the slope, the rock debris could not have been picked up in the upper fans or in the transport couloir. The rock debris was definitely plucked from the plateau edge by the cornice and transported downslope. The falling cornice must have also incorporated loose rock debris from the horizontal ledges of the vertical free rock face, originated by melting cornices and rockfall, visible by the cleared snow-free area.

The largest maximum extent of avalanche snow-deposits (m^2) was measured in catchment N1 in 2007/2008 and 2008/2009 (Figure 7), with over 26,000 m^2 in each year (Table 2). In the same year in catchment N1, the most extensive rock debris quantification was carried out, with 28 parcels of snow inventories being sampled (Figure 7a), covering an area of 220 m^2 (Table 2). In all catchments during the entire observation period, a minimum of 12 m^2 of snow inventories (Table 2) was sampled.

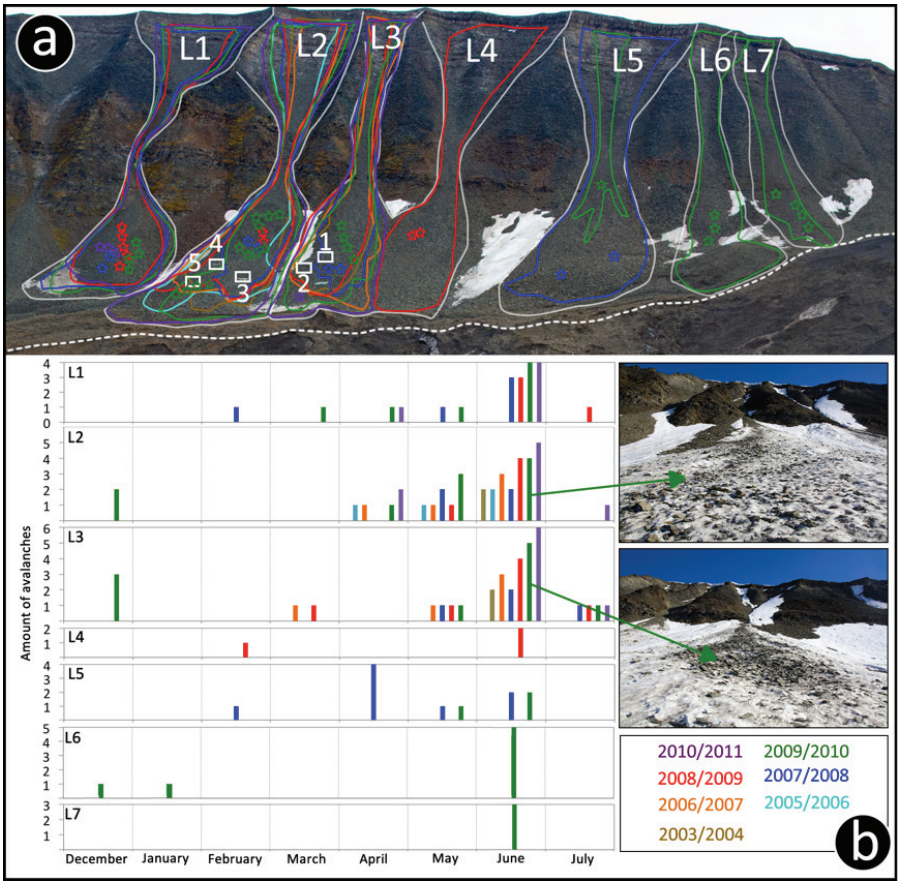

Figure 8: a) Outlines of the outermost annual extent of avalanche snow-deposits in the Nybyen slope system. The stars indicate the rock debris sampling sites. b) Annual number of avalanches that released in each catchment. The two pictures exemplify two avalanches snow-deposits in which snow inventories were carried out. The avalanches released in catchments L2 and L3 in 2009/2010. Note the high visible rock debris content in both avalanches.

At Larsbreen, from 2003/2004 to 2010/2011, with the exception of 2004/2005, 120 avalanche deposits were analyzed (Figure 8b). A total of 156 avalanches were recorded, thus 77 % of all avalanches are taken into account. However, not all catchments were sampled equally over the entire observation period, as done at Nybyen (Figure 2, Table 2). Out of 120 avalanches, 55 % stopped in the lower third, and 45 % in the middle third of the maximum runout zone (white line, Figure 6). Rock sediment was visible in 91 % of all investigated deposits, with 66 % having “high amounts of visible rock debris”.

The maximum extent of avalanche snow-deposits is comparably smaller at Larsbreen than at Nybyen (Table 2), owing to the slope system being shorter in vertical height and slide distance. However, the largest avalanches in all catchments approached closely the furthest visible slope deposition, which is at present found on the ice-cored marginal moraine of Larsbreen glacier (Figure 8).

In 2003/2004, 2006/2007 and 2009/2010 all five permanent sediment traps (Figure 8a) were cleared and the rock debris weighed. In all the other years, some of the plastic sheets were either destroyed or remained snow covered throughout the summer (L3 in 2005/2006). However, we also carried out snow inventories both in L2 and L3, therefore the long records exist from these two catchments. T2, the large boulder, located the furthermost down on the avalanche fan (Figure 4a, c), was covered with rock de-

bris and thus sampled each year, except in 2007/2008. This indicates that avalanches must be the primary rock debris transport agent, as rockfalls are unlikely to move debris this far down on the avalanche fan and up a large boulder. Due to the permanent sediment traps, catchments L2 and L3 have the longest and most persistent sediment quantification record, followed by catchment L1 (Table 2). In September 2010, sediment trap T3 was filled with almost 6,700 kg of rock debris. As T3 was emptied the year before, these large amounts of rock were deposited during the winter 2009/2010, possibly a cornice that plucked large rock pieces from the headwall.

Avalanche sedimentation rates (mm/yr)

For each catchment at both slope systems, we have calculated mean rock debris sedimentation rates (kg/m^2) (Table 2) that have a large interannual variability. Mean annual rock debris sedimentation at Nybyen ranged from 8.2 kg/m^2 (N1 in 2008/2009) to 38.7 kg/m^2 (N2 in 2009/2010) (Table 2). At Larsbreen, rock debris sedimentation was as low as 0.8 kg/m^2 (L2 in 2006/2007) and as high as 55.4 kg/m^2 (L4 in 2008/2009) (Table 2). Corresponding (avalanche) sedimentation rates ranged at Nybyen between 225,190 kg/yr (N1 in 2008/2009) and 704,105 kg/yr (N4 in 2010/2011) (Table 2). At Larsbreen, annual avalanche sedimentation rates exhibit a larger range from 5,615 kg/yr (L2 in 2006/2007) to 283,686 kg/yr (L4 in 2008/2009) (Table 2). There is no correlation between the maximum area of avalanche snow-deposition, and corresponding avalanche sedimentation rates on an annual basis for each catchment at both slope system, with R^2 values of 0.003 for Nybyen and 0.004 for Larsbreen. Also, large rock debris sampling areas did not result in larger annual avalanche sedimentation rates for each catchment at both slope systems ($R^2 = 0.05$ for Nybyen and $R^2 = 0.06$ for Larsbreen).

Avalanche fan-surface accretion and rockwall retreat rates (mm/yr)

Table 3: Calculations of annual avalanche fan-surface accretion and rockwall retreat rates (mm/yr) for each catchment at the Nybyen (N1-N5) and Larsbreen (L1-L7) slope systems. The source and depositional areas for each catchment are visualized in Figure 5 and Figure 6 with the white outline. The annual averages for Nybyen and Larsbreen are given in bold. The highest values and rates for each calculation step are given in italic. The values and rates marked with a star are from 2 years of observations.

	Source area (m^2)	**Depositional area (m^2)**		**Source area (m^2)**	**Depositional area (m^2)**
N1	116,541	*27,422*	**L1**	54,150	7,282
N2	137,665	21,897	**L2**	42,964	*8,623*
N3	169,359	21,454	**L3**	25,007	7,771
N4	*222,854*	23,016	**L4**	*61,139*	5,890
N5	146,252	18,771	**L5**	47,763	8,410
			L6	6,561	5,835
			L7	13,406	3,904
	676,130	**112,560**		**250,990**	**47,715**

	2007/2008	**2008/2009**	**2009/2010**	**2010/2011**		**2003/2004**	**2005/2006**	**2006/2007**	**2007/2008**	**2008/2009**	**2009/2010**	**2010/2011**
Total avalanche sedimentation rate (kg/yr) / Mean rock density of 2,250 kg/m^3 = Volume rock debris (m^3)												
N1	108.32	100.08			**L1**				62.12	36.63	43.03	115.87
N2			163.04	115.80	**L2**	12.37	34.00	2.50	33.99	80.58	72.29	75.83
N3				223.86	**L3**	8.10		*7.89	16.58	33.16	47.07	56.33
N4		111.33		*312.94*	**L4**					*126.08*		
N5	105.58		126.56		**L5**				44.55		35.80	
					L6						67.09	
					L7						19.67	
	215.29	**162.86**	**278.21**	**638.07**		**20.48**	**34.00**	**11.60**	**145.52**	**255.57**	**282.83**	**226.35**
Avalanche fan-surface accretion rate (mm/yr)												

N1	3.95	3.65			**L1**				8.53	5.03	5.91	15.91
N2			7.45	5.29	**L2**	1.43	3.94	0.29	3.94	9.34	8.38	8.79
N3				10.43	**L3**	1.04		*1.02	2.13	4.27	6.06	7.25
N4		4.84		*13.60*	**L4**					*21.41*		
N5	5.62		6.74		**L5**				5.30		4.26	
					L6						13.21	
					L7						5.04	
	1.91	**1.45**	**2.47**	**5.67**		**0.43**	**0.71**	**0.24**	**3.05**	**5.36**	**5.93**	**4.74**
Rockwall retreat rate (mm/yr)												
N1	0.93	0.86			**L1**				1.15	0.68	0.79	2.14
N2			1.18	0.84	**L2**	0.29	0.79	0.06	0.79	1.88	1.68	1.77
N3				1.32	**L3**	0.32		*0.32	0.66	1.33	1.88	2.25
N4		0.50		*1.40*	**L4**					2.06		
N5	0.47		0.57		**L5**				0.93		0.75	
					L6						*5.00*	
					L7						0.75	
	0.32	**0.24**	**0.41**	**0.94**		**0.08**	**0.14**	**0.05**	**0.58**	**1.02**	**1.13**	**0.90**

At the Nybyen slope system, the source and depositional areas are larger than at Larsbreen, consisting of the free vertical rock faces, the first depositional areas and the transport couloirs (Figure 5b). However, this did not lead to larger avalanche fan-surface accretion and rockwall retreat rates (Table 3). But in both slope systems, the highest avalanche fan-surface accretion rates with 13.5 mm at Nybyen and 21.41 mm/yr at Larsbreen respectively were calculated in the catchments with the largest source areas (N4 and L4).

At Nybyen, the size of the maximum avalanche snow-deposits does not determine annual avalanche surface fan accretion rates ($R^2 = 0.01$) for each catchment. The same accounts for Larsbreen, where the size of the maximum avalanche snow-deposits also does not determine annual avalanche fan accretion rates ($R^2 = 0.01$). However, annual average maximum avalanche snow depositional areas correlate weakly with surface fan accretion rates ($R^2 = 0.28$) at Nybyen. Strong correlations were found at Larsbreen between annual average maximum avalanche snow depositional areas and annual average avalanche fan accretion rates ($R^2 = 0.86$ for both).

Discussion

Avalanche sedimentation rates and their geomorphological effect

Monitoring the Nybyen and Larsbreen slope systems enabled us to establish an improved understanding of the role of cornice fall avalanche sedimentation and the particular process dynamics involved. Due to the geomorphological work of cornices (Eckerstorfer et al., 2012) a significant majority of cornice fall avalanches at both slope systems have a high visible rock debris content throughout the entire winter (Figure 9b, c), making avalanche sedimentation very efficient. This is opposed to many earlier studies that did not recognize such efficient rock debris transport by avalanches. In addition, both slope systems consists of for frost weathering very susceptible sandstones and shales, with a rather moderate rock strength and high amount of fractures (Siewert et al., 2012). As a result, the annual avalanche fan-surface accretion rates we present for each catchment are comparably high. In some years, the surface of an avalanche fan raised over 21 mm (L4 in 2008/2009) by cornice fall avalanche sedimentation. The rock debris, accumulated on the avalanche fans are the sandstones from the Grumantbyen formation, varying in clast size from boulders to stones, and shales from the Basilika formation (only at Nybyen) accounting for all the fines, as these shales are broken down in the transport process (Figure 4e). Sedimentation by rockfall would produce primarily only coarse-grained debris. During the many snow inventory samplings, we found perched rock debris on larger blocks (Figure 9f). Rock debris only get perched this way by avalanche sedimentation, when rock debris settle on top of each other during avalanche snow melting. All primary fans at both slope systems consist primarily of avalanche deposits, containing unsorted rock debris of very different clast size. Only avalanches are able to transport rock debris as far out on the slope systems, as we observed it. At some places these avalanche deposits reach at Nybyen almost as far as the outermost fans that consist of periglacially-reworked debris and slush

flow deposits. At Larsbreen, avalanche deposits are clearly visible beyond the slope system limit, having been transported upslope the rock glacier ridges and quite some distance onto the otherwise much more fine-grained ice-cored moraine of the Larsbreen glacier (Figure 9a, d). Furthermore, at several of the avalanche fans at Larsbreen, avalanche snow has been turned to ice by the relatively high sedimentation rates and is thus preserved underneath the talus (Figure 9e). This stratigraphy of rock debris and avalanche snow turned to ice was visible in a cave underneath the rock glacier (Humlum et al., 2007). Thus the cornice fall avalanches provide enough fresh rock debris and snow to the root of a rock glacier to allow it to have grown to its relatively large size (Humlum et al., 2007) (Figure 9a). Presumably the prevailing southeasterly airflow over the Gruvefjellet plateau favours the build-up of the largest cornices at Larsbreen compared to Nybyen, resulting in a higher release frequency, providing enough snow and debris to supply the Larsbreen rock glacier. It is also likely, that the avalanche derived rock glacier at Larsbreen is located right above the rock glacier initiation line altitude (based on climate), which could coincide with the equilibrium line altitude for the cirque glaciers in the area.

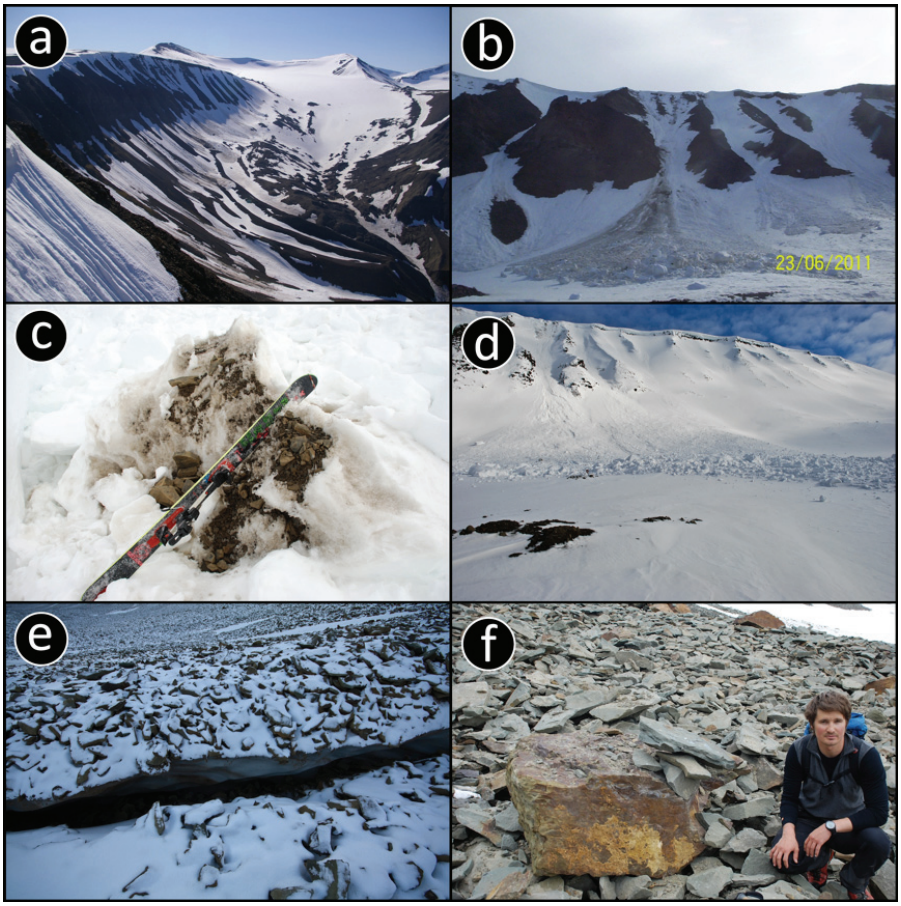

Figure 9: a) Automatic time-lapse photograph of the entire Larsbreen slope system. The photo shows avalanche activity 10 June 2008. Rock debris is clearly visible in the avalanches, as well as long runouts onto the ice-cored moraine of Larsbreen glacier. The avalanche derived rock glacier, with its three separate ridges is visible in the foreground. It was deflected by the LIA push of Larsbreen glacier. b) Automatic time-lapse photographs covering catchments L1-L3 at Larsbreen. The collapsed part of the cornice is visible, as well as the high rock debris content in the avalanche deposit. c) Collapsed piece of a cornice with rock debris of different grain sizes plucked directly from the plateau edge and transported downslope by a cornice fall avalanche, 12 May 2010 in catchment L3. d) Large cornice fall

avalanche 10 May 2011, which nearly hit the time-lapse camera (Lars cam) in front of the avalanche fan, and stopped on the ice-cored moraine of the Larsbreen glacier. e) A fluvial channel eroded through avalanche deposits exposing ice inside the avalanche fan, accumulated due to the insulating effect of the avalanche sedimentation at catchment L5. The crack is about 100 cm in width at maximum f) Perched avalanche deposited rock debris onto a boulder located at the foot of the avalanche fan in catchment L1 at Larsbreen.

The differences in avalanche sedimentation rates between the Nybyen and Larsbreen slope systems

Both the Nybyen and Larsbreen slope systems are developed in a similar geological setting with roughly similar slope aspect towards W and NW. The slope systems are part of the same plateau edge that steadily rises in elevation from north to south (Figure 1). The Nybyen slope system has a larger vertical relief than Larsbreen, as well as a larger run (600 m and 200 to 350 m respectively). The relationship between height and run is roughly similar for the two systems (ranging from 0.48 to 0.6), but the slope profiles are quite different with much deeper incised gullies or couloirs at Nybyen, which cause intermediate depositional areas to exist in the upper part of the slope as well (Figure 5). The Larsbreen slope system is topographically smoother with a much larger source-to-depositional area ratio, and no intermediate storage landforms (Figure 6).

Thus the different slope system-specific avalanche sedimentation rates are a function of the complexity of the catchments. The intermediate storage at the Nybyen slope (Krautblatter and Dikau, 2007) is, in contrast to Larsbreen, well developed as several catchments have a thick sediment cover already in the first depositional area (Figure 5a). In the upper catchments, the vertical free rock face transitions immediately into the primary fans. When cornices melt down *in-situ* instead of collapsing, embedded rock debris is deposited on the plateau edge, the horizontal ledges of the free rock face and the upper fans, acting as yet another intermediate storage. This intermediate storage is also to some degree filled with rockfall debris from the free face above. Consequently, large cornice fall avalanches not only transport plucked rock debris from the plateau edge, but also sweep rock debris deposited by melting cornices and rockfall the previous years from the ledges on the free rock face and the upper fans. Avalanche and rockfall deposits stored temporarily in the transport couloirs are typically only swept away by cornice fall avalanches at the end of the snow season, during full-depth avalanching, when just little snow is left on the slopes. Only by cornice fall avalanche transportation can larger quantities of rockfall debris reach the primary fans. Rockfall debris from the protruding rock noses accumulate in very steep, well sorted fans between the primary avalanche fans, especially at Nybyen, but also at Larsbreen in the northern part (Figure 5a).

The sedimentology and geomorphology of the individual catchments also lead to different avalanche sedimentation rates. The most striking geomorphological difference is the steeper transition from the plateau to the free rock face at Larsbreen, being almost entirely vertical above catchments L5 – L7. Due to this vertical backwall, about 15-20 m high, a downwards-deforming cornice very fast becomes unstable, as it is relatively unsupported compared to a cornice accreting on a less steep backwall. When such a cornice detaches from the plateau it often results in entire cornice collapses, which very efficiently plucks rock debris from the backwall. A significant sedimentological difference between catchments is the sediment thickness particularly in the transport couloirs at Nybyen (Figure 5a). When an avalanche sweeps down these couloirs containing a thick sediment cover, it can entrain more rock debris.

Present-day and Holocene rockwall retreat rates

Having quantified avalanche sedimentation it is possible to contribute to the discussion on how much of the rockwall retreat is caused by the geomorphological activity of avalanches, and how much is the effect of rockfalls. The average annual rockwall retreat rates are as high as 0.94 mm/yr at Nybyen and 1.13 mm/yr at Larsbreen (Table 3), with catchment specific rockwall retreat rates as high as 1.40 mm/yr (N4 in 2010/2011) at Nybyen, and 5 mm/yr (L6 in 2009/2010) at Larsbreen. In this catchment L6, the depositional area is only 11 % smaller than the source area.

We assume, based on almost 10 years of frequent field observations, that rockfalls contribute to the rockwall retreat rates with a maximum of 10 %. This assumption is supported by our time-lapse photography monitoring, showing that at least one cornice fall avalanche released in each catchment at both slope systems every year. Therefore the upper depositional areas at Nybyen and the transport couloirs at Larsbreen got swept annually. This keeps the rock fall contribution small and makes the rockwall retreat rates annual rates.

Siewert et al. (2012) calculated Holocene rockwall retreat rates, based on GPR mapping of the thickness of the entire avalanche fan deposits at both sides of the Longyeardalen valley. Their calculations indicate slightly higher average Holocene rockwall retreat rates of 1.1 mm/yr at the Nybyen slope system, and 0.5 mm/yr on the SE facing side of the valley. Hartmann-Brenner (Hartmann-Brenner, 1974) also calculated average Holocene rockwall retreat rates of 0.7 mm/yr for the SE facing slopes in the Longyeardalen valley.

The average Holocene rockwall retreat rates are within the range of our present-day rates (Table 3), but generally in the lower end of the present-day rates at both the Nybyen slope system, but primarily at the Larsbreen slope system. This is most likely due to the large activity of cornice fall activity at the two slope systems, dominating the NW facing side, while a combination of avalanches and rockfalls dominate the SE side of the Longyeardalen valley. From a large debris flow event in 1972 Larsson (1982) reported rockwall retreat rates of maximum 0.0125 mm/yr, which shows that also debris flows are of much less importance for rockwall retreat than cornice fall avalanching in the Longyeardalen valley.

Possible errors and uncertainties

Cornice fall avalanche activity was monitored by automatic time-lapse photography and direct field observations and we are sure that this combination of methods enabled us to have observed the entire record of major avalanche activity. The extent of each avalanche was calculated in ArcGIS 10, based on an outline drawn from the photographs. There might be a small overestimation of the depositional area due to a more generalized outline drawn in ArcGIS 10, but this error is consistent throughout the dataset.

Rock debris was collected in five permanent sediment traps and in numerous snow inventories. While the permanent sediment traps provide the longest and most persistent record of avalanche sedimentation, the snow inventories are somewhat biased by the individual sampling location, and its position on the avalanche deposits. Obviously, sampling locations were chosen to be were large quantities of rock debris were seen to ablate out of the snow. Still, in many catchments a high number of sampling sites could be established each year, giving this preferential sampling less significance. A large difference between the permanent sediment traps and the snow inventories is their timing of collection. Summer rockfall is only to a very small degree affecting the avalanche fans as far down on the primary fans as where the sediment traps were located. But due to the timing of sampling at the snow minimum in September, potentially some few rocks from really large rockfalls could have been included in the quantification of the permanent sediment traps.

All these permanent sediment traps and snow inventories are single point measurements of rock debris that were summed up and extrapolated onto the entire avalanche snow deposit area, which is the annual maximum extent, all avalanches have reached in one year in a catchment. However, a larger number of rock debris samples did not necessarily result in a larger amount of rock debris. We therefore know that the determined avalanche sedimentation rates and avalanche fan-surface accretion rates are maximum rates.

Conclusion

In this study, we present a record of maximum 7 years of avalanche sedimentation rates from two slope systems in the valley Longyeardalen, in central Svalbard. Avalanche monitoring was carried out by daily time-lapse photography and direct field observations ensuring a complete record. Avalanche transported rock debris quantification was carried out directly by sampling it in permanent sediment traps on avalanche fans in end of summer and by snow inventories during the snow melting season.

Annual avalanche sedimentation rates are expressed as the amount of rock debris accumulated by avalanches in kg, as well as the annual surface accretion on the avalanche fan in mm. At both slope systems these rates are high due to the highly weathered, moderately strong sedimentary rock, and the high magnitude and frequency of dirty cornice fall avalanches. These avalanches efficiently pluck and transport rock debris from the free rock face onto the primary fans, and sweep the transport couloirs clean of rock debris deposited by melting cornices and rockfall. This process took place every year in all catchment at both slope systems, however, we did not quantify it every year. The significant geomorphological work of cornices and cornice fall avalanches cause erosion of the plateau edges, and a high ice-content in the aggrading permafrost in the distinct avalanche fans, consisting of a layering of avalanche snow and rock debris. Most evidently, cornice fall avalanching causes the formation of a large avalanche-derived rock glacier right below the Larsbreen slope system. The calculated avalanche sedimentation rates reflect the magnitude and frequency of this cornice fall avalanching in the present climate. Humlum et al. (2007) suggested that the rock glacier is of late Holocene age (<5000 years), which means that significant cornice fall activity and rock debris transport must have occurred since then. Magnitude and frequency of avalanching must have been comparable, as the median Holocene rockwall retreat rate, calculated by Siewert et al. (2012) is comparable to the present-day rates.

The larger avalanche sedimentation at Larsbreen is caused by a simpler system with a shorter distance from the cornice source are to the one depositional area. The Nybyen slope system has more complex, deeper insisted catchments, where rock debris gets deposited in intermediate storage landforms.

Differences in avalanche sedimentation rates between years within each slope systems are mainly due to a higher cornice fall frequency resulting in larger avalanches, transporting more rock debris downslope.

In conclusion, cornice fall avalanches are at present by far the most efficient sediment erosion and transport agent on NW facing slopes in the valley Longyeardalen. As cornice fall avalanches are the most dominant type of avalanche in the Longyearbyen area, with 45.2 % of the total (Eckerstorfer and Christiansen, 2011b), they are likely to be the dominant mode of sediment transport of any leeward slope.

Acknowledgements

Thanks Jonas Ellehauge, Knut Stalsberg, Jordan R. Mertes, Ulli Neumann, Jørgen Haagensli, Ole Humlum and the IPY Summer School 2009 students for help with rock debris sampling. Thanks to Wesley R. Farnsworth for fieldwork assistance during geomorphological mapping. We acknowledge the thorough comments and suggestions by Associate Editor Martin Schneebeli, Brian H. Luckman and two anonymous reviewers that improved an earlier version of this paper significantly.

References

Ackroyd, P, 1987. Erosion by snow avalanche and implications for geomorphic stability, Torlesse Range, New Zealand. *Arctic and Alpine Research*, **19**(1), 65-70.

Åkerman, HJ, 1984. Notes on talus morphology and processes in Spitsbergen. *Geografiska Annaler*, **66A**(4), 17.

Åkerman, HJ, 2005. Relations between slow slope processes and active-layer thickness 1972-2002, Kapp Linne, Svalbard. *Norsk Geografisk Tidsskrift - Norwegian Journal of Geography*, **59**(2), 116 - 128.

André, M-F, 1990. Geomorphic impact of spring avalanches in Northwest Spitsbergen (79°N). *Permafrost and Periglacial Processes*, **1**(2), 97-110. doi: 10.1002/ppp.3430010203

André, M-F, 1995. Holocene climate fluctuations and geomorphic impact of extreme events in Svalbard. *Geografiska Annaler*, **77A**(4), 241-250.

André, M-F, 1996. Geological control of slope processes in northwest Spitsbergen. *Norsk Geografisk Tidsskrift - Norwegian Journal of Geography*, **50**, 4.

André, M-F, 1997. Holocene rockwall retreat in Svalbard: A triple-rate evolution. *Earth Surface Processes and Landforms*, **22**(5), 423-440.

Bell, I, Gardner, J, DeScally, F, 1990. An estimate of snow avalanche debris transport, Kaghan Valley, Himalaya, Pakistan. *Arctic, Antarctic, and Alpine Research*, **22**(3), 317-321.

Blikra, LH, Selvik, SF, 1998. Climatic signals recorded in snow avalanche-dominated colluvium in western Norway: depositional facies successions and pollen records. *The Holocene*, **8**(6), 631-658.

Caine, TN, 1976. A uniform measure of subaerial erosion. *Geological Society of America Bulletin*, **87**, 137-140.

Christiansen, HH, 2001. Snow-cover depth, distribution and duration data from northeast Greenland obtained by continuous automatic digital camera. *Annals of Glaciology*, **32**, 102-108. doi: 10.3189/172756401781819355

Christiansen, HH, Blikra, LH, Mortensen, LE, 2007. Holocene slope processes and landforms in the northern Faroe Islands. *Earth and Environmental Science Transactions of the Royal Society of Edinburgh*, **98**, 1-13. 10.1017/s0263593307000041

Decaulne, A, Saemundsson, T, 2006. Geomorphic evidence for present-day snow-avalanche and debris-flow impact in the Icelandic Westfjords. *Geomorphology*, **80**(1-2), 80-93. doi: 10.1016/j.geomorph.2005.09.007

Eckerstorfer, M, Christiansen, HH, 2011a. The "High Arctic Maritime Snow Climate" in Central Svalbard. *Arctic, Antarctic, and Alpine Research*, **43**(1), 11-21. doi:10.1657/1938-4246-43.1.11

Eckerstorfer, M, Christiansen, HH, 2011b. Topographical and meteorological control on snow avalanching in the Longyearbyen area, central Svalbard 2006-2009. *Geomorphology*, **134**(3-4), 186-196. doi:10.1016/j.geomorph.2011.07.001

Eckerstorfer, M, Christiansen, HH, Vogel, S, Rubensdotter, L, 2012. Snow cornice dynamics as a control on plateau edge erosion in central Svalbard *Earth Surface Processes and Landforms*. doi: 10.1002/esp.3292

Etzelmueller, B, Ødegård, RS, Vatne, G, Mysterud, RS, Tonning, T, Sollid, JL, 2000. Glacier characteristics and sediment transfer system of Longyearbreen and Larsbreen, western Spitsbergen. *Norsk Geografisk Tidsskrift - Norwegian Journal of Geography*, **54**(4), 157-168. 10.1080/002919500448530

French, HM, 2007. The periglacial environment, **Third edition**. John Wiley & Sons.

Hartmann-Brenner, D-C, 1974. Ein Beitrag zum Problem der Schutthaldenentwicklung an Beispielen des Schweizerichen Nationalparks und Spitzbergens. Doctoral Thesis, University of Zuerich.

Heckmann, T, Wichmann, V, Becht, M, 2002. Quantifying sediment transport by avalanches in the Bavarian Alps - first results. *Zeitschrift für Geomorphologie, N.F.*, **127**, 137-152.

Heckmann, T, Wichmann, V, Becht, M, 2005. Sediment transport by avalanches in the Bavarian Alps revisited - a perspective on modelling. *Zeitschrift für Geomorphologie, N.F.*, **138**, 11-25.

Hjelle, A, 1993. The Geology of Svalbard. Polarhåndbok, **7**. Norsk Polarinstitutt, Oslo. pp. 163 pp.

Humlum, O, Christiansen, HH, Juliussen, H, 2007. Avalanche-derived rock glaciers in Svalbard. *Permafrost and Periglacial Processes*, **18**(1), 75-88. doi: 10.1002/ppp.580

Jahn, A, 1967. Some features of mass movement on Spitsbergen slopes. *Geografiska Annaler*, **49A**(4), 213-224.

Jahn, A, 1976. Contemporaneous geomorphological processes in Longyeardalen, Vestspitsbergen (Svalbard). *Biuletyn Peryglacjalny*, **26**, 25.

Jahn, A, 1984. Periglacial talus slopes. Geomorphological studies on Spitsbergen and in Northern Scandinavia. *Polar Geography and Geology*, **8**, 177-193. 10.1080/10889378409377224

Krautblatter, M, Dikau, R, 2007. Towards a uniform concept for the comparison and extrapolation of rockwall retreat and rockfall supply. *Geografiska Annaler: Series A, Physical Geography*, **89**(1), 21-40. 10.1111/j.1468-0459.2007.00305.x

Krautblatter, M, Moser, M, 2009. A nonlinear model coupling rockfall and rainfall intensity based on a four year measurement in a high Alpine rock wall (Reintal, German Alps). *Natural Hazards and Earth System Sciences*, **9**, 1425-1432.

Larsson, S, 1982. Geomorphological effects on the slopes of Longyear valley, Spitsbergen, after a heavy rainstorm in July 1972. *Geografiska Annaler*, **64A**(2), 105-125.

Luckman, BH, 1977. The geomorphic activity of snow avalanches. *Geografiska Annaler. Series A, Physical Geography*, **59**, 31-48.

Luckman, BH, 1978a. Geomorphic work of snow avalanches in the Canadian Rocky Mountains. *Arctic and Alpine Research*, **10**(2), 261-276.

Luckman, BH, 1978b. The measurement of debris movement on alpine talus slopes. *Zeitschrift für Geomorphologie, N.F.*, **Suppl. Bd. 29**, 117-129.

Luckman, BH, 1988. Debris accumulation patterns on talus slopes in Surprise Valley, Alberta. *Geographie physique et Quaternaire*, **42**(3), 247-278.

Matsuoka, N, Sakai, H, 1999. Rockfall activity from an alpine cliff during thawing periods. *Geomorphology*, **28**, 309-328.

Met.no, 2012. eklima. Free access to weather- and climate data from Norwegian Meteorological Institute form historical data to real time observations. http://www.eklima.no.

Rapp, A, 1960a. Recent developments of mountain slopes in Kärkevagge and surroundings, northern Scandinavia. *Geografisk Annaler*, **XLII**, 71-200.

Rapp, A, 1960b. Talus slopes and mountain walls at Tempelfjorden, Spitsbergen. *Norsk Polarinstitut Skrifter*, **119**.

Sass, O, Hoinkis, R, Wetzel, K-F, 2010. A six-year record of debris transport by avalanches on a wildfire slope (Arnspitze, Tyrol). *Zeitschrift für Geomorphologie, N.F.*, **54**(2), 181-193.

Schrott, L, Niederheide, A, Hankammer, M, Hufschmidt, G, Dikau, R, 2002. Sediment storage in a mountain catchment: geormorphic coupling and temporal variability (Reintal, Bavarian Alps, Germany). *Zeitschrift für Geomorphologie, N.F.*, **Suppl.-Bd. 127**, 175-196.

Siewert, MB, Krautblatter, M, Christiansen, HH, Eckerstorfer, M, 2012. Arctic rockwall retreat rates estimated using laboratory-calibrated ERT measurements of talus cones in Longyeardalen, Svalbard. *Earth Surface Processes and Landforms*. 10.1002/esp.3297

Vogel, S, Eckerstorfer, M, Christiansen, HH, 2012. Cornice dynamics and meteorological control at Gruvefjellet, Central Svalbard. *The Cryosphere*, **6**, 157-171. doi:10.5194/tc-6-157-2012

Whalley, WB, 1984. Rockfalls. In: D. Brunsden, D.B. Prior (Eds.), Slope Instability. Wiley & Sons, Chichester, pp. 217-256.